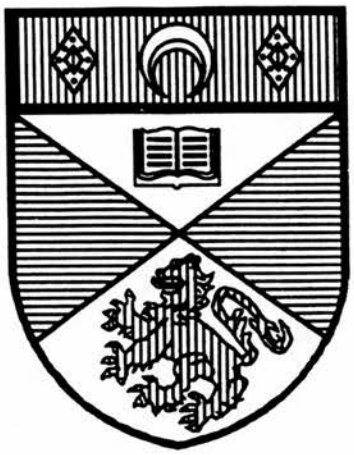

Synthetic and Kinetic Studies of Macrocyclic Metal Complexes

A thesis presented by Andrew Danby to the University of St. Andrews

in application for the degree of Doctor of Philosophy

April 1996.

Th C 20

Declarations

I, Andrew Mark Danby, hereby certify that this thesis has been composed by myself, that it is a record of my work and that it has not been accepted in partial or complete fulfilment of any other degree or professional qualification.

Signed_ Date 30th April 1996

I was admitted to the Faculty of Science of the University of St. Andrews under Ordinance General No. 12 on the 1st of October 1992 and as a candidate for the degree of Ph.D. on the 1st of October 1993.

Signed_ Date 30th April 1996.

I hereby certify that the candidate has fulfilled the conditions of the Resolution and Regulations appropriate to the degree of Ph.D.

Signature of Supervisor_ Date 30/April/96

Copyright

Contents

Declarations i

Copyright ii

Contents iii

Acknowledgements vii

Abstract viii

Chapter 1

Studies of "Padlock" penta- and hexa-aza Macrocycles

1.1 Introduction 1

1.2 Experimental

1.2.1 Synthesis 12

1.2.2 Kinetic Measurements 18

1.2.3 Equilibrium Measurements 18

1.2.4 Crystal Srtucture Determinations 19

1.3 Results and Discussion

1.3.1 Crystal Structure of (3-ethyl-1,3,5,8,12-pentaaza-cyclotetradecane)-nickel(II) perchlorate 23

1.3.2 Crystal Structure of [(1,3,6,10,12,15-hexaazatricyclo-[13.3.1.$1^{6,10}$]-eicosane)nickel] perchlorate 31

1.3.3 Kinetics of Metal Exchange 38

1.3.4 Square Planar-Octahedral Equilibria 45

1.3.5 Square Planar-Octahedral Equilibria in Acidic Solution 51

1.4 References 56

Chapter 2

Kinetic Studies of Binuclear Hexaaza Macrocycles

2.1 Introduction 63

2.2 Experimental

2.2.1 Synthesis 75

2.2.2 Physical Measurements 83

2.3 Results and Discussion

2.3.1 Synthesis 84

2.3.2 Acid Catalysed Dissociation Kinetics of Cu_2PEA 86

2.3.3 Acid Catalysed Dissociation Kinetics of Cu_2MPA and Cu_2PPA 96

2.4 References 101

Chapter 3

Studies of Cobalt(III) Complexes of [15]aneN$_4$

3.1 Introduction

3.1.1 Tetraaza Macrocyclic Complexes 106

3.1.2 Cobalt(III) Complexes of 1,4,8,12-tetraazacyclopentadecane 108

3.1.3 Kinetic Studies of the Acid Catalysed Aquation of $[Co([15]aneN_4)Cl_2]^+$ 111

3.1.4 Acid catalysed aquation of the $[Co([15]aneN_4)CO_3]^+$ 113

3.2 Experimental

3.2.1 Synthesis 115

3.2.2 Physical Measurements 120

3.3 Results and Discussion

3.3.1 Synthesis 122

3.3.2 Acid Catalysed Decarboxylation of *cis*-$[Co([15]aneN_4)(CO_3)]^+$ 124

3.3.3 Aquation of *trans* I-$[Co([15]aneN_4)Cl_2]^+$ 148

3.4 References 154

Chapter 4

Studies of the Formation of *trans*[14]dieneN$_4$

4.1 Introduction 157

4.2 Experimental

4.2.1 Synthesis 164

4.2.2 Kinetic Measurements 168

4.2.3 Crystal Structure Determination 169

4.3 Results and Discussion

4.3.1 Synthesis 171

4.3.2 Crystal Structure of [(14-amino-4,4,9,11,11-pentamethyl-5,8,12-triazatetradec-8-en-2-one)copper(II)]$(ClO_4)_2 \cdot CH_3CN$ 172

4.3.3 Kinetic studies 178

4.4 References 187

Chapter 5

Synthesis of Tetraamide Macrocycles

5.1 Introduction

5.1.1 Uses of Macrocyclic Oxopolyamines 192

5.1.2 Synthetic Strategies 200

5.2 Experimental

5.2.1 Synthesis 205

5.2.2 Crystal Structure Determination of $[Cu(mal)(pn)Cl_2]^{2-}(pnH_2)^{2+}$ 208

5.3 Results and Discussion 210

5.4 References 218

Appendix 1 224

Acknowledgments

I am indebted to the School of Chemistry, University of St. Andrews for the award of a Research Stundentship. The British Council is acknowledged for financial assistance towards a five week study period at the Universität Heidelberg and the Gesellschaft Deutscher Chemiker for a bursary for attendance at a conference at Wiesbaden, Germany.

I sincerely thank my supervisor Professor R.W.Hay for his guidance, encouragement and humour throughout the duration of my studies. Thanks are also extended to Dr. P. Lightfoot for determining all of the crystal structures. Professor P. Comba and Dr. D.T. Richens are thanked for their assistance in arranging my visit to Heidelberg. Advice was gratefully received from Professors N.F. Curtis (University of Wellington) and Y.A. Lampeka (Ukranian Academy of Science, Kiev).

Thanks are also due to the numerous people who have worked in Lab. 229 during my studies. They provided much needed distractions from the monotony of research.

Finally, I should like to thank my family for their continued support and patience.

Abstract

The chemistry of a series of pentaaza and hexaaza macrocycles formed by the metal directed condensation of formaldehyde, diamines and primary amines has been investigated. Structural studies were carried out and the results used to determine the extent of any long range interactions between the coordinated metal ion and non-coordinating amino groups. The effect of the uncoordinated tertiary amine on the square planar-octahedral spin equilibria was also studied.

Chapter 2 investigates kinetic aspects of the chemistry of binuclear complexes of hexaaza macrocycles. The acid catalysed metal dissociation reactions of the copper(II) complexes of three ligands were studied. It was found that the two metal centres in such complexes act independently of each other. Activation parameters for the metal dissociation reactions have been determined.

Chapter 3 discusses cobalt(III) complexes of the tetraaza macrocycle [15]aneN$_4$. Kinetic and mechanistic studies have been carried out to study the decarboxylation reaction of [Co([15]aneN$_4$)(CO$_3$)]$^+$. A mechanism for this reaction is described. The kinetics of the hydrolysis of [Co([15]aneN$_4$)Cl$_2$]$^+$ have also been investigated.

The ring closure reactions of a linear β-aminoketone copper(II) complex to form the macrocyclic complex [Cu(*trans*[14]dieneN$_4$)]$^{2+}$ have been studied kinetically. A mechanism involving an intramolecular reaction with a coordinated hydroxide group has been proposed.

Attempts to synthesise macrocyclic tetraamide complexes via a literature method are described. Evidence is presented which suggests that the preparation of such complexes by metal template directed condensation of diacids and diamines is not viable and this view has been confirmed by crystallographic studies.

Chapter 1

Studies of "Padlock" Macrocycles

1.1 Introduction

Many complexes have been synthesized by the condensation of amines with aldehydes or ketones in the presence of a metal ion template. Formaldehyde in particular has been used to bridge two amine moieties. The reaction of two molecules of ethylenediamine with four molecules of formaldehyde to give 1,3,6,8-tetraazatricyclo[4,4,1,13,8]dodecane[1] has been well studied. Formaldehyde has also been used in intramolecular cyclisation reactions to form macrocyclic ligands. Two molecules of butane-2,3-dione dihydrazone complexed to a divalent metal ion will undergo amine condensation[2] with formaldehyde to form a macrocyclic complex as shown in Figure 1.1.1.

Figure 1.1.1 Condensation of butane-2,3-dione dihydrazone with formaldehyde to give a macrocyclic complex.

A similar procedure has been used to cyclise the dihydrazine[3], Figure 1.1.2;

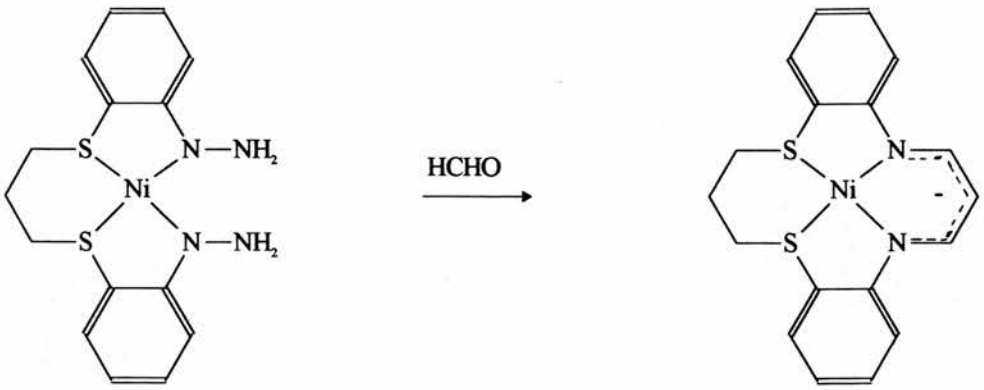

Figure 1.1.2.

Such formaldehyde condensations have proved useful in the synthesis of polydentate and macrocyclic ligands and have been further developed by introducing a "molecular padlock". Thewalt and Weiss[4] were the first to report the use of a molecular padlock in the synthesis of the polydentate N_2S_2 donor ligand shown in Fig 1.1.3.

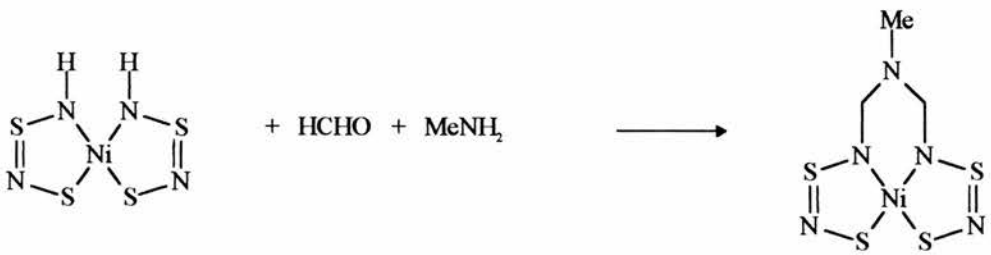

Figure 1.1.3.

A possible mechanism for the formation of such padlock bridges is shown in Figure 1.1.4.

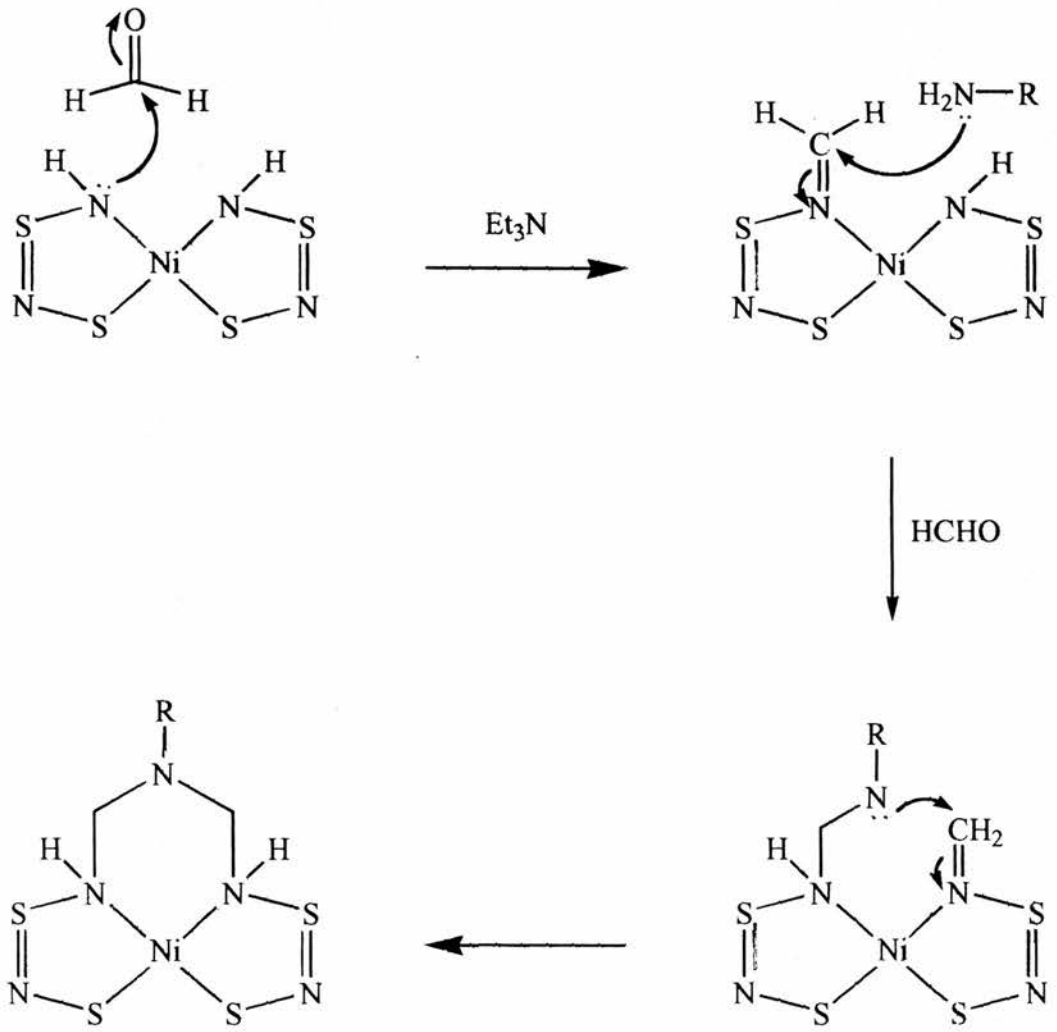

Figure 1.1.4. Mechanism of formaldehyde condensation with an amine "padlock".

The reaction is initiated by the formation of an imine by the reaction of formaldehyde with a coordinated amino group. The imine is then attacked by the alkylamine to yield

a *gem*-diamine which subsequently condenses with a neighbouring imine group resulting in the formation of the six membered chelate ring.

The analogous reaction using ammonia as the locking fragment has been reported[5]. This class of reactions was developed further with the synthesis by Creaser *et al* [6,7] of (S)-[(1,3,6,8,10,13,16,19-octaazabicyclo-[6.6.6]eicosane)cobalt]Cl_3 or, as it is more commonly known, [Co(sepulchrate)]Cl_3. The synthesis of large macrocycles and cages had previously proved complicated because of the unfavourable entropy effects involved. By introducing a template the organic chemistry can be split into several smaller, more favourable steps. The preparation involves the condensation of $[Co(en)_3]^{3+}$ with formaldehyde and ammonia to yield the Co(III) complex of the sexadentate "sepulchrate" ligand, Figure 1.1.5. Ammonia acts as the capping fragment and being triprotic, causes a three dimensional condensation to occur. The trigonal symmetry about the capping nitrogen atoms is precisely that required to fit on the trigonal axis of the *tris*-(ethylenediamine)metal complex, however, the crystal structure of the nickel(II) complex[8] shows distortion from the expected trigonal stereochemistry.

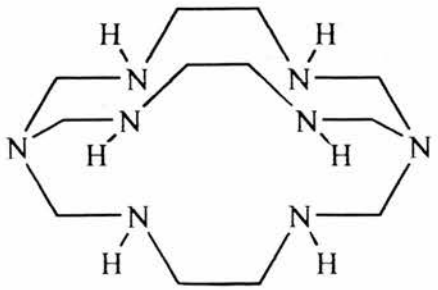

Figure 1.1.5. 1,3,6,8,10,13,16,19-octaazabicyclo-[6.6.6]eicosane (sepulchrate)

Recently Suh and Kang[9] extended this type of reaction to the preparation of diaza-cyclam macrocycles by the nickel(II) template condensation of ethylenediamine, formaldehyde and alkylamines, Figure 1.1.6.

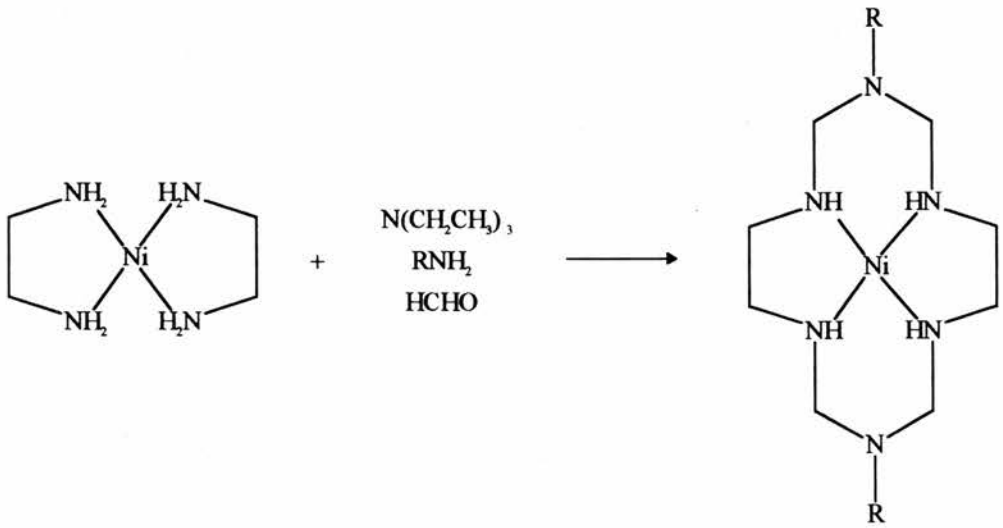

Figure 1.1.6. Hexaaza macrocycles via formaldehyde condensation.

Attempts to use ammonia as the locking fragment were unsuccessful yielding the non-cyclic tetradentate ligand[10], Figure 1.1.7, instead of the hexaaza macrocycle, Figure 1.1.8. It is known that methylenediamine groups are unstable when they contain primary or secondary amines[11] and usually they can only be isolated when they contain tertiary amines. However, methylenediamine groups containing secondary amines can be stabilized by the coordination of the secondary amines to a metal ion[8].

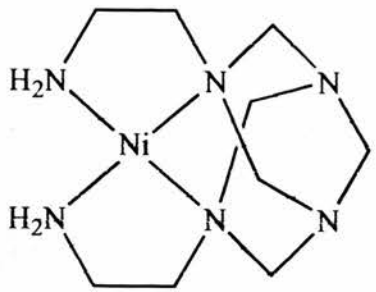

Figure 1.1.7.

Further evidence for the instability of methylenediamine bridges (even when they are stabilized by coordination to a metal ion) was demonstrated by Suh and Kim[12] in their attempt to synthesize $[Ni(sepulchrate)]^{2+}$ from $[Ni(semisepulchrate)]^{2+}$ via the condensation of $[Ni(semisepulchrate)]^{2+}$ with formaldehyde and ammonia. The nickel(II) complex of the non-cyclic tetradentate ligand, Figure 1.1.7, was isolated. This result suggests that the secondary nitrogens of the $[Ni(semisepulchrate)]^{2+}$ methylenediamine groups are still sufficiently reactive to produce tertiary nitrogens upon reaction with formaldehyde in the presence of primary amines.

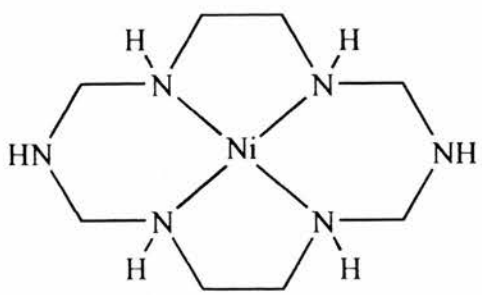

Figure 1.1.8.

Several other amines in addition to the linear primary alkylamines have been used as padlocks in the synthesis of diazacyclams. For example, benzidine[13] has been used as a padlock and hexaazacyclams with hydroxyl[14,15] and nitrile[16] pendant arms have been synthesized using ethanolamine and β-aminopropionitrile. The nickel(II) complex with the nitrile pendant arms forms an interesting intermolecular coordination polymer in which the nitrile group of one macrocycle molecule coordinates axially to the metal atom of an adjacent molecule and its structure has been determined by X-ray crystallographic techniques.

N-substituted pentaazacyclam derivatives can be synthesized[15] by the nickel(II) template condensation reaction of formaldehyde, methylamine and 3,7-diazanonane-1,9-diamine (2,3,2-tet). There has been interest[18] in the synthesis of macrocycles using long chain primary amines (up to $C_{18}H_{37}NH_2$) as the padlock because the macrocycle possesses a hydrophobic aliphatic chain and a hydrophilic macrocyclic head. Such complexes have been studied as they can form molecularly organized systems, for example, Langmuir-Blodgett films and are potential mesogens for the formation of liquid-crystals[19,20].

Lampeka has reported[21] the synthesis of (1,3,5,8,12-pentaazacyclotetradecane)-nickel(II) perchlorate by the condensation of $[Ni(2,3,2\text{-tet})]^{2+}$, formaldehyde and ammonia. This macrocycle containing two methylenediamine bridges to secondary amines might be expected to be unstable in view of Suh's earlier unsuccessful attempts to synthesize the hexaamine analogue. It is of particular interest because the uncoordinated distal secondary amine group is a potential reaction site that would allow various substituents to be introduced into the macrocycle.

An interesting class of compound can be prepared by the condensation of $[Ni(2,3,2\text{-tet})]^{2+}$, formaldehyde and an aliphatic α,ω-diamine to give a *bis*-(macrocyclic) dinickel(II,II) complex. Molecules containing two or more spatially separated reactive sites are of interest because they can act as multielectron redox agents or catalysts and can be regarded as models for polynuclear metalloenzymes. In addition they can exhibit interesting physical properties due to metal-metal interactions. Complexes of the type shown in Figure 1.1.9 have been reported [22,23] (n = 2-5). These compounds may also be of importance as anti AIDS drugs[24].

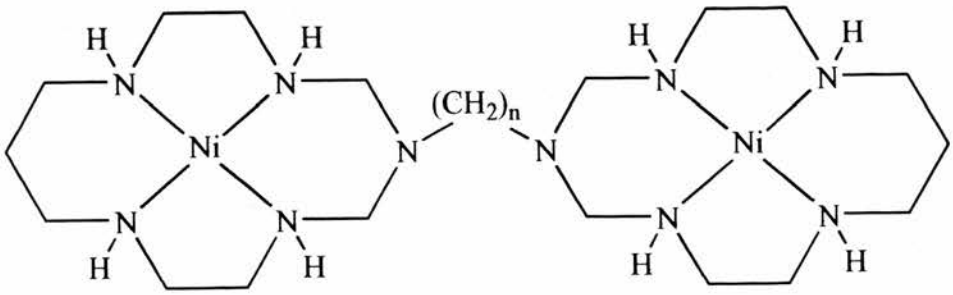

Figure 1.1.9. *bis*-((pentaazacyclam)Ni^{II})

Variations on this structure by replacing $[Ni(2,3,2\text{-tet})]^{2+}$ with the nickel complex of a different ligand have been reported [25,26]. Interestingly attempts to prepare similar complexes using the copper(II) and nickel(II) complexes of 2,2,2-tet (1,9-diamino-3,6-diazanonane) and 3,2,3-tet (1,10-diamino-4,7-diazadecane) have unexpectedly resulted in the monomacrocyclic compounds as shown in Figure 1.1.10.

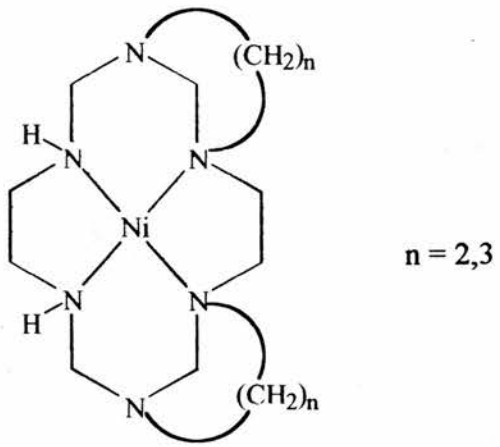

Figure 1.1.10.

This result is probably due to the different coordination modes of the tetraamines about the metal ions. The ligand 2,3,2-tet will occupy the equatorial plane about the nickel(II) ion and two *trans* axial coordination sites will be vacant for the coordination of further ligands. Such coordination of the tetraamine prevents the bidentate binding of the padlock α,ω–diamine and compels each amino group of the diamine to undergo a formaldehyde condensation reaction in the coordination sphere of a different metal ion. The ligands 2,2,2-tet and 3,2,3-tet favour coordination, either mononuclear or polynuclear, in which two *cis* coordination sites are vacant[27] and therefore the α,ω-diamine coordinates in a bidentate manner. Intramolecular condensation then occurs leading to the products shown in Figure 1.1.10.

This argument is supported by the synthesis[28] of [(3-oxa-1,6,8,12,15-pentaazatricyclo[13.3.1.^{8,12}]eicosane)copper]$^{2+}$ from [(3,2,3-tet)Cu]$^{2+}$, formaldehyde

and ethanolamine. The coordination of the 3,2,3-tet ligand is such that two *cis* coordination sites are available for the ethanolamine to bind in a bidentate manner. The complex then undergoes an intramolecular condensation reaction with formaldehyde to form the tricyclic product.

Similar intramolecular condensations have been used to prepare bicyclic[29] and tricyclic hexa-aza macrocycles. For example, if ethylenediamine is substituted for ethanolamine in the previous reaction [(1,3,6,10,12,15-hexaazatricyclo[13.3.1.$1^{8,12}$]-eicosane)nickel]$^{2+}$ is produced[30]. Triamines can be used to prepare similar complexes with the small ring moieties *trans* to each other[31].

Apart from amines several other species have been used as locking fragments. Amides and sulfonamides will undergo a condensation reaction with formaldehyde and primary amines[32,33]. A ferrocene metallocyclam conjugate with a sulfonamide bridge has recently[34] been synthesized and characterized, Figure 1.1.11.

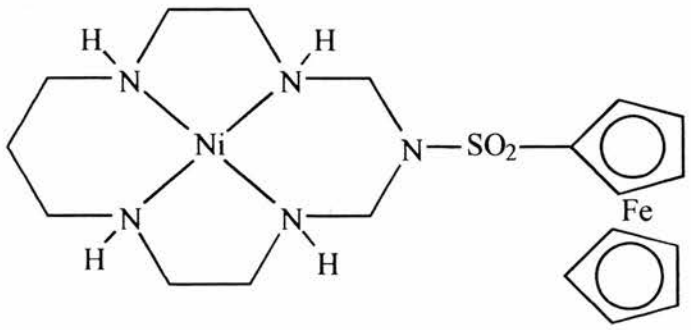

Figure 1.1.11. Ferrocene metallocyclam.

Carbon acids have also been extensively used in the synthesis of macrocycles. Nitroalkanes have been used as padlocks to form both cryptates[35,36,37] and monocyclic cyclam-like macrocycles[38,39,40,41]. The pendant nitro groups can coordinate axially with the metal ion. Reducing the nitro groups to form pendant amines which can coordinate to a central metal ion has also been widely reported[42,43,44,45]. Diethyl malonate possess an acidic central carbon which has been used as a padlock molecule in the synthesis of a macrocycle[46] although the yield was only 2% due to hydroxide ion competing with the diethylmalonato anion for the imine.

1.2 Experimental.

1.2.1 Synthesis

All materials were purchased from Aldrich, Avocado or Fisons. They were all reagent grade and were used as supplied except the amines which were redistilled prior to use.

Synthesis of (3-methyl-1,3,5,8,12-pentaazacyclotetradecane)nickel(II) perchlorate

The synthesis follows the procedure reported by Fabbrizzi *et al*[17]. $NiCl_2 \cdot 6H_2O$ (6.0 g, 25.2 mmol) was dissolved in ethanol (150 cm^3) and 3,7-diazanonane-1,9-diamine (4.04 g, 25.2 mmol) was added dropwise. To the violet solution was added triethylamine (5.04 g, 50.4 mmol), 30% aqueous methylamine solution (6 cm^3, 25.2 mmol) and 35% aqueous formaldehyde solution (11.4 g, 140 mmol). The solution was heated to reflux for 24 hours and the resulting brown solution cooled, filtered and reduced in volume (by 1/3) on a rotary evaporator. A saturated ethanolic solution (100 cm^3) of sodium perchlorate was added and the solution cooled in a refrigerator. The yellow crystalline product was filtered off, washed with ether and dried *in vacuo*. (Yield 5.71 g, 46.5 %) M.W. 474.94 g mol^{-1}, (Found: C, 25.56; H, 5.52; N, 15.00 %. Calculated for $C_{10}H_{25}N_5NiCl_2O_8$: C, 25.40; H, 5.33; N, 14.81 %); λ_{max} 448, ε = 51 $dm^3\ mol^{-1}\ cm^{-1}$ (H_2O); I.R./cm^{-1} ν(N-H); 3225; ν(C-H) 2943; ν(C:N) 1644 (KBr)

Synthesis of (3-ethyl-1,3,5,8,12-pentaazacyclotetradecane)nickel(II) perchlorate

This preparation was essentially the same as for (3-methyl-1,3,5,8,12-pentaazacyclotetradecane)nickel(II) perchlorate, but substituting the aqueous solution of methylamine with 70% aqueous ethylamine solution (1.63 g, 25.2 mmol). (Yield 7.31 g, 59.6 %) M.W. 486.96 g mol^{-1}, (Found: C, 26.94; H, 6.01; N, 14.75 %. Calculated for $C_{11}H_{27}N_5NiCl_2O_8$: C, 27.13; H, 5.59; N, 14.38 %); λ_{max} = 464 ε = 62.6 dm^3 mol^{-1} cm^{-1} ($MeNO_2$); I.R./cm^{-1}; ν(N-H); 3220; ν(C-H) 2951; ν(C:N) 1632 (KBr)

Synthesis of (3-propyl-1,3,5,8,12-pentaazacyclotetradecane)nickel(II) perchlorate

This preparation was essentially the same as for (3-ethyl-1,3,5,8,12-pentaazacyclotetradecane)nickel(II) perchlorate, but substituting the aqueous solution of methylamine with *n*-propylamine (1.49 g, 25.2 mmol). (Yield 7.74 g, 61.3 %) M.W. 500.99 g mol^{-1} (Found: C, 29.20; H, 5.67; N, 14.05 %. Calculated for $C_{12}H_{29}N_5NiCl_2O_8$: C, 28.77; H, 5.83; N, 13.98 %); λ_{max} = 464 ε = 62.6 dm^3 mol^{-1} cm^{-1} ($MeNO_2$) I.R./cm^{-1}; ν(N-H); 3225; ν(C-H) 2943; ν(C:N) 1644 (KBr)

Synthesis of (3-butyl-1,3,5,8,12-pentaazacyclotetradecane)nickel(II) perchlorate

This preparation was essentially the same as for (3-methyl-1,3,5,8,12-pentaazacyclotetradecane)nickel(II) perchlorate, but substituting the aqueous solution of methylamine with *n*-butylamine (1.85 g, 25.2 mmol). (Yield 8.04 g, 61.9 %) M.W. 515.02 g mol^{-1}, (Found: C, 30.26; H, 6.13; N, 13.36 %. Calculated for $C_{13}H_{31}N_5NiCl_2O_8$: C, 30.32; H, 6.07; N, 13.60 %); λ_{max} 449 nm (H_2O); I.R./cm^{-1} ν(N-H); 3201; ν(C-H) 2958; 1466, 1099, 1022, 626 (KBr)

Synthesis of (3-octyl-1,3,5,8,12-pentaazacyclotetradecane)nickel(II) perchlorate

This preparation was essentially the same as for (3-methyl-1,3,5,8,12-pentaazacyclotetradecane)nickel(II) perchlorate, but substituting the aqueous solution of methylamine with *n*-octylamine (3.26 g, 25.2 mmol). (Yield = 6.1 g, 42.4 %), M.W. 571.12 g mol^{-1}, (Found: C, 36.1; H, 7.1; N, 12.31 %. Calculated for $C_{17}H_{39}N_5NiCl_2O_8$: C, 35.75; H, 6.88; N, 12.26 %); λ_{max} 460 nm (H_2O);

Synthesis of (3-tridecyl-1,3,5,8,12-pentaazacyclotetradecane)nickel(II) perchlorate

This preparation was essentially the same as for (3-methyl-1,3,5,8,12-pentaazacyclotetradecane)nickel(II) perchlorate, but substituting the aqueous solution of methylamine with *n*-tridecylamine (5.03 g, 25.2 mmol). (Yield = 7.57 g, 46.8 %), M.W. 641.26 g mol^{-1}; λ_{max} 460 nm (H_2O);

Synthesis of (3-octadecyl-1,3,5,8,12-pentaazacyclotetradecane)nickel(II) perchlorate

This preparation was essentially the same as for (3-methyl-1,3,5,8,12-pentaazacyclotetradecane)nickel(II) perchlorate, but substituting the aqueous solution of methylamine with *n*-octadecylamine (6.80 g, 25.2 mmol). (Yield 6.17 g, 34.4 %), M.W. 711.39 g mol^{-1}, λ_{max} 456 nm (H_2O); I.R./cm^{-1} ν(N-H); 3210; ν(C-H) 2923; ν(C:N) 1654 (KBr)

Synthesis of (1,3,6,10,12,15-hexaazatricyclo[13.3.1.1^{6,10}]eicosane)nickel(II) perchlorate

N-(2-aminoethyl)-1,3-propanediamine (5.9 g, 50 mmol) was added to a solution of $NiCl_2 \cdot 6H_2O$ (5.95 g, 25 mmol) in methanol (50 cm^3). A 37% aqueous solution of formaldehyde (20.6 g, 0.2 mol) was added and the solution was heated to reflux for 5 hours. The resulting yellow solution was filtered to remove insoluble material and reduced to ca. 1/2 its volume on a rotary evaporator. Addition of ca. 3 cm^3 of concentrated perchloric acid followed by cooling in a refrigerator overnight yielded a yellow precipitate which was filtered off, washed with cold methanol and dried in *vacuo*. (Yield = 8.04 g, 61.95 %), M.W. 540.03 g mol^{-1}, (Found: C, 31.23; H, 5.67; N, 15.43 %. Calculated for $C_{14}H_{30}N_6NiCl_2O_8$: C, 31.14; H, 5.60; N, 15.56 %), λ_{max} 463 nm (H_2O); I.R./cm^{-1} ν(N-H) 3244; ν(C-H) 2949; ν(C:N) 1654, 1637; 1466, 1089 (KBr)

Synthesis of (1,3,6,10,12,15-hexaazatricyclo[13.3.1.1^{6,10}]eicosane)nickel(II)-dithiocyanate

The perchlorate salt (1.08 g, 2 mmol) prepared above was dissolved in warm water and an excess of saturated aqueous solution of potassium thiocyanate was added. Upon cooling the pink complex precipitated which was washed with ether and dried in *vacuo*. (Yield = 0.81 g, 88.56 %), M.W. 457.29 g mol^{-1}, (Found: C, 42.31; H,

6.96; N, 24.45 % Calculated for $C_{16}H_{30}N_8S_2Ni$: C, 42.03; H, 6.61; N, 24.50 %); λ_{max} 440 nm (H_2O); I.R./cm^{-1} ν(N-H) 3278; ν(C-H) 2965; ν(C:N) 2050; (KBr)

Synthesis of (1,3,6,9,11,14-hexaazatricyclo[12.2.1.1^{6,9}]octadecane)nickel(II)-dichloride

Diethylenetriamine (5.16 g, 50 mmol) was added to a stirred methanolic solution (30 cm^3) of $NiCl_2 \cdot 6H_2O$ (5.94 g, 25 mmol).). A 37% aqueous solution of formaldehyde (20.6 g, 0.2 mol) was added and the solution was heated to reflux for 5 hours. The resulting orange solution was filtered to remove insoluble material and reduced to ca. 1/2 its volume on a rotary evaporator. After cooling in a refrigerator overnight the orange crystals that formed were filtered off, washed with cold methanol and diethyl ether and then dried in *vacuo*. (Yield = 7.38 g, 76.9 %), M.W. 383.98 g mol^{-1}, (Found: C, 37.21; H, 6.71; N, 22.77 %. Calculated for $C_{12}H_{26}N_6NiCl_2$: C, 37.54; H, 6.83; N, 21.89 %); λ_{max} = 444 ε = 71 dm^3 mol^{-1} cm^{-1} (H_2O); I.R./cm^{-1} ν(N-H) 3446; ν(C-H) 2891, 2856; ν(C:N) 1624; 1098, 711 (KBr)

1.2.2 Kinetic Measurements

The kinetics of the metal exchange reaction with copper(II) was studied spectrophotometrically using a Perkin Elmer Lambda 5 UV/Visible spectrophotometer. The reaction was monitored at 430 nm which is λ_{max} for the planar nickel complex. Plots of $\ln(A_t-A_\infty)$, where A_t is the absorbance at time t and A_∞ the final absorbance, were linear for several half lives. Rate constants were obtained by least squares regression analysis from absorbance versus time data using a computer. The concentration of the nickel(II) complex employed in the kinetic measurements was normally *ca.* 10^{-2} mol dm^{-3} and the copper(II) was always in at least a ten fold excess so that pseudo first order kinetics were observed.

1.2.3 Equilibrium Measurements

The square planar-octahedral equilibria were measured spectrophotometrically using either a Perkin-Elmer Lambda 5 or a Perkin-Elmer Lambda 14 spectophotometer. Temperature was regulated using a Peltier electronic thermostating system.

1.2.4 Crystal Structure Determinations using X-ray Diffraction

Crystal Structure Determination of (1,3,6,10,12,15-hexaazatricyclo[13.3.1.1^{6,10}]-eicosane)nickel(II) perchlorate

An orange block crystal grown from aqueous solution mounted on a glass fibre was used in the X-ray analysis.

Crystal Data.—— $C_{14}H_{30}N_6NiCl_2O_8$, M = 540.03, orthorhombic, a = 16.432(7), b = 12.225(6), c = 10.727(9)Å, ß = °, U = 2154(3) Å^3 (by least squares refinement on diffractometer angles for 25 carefully centred reflections in the range 31.86 < 2θ < 34.85°), space group Pbca (#61), Z = 4, D_c = 1.59 g cm^{-3}, F(000) = 1080.00. Orange block. Crystal dimensions: 0.35 × 0.25 × 0.20 mm, μ(Mo-K$_\alpha$) = 11.98 cm^{-1}.

Data Collection and Processing.——Rigaku AFC7S diffractometer, ω–2θ mode with ω scan width = 1.26 + 0.35 tan θ, ω scan speed 16.0° min^{-1}, graphite monochromated Mo-K$_\alpha$ radiation; 2194 reflections measured (max. 2θ = 50.1°), 2194 unique, giving 1200 with $I > 2\sigma(I)$. Lorentz-polarization corrections made.

Structure Analysis and Refinement.——Direct methods[47] followed by expansion using Fourier techniques[48]. Non-hydrogen atoms refined anisotropically. Hydrogen ions were included but not refined. Full-matrix least-squares[49] refinement was based

on 1200 observed reflections and 142 variable parameters and converged with unweighted and weighted agreement factors of:

$$R = \sum \| Fo| - |Fc| \| / \sum |Fo| = 0.041$$

$$R_w = \sqrt{\left(\sum \left(|Fo| - |Fc| \right)^2 / \sum wFo^2 \right)} = 0.034$$

The standard deviation[50] of unit weight was 2.16. The weighting scheme was based on counting statistics and included a factor (p = 0.002) to down-weight intense reflections. Plots of $\Sigma w(|Fo|-|Fc|)^2$ versus $|Fo|$, reflection order in data collection, $\sin\theta/\lambda$ and various classes of indices showed no unusual trends. The maximum and minimum peaks on the final difference Fourier map corresponded to 0.51 and –0.39 e^- /Å^3, respectively. Final R and R_w values are 0.041 and 0.034 respectively. All calculations were performed using the teXsan[51] crystallographic software package of Molecular Structure Corporation.

Crystal Structure Determination of (3-ethyl-1,3,5,8,12-pentaazacyclotetradecane)nickel(II) perchlorate

An orange block crystal grown from aqueous solution mounted on a glass fibre was used in the X-ray analysis.

Crystal Data.—— $C_{11}H_{27}N_5NiCl_2O_8$, M = 486.96, monoclinic, a = 13.521(2), b = 9.252(1), c = 9.105(2) Å, ß = 117.226(8)°, U = 1012.8(2) Å^3 (by least squares refinement on diffractometer angles for 25 automatically centred reflections in the range 8.48 < 2θ < 17.67°, λ = 0.71069 Å), space group Cm (#8), Z = 2, D_c = 1.60 g cm^{-3}, F(000) = 508.00. Orange block. Crystal dimensions: 0.40 × 0.25 × 0.15 mm, μ(Mo-K_α) = 12.69 cm^{-1}.

Data Collection and Processing.——Rigaku AFC7S diffractometer, ω–2θ mode with ω scan width = 1.63 + 0.35 tan θ, ω scan speed 16.0° min^{-1}, graphite monochromated Mo-K_α radiation; 1000 reflections measured (max. 2θ = 50.0°), 956 unique [merging R = 0.012 after absorption correction (max.,min. transmission factors = 0.37, 0.10)], giving 878 with $I > 3\sigma(I)$. Lorentz, polarization and absorption corrections made.

Structure Analysis and Refinement.——Direct methods[47] followed by expansion using Fourier techniques[48]. Non-hydrogen atoms refined anisotropically. Hydrogen ions were included but not refined. Full-matrix least-squares[49] refinement was based

on 878 observed reflections and 158 variable parameters and converged with unweighted and weighted agreement factors of:

$$R = \sum \| Fo| - |Fc| \| / \sum |Fo| = 0.041$$

$$R_w = \sqrt{\left(\sum \left(|Fo| - |Fc| \right)^2 / \sum wFo^2 \right)} = 0.034$$

The standard deviation[50] of unit weight was 2.87. The weighting scheme was based on counting statistics. Plots of $\Sigma w(|Fo|-|Fc|)^2$ versus $|Fo|$, reflection order in data collection, sin θ/λ and various classes of indices showed no unusual trends. The maximum and minimum peaks on the final difference Fourier map corresponded to 0.32 and -0.29 $e^-/Å^3$, respectively. Final R and R_w values are 0.031 and 0.027 respectively. The perchlorate anions were initially refined anisotropically, but after finding large anisotropic disorder about the O(3)—Cl(2) axis the model was replaced with one that allowed six positions about the axis for one perchlorate anion rather than three and the model refined isotropically. All calculations were performed using the teXsan[51] crystallographic software package of Molecular Structure Corporation.

1.3. Results and Discussion

1.3.1 Crystal Structure of (3-ethyl-1,3,5,8,12-pentaazacyclotetradecane)-nickel(II) perchlorate

Figure 1.3.1.1 shows an ORTEP view together with the atomic numbering scheme for the complex (3-ethyl-1,3,5,8,12-pentaazacyclotetradecane)nickel(II) perchlorate. Final fractional atomic coordinates are given in Table 1.3.1.1 and selected bond lengths and angles are listed in Table 1.3.1.2. The four secondary amine nitrogen atoms are bound to the nickel ion in an almost regular square planar geometry and they adopt an RSRS configuration. The N—Ni—N bite angles deviate slightly from those expected for ideal square planar geometry; those in six membered rings are expanded to 92.9 (3)° with a bite distance of 2.801 Å and those of five membered rings contracted to 87.0 (1)° with a bite distance of 2.064 Å. The Ni—N bond lengths are 1.959 (5) Å and 1.906 (5) Å and lie in the range expected for such low spin tetra-amine complexes[52]. Both six membered chelate rings adopt a chair configuration and the five membered rings a *gauche* configuration. The ethyl group on the tertiary N(1) is axial.

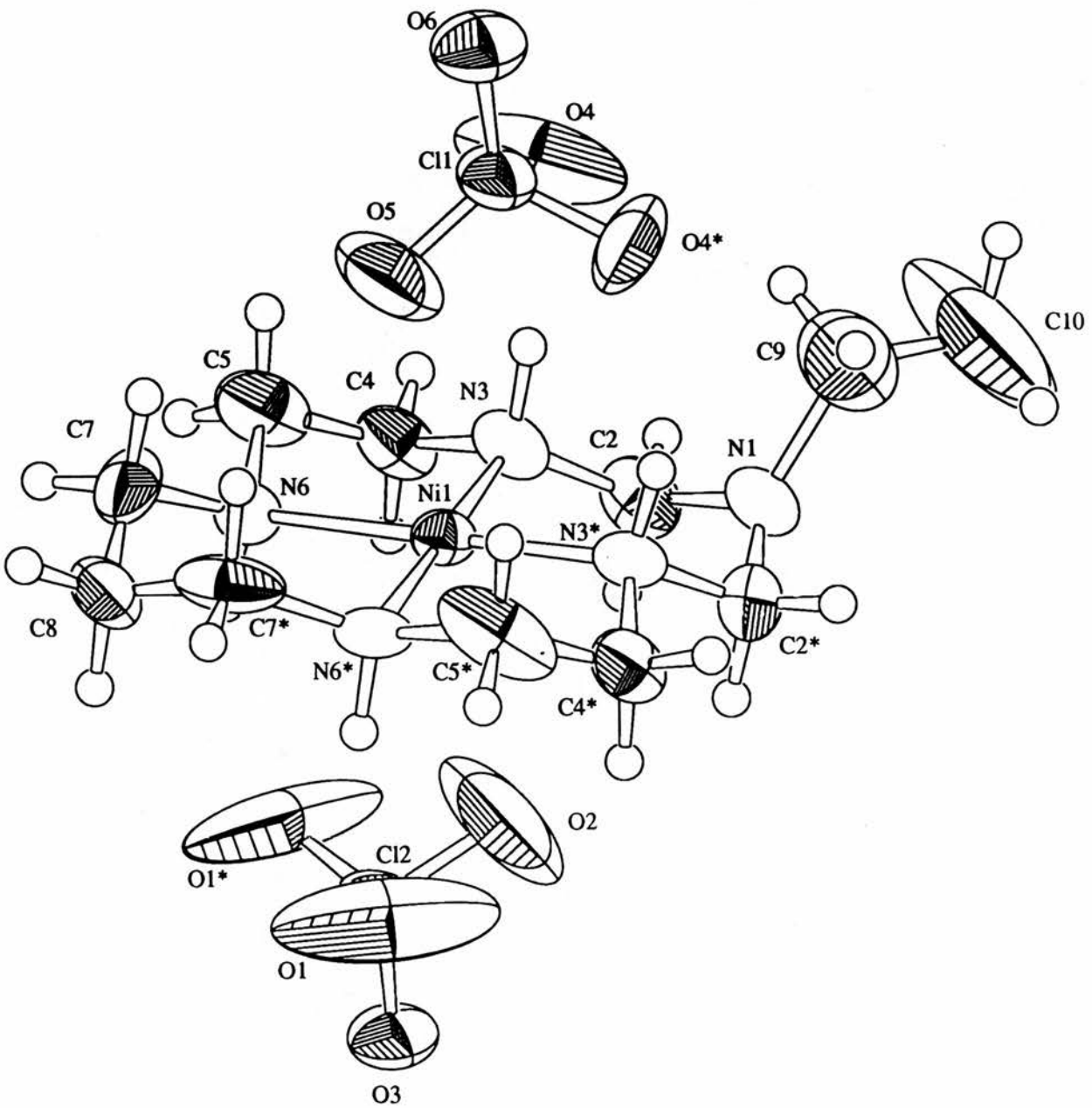

Figure 1.3.1.1. ORTEP view of (3-ethyl-1,3,5,8,12-pentaazacyclotetradecane)-nickel(II) perchlorate with numbering scheme.

Table 1.3.1.1. Fractional atomic coordinates (3-ethyl-1,3,5,8,12-pentaaza-cyclotetradecane)nickel(II) perchlorate.

Atom	x	y	z
Ni(1)	0.2416	0.5	0.3356
N(1)	–0.0013(6)	0.5	–0.003(1)
N(3)	0.1362(4)	0.3465(6)	0.2132(6)
N(6)	0.3436(4)	0.3506(7)	0.4560(6)
C(2)	0.0714(5)	0.3648(8)	0.0416(8)
C(4)	0.2003(5)	0.2170(9)	0.245(1)
C(5)	0.2824(6)	0.2068(8)	0.424(1)
C(7)	0.4260(6)	0.372(1)	0.6427(7)
C(8)	0.4893(8)	0.5	0.677(1)
C(9)	–0.1009(8)	0.5	0.023(2)
C(10)	–0.199(1)	0.570(2)	–0.118(2)

Table 1.3.1.2. Molecular geometry dimensions (lengths in Å, angles in °)

Atoms		Bond length	Atoms		Bond length
Ni(1)	N(3)	1.959(5)	N(6)	C(5)	1.522(9)
Ni(1)	N(6)	1.906(5)	N(6)	C(7)	1.561(7)
N(1)	C(2)	1.526(8)	C(4)	C(5)	1.495(6)
N(1)	C(2)	1.526(8)	C(7)	C(8)	1.41(1)
N(1)	C(9)	1.47(1)	C(9)	C(10)	1.51(2)
N(3)	C(2)	1.409(8)	C(9)	C(10)	1.51(2)
N(3)	C(4)	1.429(9)	C(10)	C(10)	1.29(3)

Atoms			Angle	Atoms			Angle
N(3)	Ni(1)	N(3)	92.9(3)	Ni(1)	N(6)	C(7)	120.2(5)
N(3)	Ni(1)	N(6)	87.0(1)	C(5)	N(6)	C(7)	111.9(6)
N(3)	Ni(1)	N(6)	179.4(3)	N(1)	C(2)	N(3)	113.0(6)
N(6)	Ni(1)	N(6)	93.0(3)	N(3)	C(4)	C(5)	110.8(7)
C(2)	N(1)	C(2)	110.0(7)	N(6)	C(5)	C(4)	102.8(6)
C(2)	N(1)	C(9)	118.9(5)	N(6)	C(7)	C(8)	114.0(6)
Ni(1)	N(3)	C(2)	117.7(5)	C(7)	C(8)	C(7)	114.3(9)
Ni(1)	N(3)	C(4)	106.0(4)	N(1)	C(9)	C(10)	112(1)
C(2)	N(3)	C(4)	109.8(6)	C(10)	C(9)	C(10)	51(1)
Ni(1)	N(6)	C(5)	109.7(4)	C(9)	C(10)	C(10)	64.6(7)

The tertiary amine N(1) appears to exhibit slight sp^2 character in that its geometry differs from that expected for an unstrained trialkylamino group. For comparison the NC_3 group of hexamethylenetetraamine investigated in the X-ray structure of the hexamethylenetetramine-thiourea adduct[53] was taken as a reference system. The mean N(1)—C bond length in the nickel(II) complex is 1.507 ± 0.032 Å, although this is the mean of 1.526 (8) Å and a much shorter bond of 1.47 (1)Å. Hexamethylenetetraamine has C—N bond lengths of 1.47 Å. A greater difference exists when the C—N—C bond angles are considered. The expected value for an sp^3 hybridized nitrogen atom is 109° which is found in the hexamethylenetetraamine system. Significantly, the C—N(1)—C angles have a mean value of 115.93°; two angles of 118.9(5)° and a third of 110(7)°. Such flattening of the NC_3 group has been observed previously in the analogous compound (3-methyl-1,3,5,8,12-pentaazacyclotetradecane)nickel(II) perchlorate[17] and in the sepulchrand complexes of nickel(II)[8], cobalt(II)[7] and cobalt(III)[6]. Sargeson *et al* attributed the flattening of the NC_3 groups in the cobalt(II) sepulchrand complexes, on the basis of molecular modeling calculations, to either steric constraints or the electrostatic attraction between the metal centre and the tertiary nitrogen atom. Fabrizzi *et al* suggest that in the complex (3-methyl-1,3,5,8,12-pentaazacyclotetradecane)nickel(II) perchlorate the flattening of the tertiary N(1) nitrogen is due to long-range M—N electrostatic interactions rather than steric effects since the $N(1)C_3$ group is incorporated into the macrocyclic ring through only two C—N bonds, the third being bound to a methyl group. The C—N—C bond angles and C—N bond lengths for several tertiary amine complexes that demonstrate such a flattening are given in Table 1.3.1.3.

Table 1.3.1.3. Molecular geometry about the distal nitrogen atom of various penta- and hexa-aza macrocycles.

Complex	C—N—C (°)	C—N (Å)	Reference
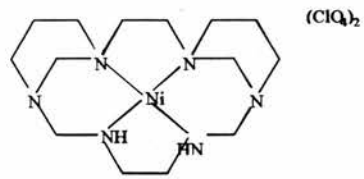	113.67 ± 2.47	1.446 ± 0.022	29
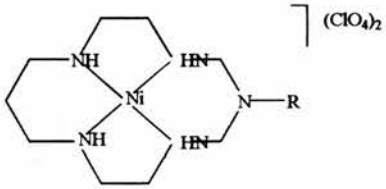			
R = —CH_3	114.97 ± 1.10	1.447 ± 0.014	17
R = —SO_2CH_3	118.93 ± 2.58	1.448	31
R = 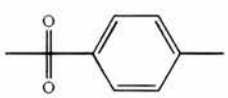	120.00 ± 3.51	1.443 ± 0.002	32
R = —CH_2CH_3	115.93 ± 5.13	1.507 ± .032	This work

All exhibit some flattening of the tertiary amine and contraction of the C—N bond lengths. This phenomena was first observed[54] in $[Fe(trenpy)]^{2+}$ and has been explained

as a long range interaction between the t_{2g} orbitals on the metal atom with the empty π^* orbitals on the uncoordinated tertiary nitrogen[8]. This idea was developed by Abba *et al* [33] who examined the effect of the locking fragment on the metal-tertiary amine distance (or equivalent methylene carbon in the case of $[Ni(cyclam)]^{2+}$). Table 1.3.1.4 shows how this distance varies and how the present system differs.

Table 1.3.1.4. Structural parameters for low-spin Ni(II) complexes of azacyclam macrocycles containing various locking fragments R.

	Distance in Angstroms				
R	$-CH_2-$	$-N(CH_3)-$	$-N(CH_2CH_3)-$	-N(CO)-	$-N(SO_2)-$
Ni^{II}—R	3.35	3.32	3.32	3.25	3.21
Ni^{II}—C	3.35	3.35	3.37	3.34	3.33

The nickel(II) complex of cyclam[55] is used for comparative purposes. Replacing the central $-CH_2-$ groups of one of the trimethylene chains in cyclam with an $-N(CH_3)-$ group contracts the distance by 0.03 Å. The value obtained for the $-N(CH_2CH_3)-$ fragment is 3.32 Å which is identical to the value for (3-methyl-1,3,5,8,12-pentaazacyclotetradecane)nickel(II) perchlorate. These contractions are somewhat smaller than those induced when the locking fragment is an amide (–0.1 Å) or a sulfonamide (–0.14 Å). It is unlikely that the metal-tertiary nitrogen interaction is of the dipolar type since the partial negative charge on the nitrogen group should be

smaller when electron withdrawing groups (amides, sulfonamides) are appended and higher with electron donating groups such as methylene. However, the interaction appears to be greater with the amides and sulfonamides and smaller with the methylene group.

Abba *et al*[33] therefore suggest that a completely different interaction is responsible. A filled metal *d* orbital can superimpose upon an empty π* molecular orbital of the locking fragment and back donate electron density. Such back donation should be enhanced if an electron withdrawing group is attached to the tertiary nitrogen and that appears to be observed. The methyl and ethyl amine do not present, or present to a lesser extent, an empty π* orbital and therefore there is very little contraction of the Ni—N(1) distance.

The Ni—C(8) distance (to the carbon atom opposite the locking fragment) is listed for comparison purposes. This value varies by *ca.* 0.02 Å across the range of samples, a similar variation to that found when comparing the amine padlock macrocycles with $[Ni(cyclam)]^{2+}$.

Another interesting observation was made when refining the crystal structure. The perchlorate anions were initially refined anisotropically and the overall final R value was 0.035. This gave bond angles about N(1) of 117.9° (C(9)—N(1)—C(2)(*)) and 116.5°(C(2)*—N(1)—C(2)) with bond lengths of N(1)—C(2) = 1.47Å and N(1)—C(9) = 1.54 Å. Further refinement, in particular allowing a greater degree of disorder in one perchlorate anion by modeling the anion with seven oxygen positions, although with a total occupancy of four, altered the structural configuration of the macrocycle considerably. In particular the C—N(1) bond angles and C—N(1) bond lengths were

altered. Obviously the nature of the crystal packing will affect the structural configuration of the macrocyclic complex. This aspect should not be overlooked when interpreting the structures of these complexes.

1.3.2 Crystal Structure of [(1,3,6,10,12,15-hexaazatricyclo[13.3.1.1^{6,10}]-eicosane)nickel] perchlorate

The reaction in refluxing methanol of formaldehyde and the nickel(II) complexes of both the unsymmetrical triamine N-(2-aminoethyl)-1,3-diaminopropane and the symmetrical triamine diethylenetriamine gives good yields of the planar nickel(II) complexes of the tricyclic ligands [(1,3,6,10,12,15-hexaazatricyclo[13.3.1.1^{6,10}]-eicosane)nickel]$^{2+}$ (HATCEI) and [(1,3,6,9,11,14-hexaazatricyclo[12.2.1.1^{6,9}]-octadecane)nickel]$^{2+}$ (HATCOD) shown in Figure 1.3.2.1. The perchlorate salts were readily isolated and form orange block crystals upon recrystallisation from aqueous solution.

An ORTEP view of the [Ni(HATCEI)]$^{2+}$ cation together with the atomic numbering scheme is shown in Figure 1.3.2.2. Final fractional atomic coordinates are given in Table 1.3.2.1 and selected bond lengths and angles are shown in Table 1.3.2.2. The nickel ion is coordinated to the two tertiary and two secondary nitrogen atoms of the diazacyclam ring with square planar geometry. The centrosymmetric structure has Ni-N bond lengths of 1.969 (4) and 1.936 (3) Å. The basic diazacyclam ring system has the *trans* III configuration with the two additional six membered rings fused in chair

conformations[56]. The N—C—C—N torsion angle in the ethylenediamine moiety is 55.1 (5)°. The bite angle in the five membered chelate ring is 87.2 (2)° and the bite distance is 2.6931 Å. In the six membered chelate ring the bite angle is 92.8 (2) and the bite angle is 2.828 Å. These values are in the range commonly found in nickel(II) complexes of macrocycles.

Figure 1.3.2.1. [(1,3,6,9,11,14-hexaazatricyclo[12.2.1.$1^{6,9}$]octadecane)nickel]$^{2+}$

(HATCOD)

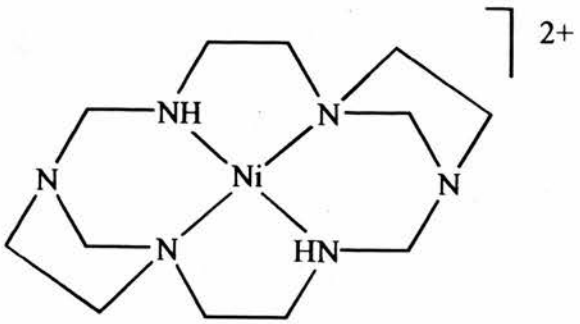

[(1,3,6,10,12,15-hexaazatricyclo[13.3.1.$1^{6,10}$]eicosane)nickel]$^{2+}$ (HATCEI)

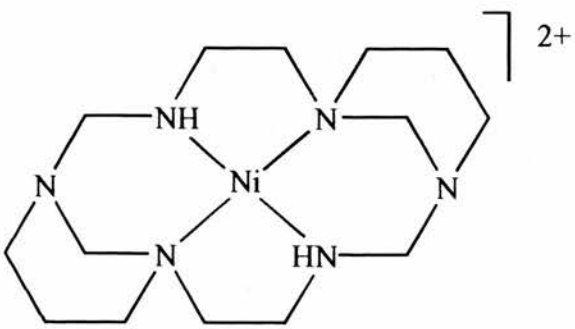

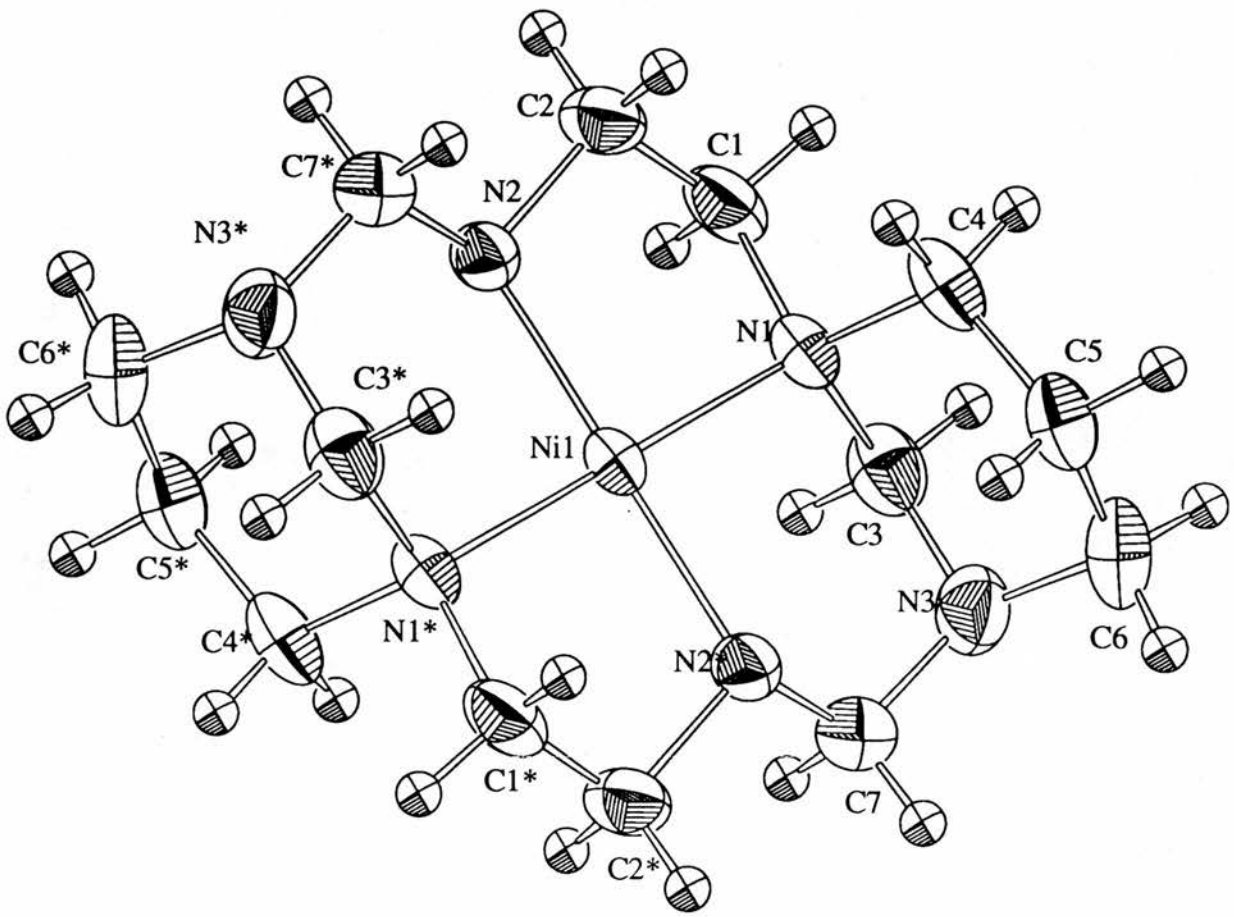

Figure 1.3.2.2. ORTEP view of [(1,3,6,10,12,15-hexaazatricyclo[13.3.1.$1^{6,10}$]-eicosane)nickel(II)] perchlorate with numbering scheme.

Table 1.3.2.1. Fractional atomic coordinates for (1,3,6,10,12,15-hexaazatricyclo[13.3.1.1^{6,10}]eicosane)nickel(II) perchlorate.

Atom	x	y	z
Ni(1)	1.0000	0	0.5
Cl(1)	0.88739(8)	0.3060(1)	0.5388(1)
O(1)	0.8757(3)	0.4040(4)	0.4746(5)
O(2)	0.9365(3)	0.3291(4)	0.6438(5)
O(3)	0.8120(2)	0.2668(4)	0.5812(5)
O(4)	0.9297(2)	0.2254(3)	0.4660(4)
N(1)	0.8947(2)	-0.0764(3)	0.5092(4)
N(2)	1.0033(3)	-0.0080(3)	0.6802(3)
N(3)	0.8890(3)	-0.1315(3)	0.2907(4)
C(1)	0.8908(3)	-0.1229(4)	0.6384(5)
C(2)	0.9212(3)	-0.0385(4)	0.7263(5)
C(3)	0.8890(3)	-0.1683(4)	0.4161(5)
C(4)	0.8210(3)	-0.0038(4)	0.4893(5)
C(5)	0.8087(3)	0.0313(4)	0.3551(5)
C(6)	0.8169(3)	-0.0632(4)	0.2641(6)
C(7)	0.9669(3)	-0.0899(4)	0.2491(5)

Table 1.3.1.2. Molecular geometry dimensions (lengths in Å, angles in °)

Atoms		Bond Length	Atoms		Bond Length
Ni(1)	N(1)	1.969(4)	N(3)	C(3)	1.419(6)
Ni(1)	N(2)	1.936(3)	N(3)	C(6)	1.476(6)
N(1)	C(1)	1.500(6)	N(3)	C(7)	1.449(6)
N(1)	C(3)	1.506(6)	C(1)	C(2)	1.485(7)
N(1)	C(4)	1.516(6)	C(4)	C(5)	1.516(7)
N(2)	C(2)	1.484(6)	C(5)	C(6)	1.519(7)
N(2)	C(7)	1.499(6)			

Atoms			Angle	Atoms			Angle
N(1)	Ni(1)	N(1)	180.00	C(2)	N(2)	C(7)	109.2(4)
N(1)	Ni(1)	N(2)	87.2(2)	C(3)	N(3)	C(6)	111.3(4)
N(1)	Ni(1)	N(2)	92.8(2)	C(3)	N(3)	C(7)	113.7(4)
N(2)	Ni(1)	N(2)	180.00	C(6)	N(3)	C(7)	116.9(4)
Ni(1)	N(1)	C(1)	105.3(3)	N(1)	C(1)	C(2)	108.0(4)
Ni(1)	N(1)	C(3)	112.0(3)	N(2)	C(2)	C(1)	105.6(4)
Ni(1)	N(1)	C(4)	114.7(3)	N(1)	C(3)	N(3)	113.1(4)
C(1)	N(1)	C(3)	109.1(4)	N(1)	C(4)	C(5)	114.0(4)
C(1)	N(1)	C(4)	108.6(4)	C(4)	C(5)	C(6)	112.5(5)
C(3)	N(1)	C(4)	107.1(4)	N(3)	C(6)	C(5)	112.2(4)
Ni(1)	N(2)	C(2)	108.7(3)	N(2)	C(7)	N(3)	114.4(4)
Ni(1)	N(2)	C(7)	118.3(3)				

The average C—N bond length for the uncoordinated tertiary nitrogen N(3) is 1.448 ± 0.028 Å whereas for the coordinated tertiary nitrogen N(1) the value is 1.507 ± 0.007 Å. The Ni—N bond length of the secondary nitrogen N(2) at [1.936 (3) Å] is 0.033 Å shorter than that of the tertiary nitrogen N(1) [1.969 (4) Å]. The difference of *ca.* 8σ shows that the Ni—N bond distances to the secondary nitrogens are significantly longer than those involving tertiary nitrogens. This is perhaps to be expected since previous studies have shown that N-methylation of the secondary nitrogen donors of macrocyclic complexes results in a decrease in ligand field strength and therefore an increase in Ni—N bond lengths in N-methylated complexes when compared to their non-methylated analogues[57,58,59,60]. These observations were all made for complexes in which the coordinated nitrogens were either all secondary or all tertiary. For complexes with a mixture of secondary and tertiary donors there does not appear to be a consistent trend in the Ni—N bond distances. However, this study confirms the studies of Suh *et al*[31], and Freeman *et al*[61] which show that Ni—N tertiary bonds are significantly longer than secondary Ni—N bonds within the same complex.

The axial sites on the nickel ion are not sterically hindered and are accessible to additional ligands so that square planar-octahedral equilibria are observed in complexes of this type.

1.3.3 Kinetics of Metal Exchange

1.3.3.1 (1,3,6,10,12,15-hexaazatricyclo[13.3.1.1^{6,10}]-eicosane)nickel(II) perchlorate

Heating $[Ni(HATCEI)]^{2+}$ with Cu^{2+} in aqueous solution leads to rapid metal exchange and the formation of the blue-violet $[Cu(HATCEI)]^{2+}$ cation with λ_{max} = 606 nm. The kinetics of the reaction were studied using an excess of copper(II) ion (at least a ten fold excess) so that first order kinetics were observed. The reaction was monitored by following the decay of the planar nickel band at 464 nm and verified by monitoring the growth of the band due to the copper complex. The first order rate constants (k_{obs}) obtained at the two wavelengths were in excellent agreement and were averaged. Table 1.3.3.1 lists the rate constants obtained at various copper(II) concentrations at 40°C, 50°C and 60°C.

Table 1.3.3.1 Rate constants (k_{obs}) obtained for the metal exchange reaction, $[Ni(HATCEI)]^{2+} \longrightarrow [Cu(HATCEI)]^{2+}$

	k_{obs} at:		
$[Cu^{2+}]$	40°C	50°C	60°C
0.005	1.25×10^{-5}	3.63×10^{-5}	1.04×10^{-4}
0.02	1.65×10^{-5}	5.35×10^{-5}	1.65×10^{-4}
0.04	1.53×10^{-5}	6.12×10^{-5}	1.90×10^{-4}
0.05	1.85×10^{-5}	6.48×10^{-5}	1.70×10^{-4}
0.1	1.86×10^{-5}	8.96×10^{-5}	1.87×10^{-4}
0.2	3.28×10^{-5}	1.60×10^{-4}	3.25×10^{-4}

The reaction *appears* to show some dependence upon the copper(II) concentration. However, it proved difficult to maintain constant ionic strength during the reaction as the addition of an inert electrolyte led to the formation of precipitates. If allowances are made for ionic strength effects the reaction is found to be essentially independent of copper(II) concentration. The limited rate increase at high copper(II) concentrations can be accounted for in terms of a positive salt effect arising from the reaction of two cationic species. In a reaction where the two reactants have charges of the same sign the activated complex will be more highly charged than the reactants. Therefore increasing the ionic strength of the solution will favour interaction between the activated complex and the adjacent ions relative to the interaction between the

reactants and the ionic atmosphere thus increasing the rate constant for the reaction. The Brønsted-Bjerrum equation $\log k = \log k_0 + Az_Az_B\sqrt{I}$ predicts that a plot of log k *versus* $\sqrt{I}$ will be linear where A is a constant (1.018 in water at 25°C) and z_Az_B is the product of the charges on the reacting species A and B. This is found to be the case for this transmetalation reaction (Figure 1.3.3.1) with Az_Az_B equal to 0.476 ± 0.090, 0.770 ± 0.042 and 0.517 ± 0.107 at 40, 50 and 60°C respectively. These values are lower than would be expected for a reaction involving two dications.

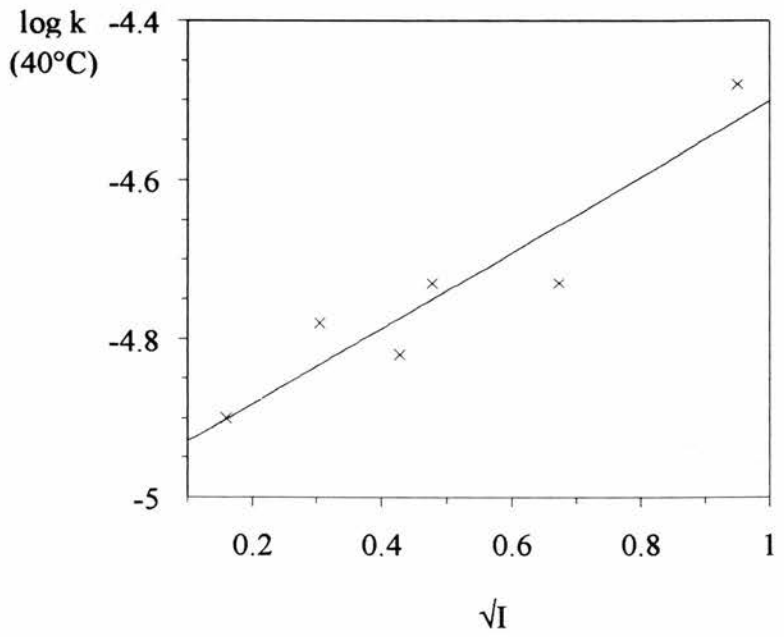

Figure 1.3.3.1. Brønsted-Bjerrum plot of log k_{obs} versus $\sqrt{I}$

As the reaction does not show a dependence on the copper(II) concentration, it appears that the copper(II) acts purely as a scavenger for the ligand produced in the dissociation step. The results can be accounted for by the reaction scheme;

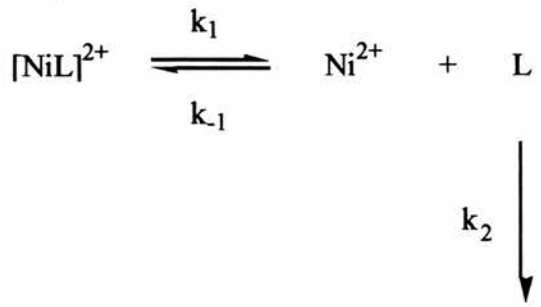

Scheme 1.3.3.1.

Macrocyclic nickel(II) complexes have quite high formation constants ($K = k_{-1}/k_1$) which results from the slow dissociation rate of the macrocyclic complex (k_{-1}). The reaction of copper(II) with L (k_2) is fast and not rate determining. The first order rate constant obtained experimentally is effectively the dissociation rate of the nickel(II) macrocyclic complex. This suggestion can be confirmed by using an excess of a "scavenger" ligand to complex the nickel(II) ion as it dissociates from the macrocyclic ligand. Ethylenediaminetetraacetic acid (EDTA) can be used as such a scavenger as it rapidly forms stable complexes with nickel(II). Measuring the rate of formation of Ni(EDTA) in an aqueous solution of $[Ni(HATCEI)]^{2+}$ and EDTA should give a rate similar to that for the dissociation of Ni(II) from the macrocycle. Using this method and monitoring the increase in absorbance of the Ni(EDTA) bands at 382 and 597 nm, a rate constant of $(1.1 \pm 0.07) \times 10^{-5}$ s^{-1} was obtained at 40°C for the dissociation of

nickel(II) from $[Ni(HATCEI)]^{2+}$. This constant is very close to those found for the transmetallation reaction and suggests that the rate determining step for the transmetallation reaction is indeed the dissociation of the nickel(II) ion from the macrocycle.

1.3.3.2 (1,3,6,9,11,14-hexaazatricyclo[12.2.1.1^{6,9}]octadecane)nickel(II) chloride

Heating $[Ni(HATCOD)]^{2+}$ with Cu^{2+} in aqueous solution gives $[Cu(HATCOD)]^{2+}$ with λ_{max} = 624 nm. The kinetics of the exchange reaction were monitored by observing the growth of this band and also the decay of the planar nickel band at 444 nm. With an excess (at least ten fold) of copper(II) identical pseudo first order kinetics were observed at both wavelengths. The rate constants at the two wavelengths were averaged and are given in Table 1.3.3.2.

Table 1.3.3.2. Rate constants (k_{obs}) obtained for the metal exchange reaction, $[Ni(HATCOD)]^{2+} \longrightarrow [Cu(HATCOD)]^{2+}$

	k_{obs} at:		
$[Cu^{2+}]$	40°C	50°C	60°C
0.005	2.82×10^{-6}	1.21×10^{-5}	4.68×10^{-5}
0.02	4.41×10^{-6}	2.40×10^{-5}	8.62×10^{-5}
0.04	6.43×10^{-6}	3.50×10^{-5}	1.38×10^{-4}
0.05	7.67×10^{-6}	3.64×10^{-5}	1.33×10^{-4}
0.1	1.33×10^{-5}	6.87×10^{-5}	2.64×10^{-4}
0.2	3.38×10^{-5}	1.20×10^{-4}	5.92×10^{-4}

As for the transmetallation reactions of $[Ni(HATCEI)]^{2+}$, maintaining constant ionic strength proved difficult because of the formation of precipitates upon the addition of inert electrolytes. Although the rates for the transmetallation are slower for this complex than for the $[Ni(HATCEI)]^{2+}$ there appears to be a better correlation with ionic strength. Whether this can be assigned solely to a positive primary salt effect or whether there is a dependence upon copper(II) concentration unrelated to ionic strength can be determined by using the Brønsted-Bjerrum equation. Figure 1.3.3.2 shows a Brønsted-Bjerrum plot for the transmetallation reactions at 40°C, 50°C and 60°C.

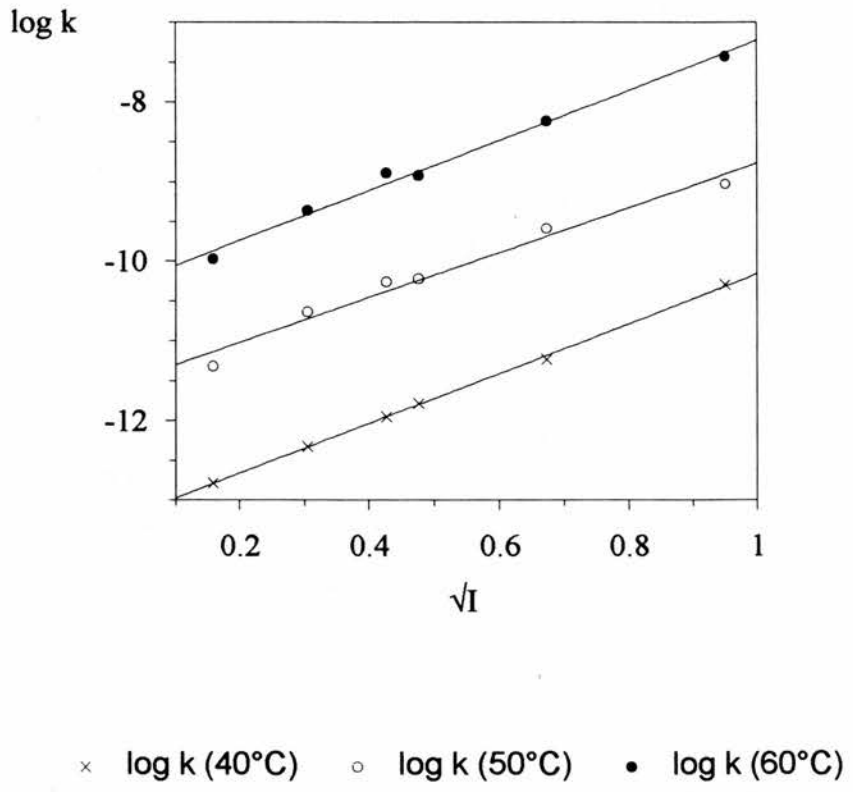

Figure 1.3.3.2. Brønsted-Bjerrum plot of log k_{obs} versus I, the ionic strength.

From the gradient of the lines values of Az_Az_B are determined to be 3.126 ± 0.045, 2.815 ± 0.227 and 3.136 ± 0.152 at 40, 50 and 60°C respectively. If the value of A is taken as ≈ 1.02 and the reactive species as dications the value of Az_Az_B should be *ca.* 4.08. The values obtained are closer to the theoretical values than was the case for $[Ni(HATCEI)]^{2+}$.

1.3.4 Square Planar-Octahedral Equilibria

An investigation of the spin interconversion equilibria of $[NiL]^{2+}$ complexes was used to investigate the chemistry of the apical N(1) amine. Planar nickel(II) complexes can exist in aqueous solution as an equilibrium mixture of two forms; the high spin octahedral form and the low spin square planar form. In the octahedral form the two axial coordination sites are occupied by water molecules. The equilibrium can be represented;

$$[NiL]^{2+} + 2H_2O \rightleftharpoons [NiL(OH_2)_2]^{2+}$$

The octahedral to square planar conversion involves the loss of two water molecules and is also an endothermic process. The equilibrium can therefore be studied by measuring the concentrations of the two forms as a function of the temperature. Higher temperatures displace the equilibrium to the left and increase the concentration of the square planar complex.

This equilibrium can be monitored by observing the band in the visible spectrum due to the square planar complex, which for $[Ni(HATCOD)]^{2+}$ has λ_{max} = 465 nm. In the non-complexing solvent nitromethane, where it is expected that the complex is 100% planar, the $[Ni(HATCOD)]^{2+}$ complex has λ_{max} = 465 nm and a molar extinction coefficient of 58 mol dm^{-3} cm^{-1}. The octahedral complex has an extinction coefficient of ~ 5 mol dm^{-3} cm^{-1} at 465 nm. Assuming the square planar complex to have the

same extinction coefficient in aqueous solution[62] the equilibrium constant at a particular temperature can be calculated from the relationship;

$$K = (\varepsilon_{lowspin} - \varepsilon_{obs}) / (\varepsilon_{obs} - \varepsilon_{highspin})$$

The equilibrium constants obtained over a temperature range for the square planar-octahedral equilibrium of $[Ni(HATCOD)]^{2+}$ are given in Table 1.3.4.1.

Table 1.3.4.1. Spin equilibria for the square planar-octahedral equilibrium of $[Ni(HATCOD)]^{2+}$. $[NiL] = 7.5 \times 10^{-3}$ mol dm^{-3}.

T (K)	10^3 1/T (K^{-1})	Abs. at 448 nm	ε_{obs}	K
298.3	3.352	0.363	48.40	0.221
303.3	3.297	0.365	48.67	0.214
308.2	3.245	0.367	48.93	0.206
313.3	3.192	0.371	49.47	0.192
318.2	3.143	0.373	49.73	0.185
323.2	3.094	0.376	50.13	0.174
328.3	3.046	0.378	50.40	0.167
333.3	3.000	0.380	50.67	0.161

A plot of ln K *versus* 1/T, Figure 1.3.4.1, gives $\Delta H° = -7.86 \pm 0.23$ kJ mol^{-1} and $\Delta S°_{298} = -38.78 \pm 0.73$ J K^{-1} mol^{-1}.

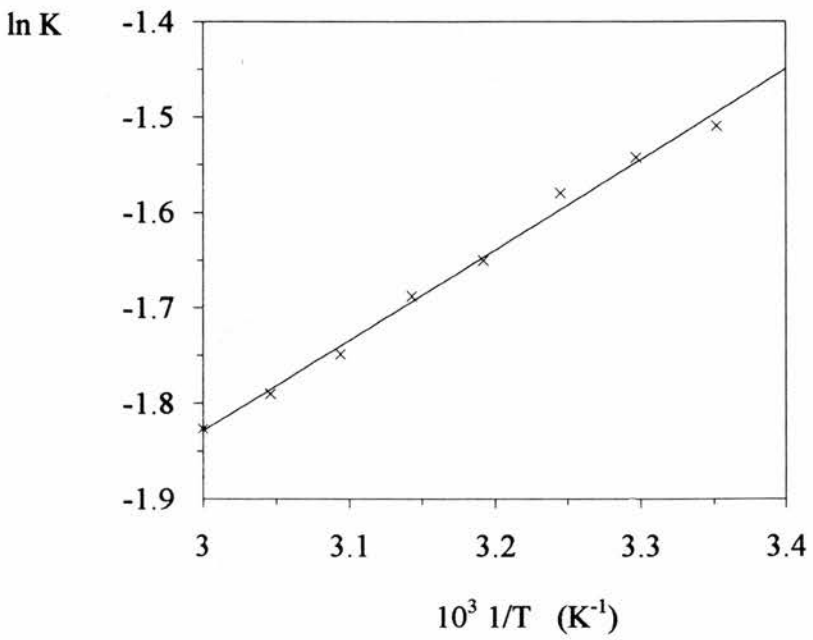

Figure 1.3.4.1. Plot of ln K *versus* 1/T for the spin equilibria of $[Ni(HATCOD)]^{2+}$ in aqueous solution. $[Ni(L)] = 7.5 \times 10^{-3}$ mol dm^{-3}.

The high spin-low spin equilibria for the nickel(II) complex of 3-ethyl-1,3,5,8,12-pentaazacyclotetradecane $[Ni(L_{Et})]^{2+}$ have also been studied. The concentration of the square planar complex increases with temperature as expected, Figure 1.3.4.2. The λ_{max} for the square planar complex is 448 nm and in nitromethane ε_{planar} ($\varepsilon_{low\ spin}$)

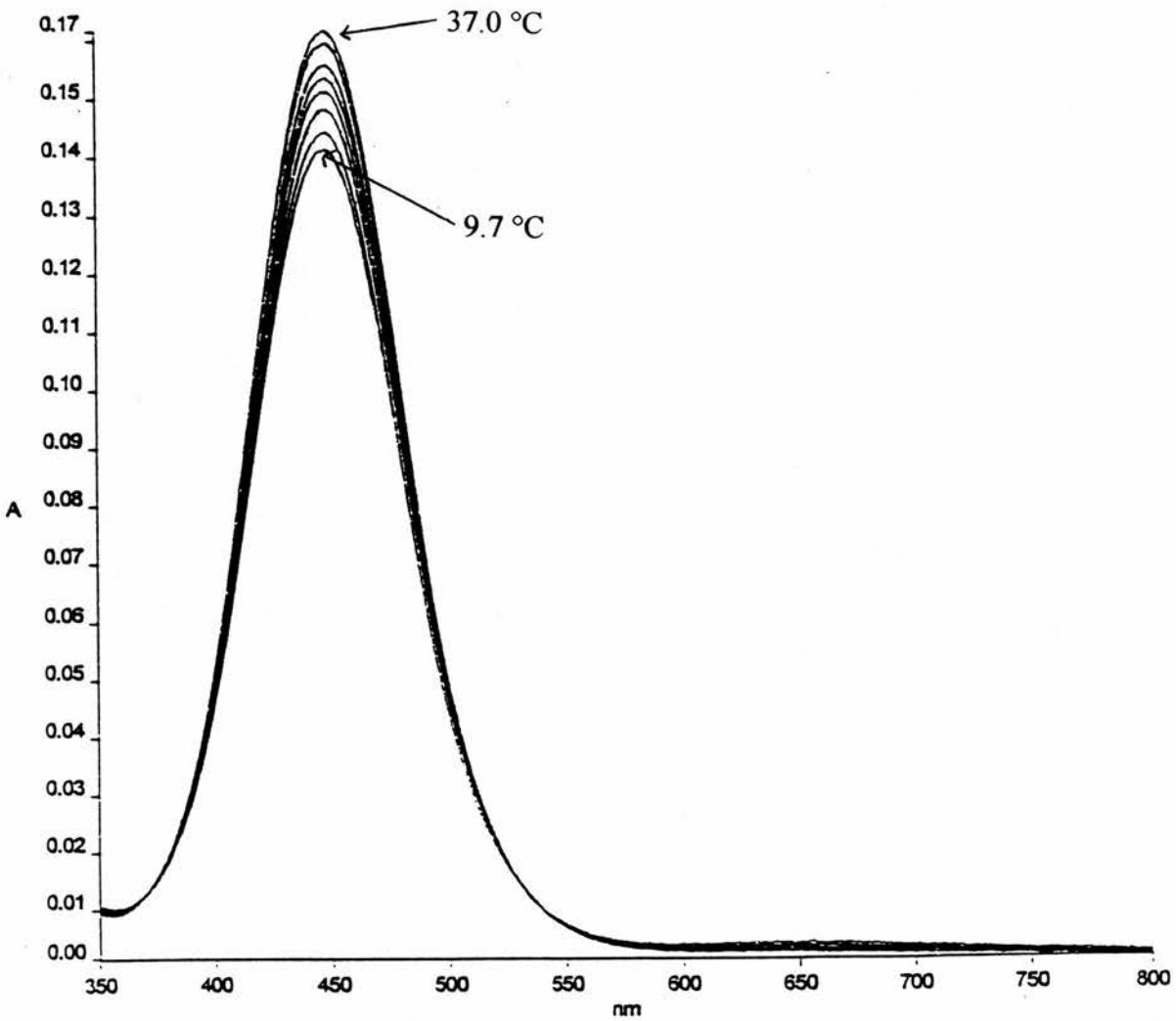

Figure 1.3.4.2. Increase in the intensity of the square planar band of $[Ni(L_{Et})]^{2+}$ with temperature. T = 9.7, 12.9, 16.9, 20.9, 23.7, 27.1, 33.2 and 37.0 °C.

$[Ni(L_{Et})]^{2+} = 3 \times 10^{-3}$ mol dm^{-3}.

has a value of 62.6 dm^3 mol^{-1} cm^{-1} at this wavelength. $\varepsilon_{octahedral}$ ($\varepsilon_{high\ spin}$) has a value ~ 6.0 dm^3 mol^{-1} cm^{-1} at this wavelength[63]. Therefore, for the equilibrium,

$$K = (\varepsilon_{lowspin} - \varepsilon_{obs}) / (\varepsilon_{obs} - \varepsilon_{highspin})$$

values of K are given in Table 1.3.4.2.

A plot of ln K *versus* 1/T, Figure 1.3.4.3, gives $\Delta H° = -19.19 \pm 0.46$ kJ mol^{-1} and $\Delta S°_{298} = -76.36 \pm 1.53$ J K^{-1} mol^{-1}.

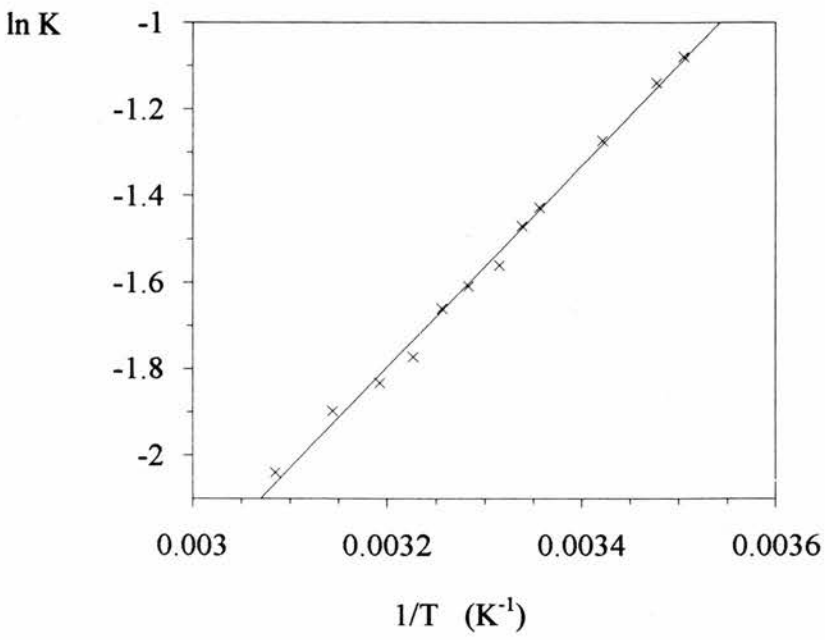

Figure 1.3.4.3. Plot of ln K *versus* 1/T for the spin equilibria of $[Ni(L_{Et})]^{2+}$ in aqueous solution. [Ni(L)] = 3.0×10^{-3} mol dm^{-3}.

Table 1.3.4.2. Spin equilibria for the square planar-octahedral equilibrium of $[NiL_{Et}]^{2+}$. $[Ni(L)] = 3 \times 10^{-3}$ mol dm^{-3}.

T (K)	10^3 1/T (K^{-1})	Abs. at 448 nm	ε_{obs}	K
285.3	3.505	0.1446	48.2	0.34
287.6	3.477	0.1468	48.9	0.32
292.3	3.421	0.1509	50.3	0.28
298.0	3.356	0.1550	51.8	0.24
299.6	3.338	0.1566	52.2	0.23
301.7	3.315	0.1581	52.7	0.21
304.6	3.283	0.1597	53.2	0.20
307.1	3.256	0.1611	53.7	0.19
309.9	3.227	0.1626	54.2	0.17
313.2	3.193	0.1642	54.7	0.16
318.1	3.144	0.1662	55.4	0.15
324.1	3.085	0.1682	56.1	0.13

1.3.5 Square Planar-Octahedral Equilibria in Acidic Solution

The square planar-octahedral equilibrium in the presence of varying concentrations of HCl was also studied. The electronic spectrum of aqueous solutions of $[Ni(L_{Et})]^{2+}$ complexes was measured in the presence of various concentrations of HCl. The concentration of the square planar complex was estimated from the absorbance at 448 nm assuming that the molar absorption coefficients in nitromethane (where the complex should be entirely square planar) were identical with those of the square planar complexes[64]. Figure 1.3.5.1 shows that as the concentration of HCl is increased the absorption, and hence the concentration, of the square planar species decreases. High concentrations of HCl favour the formation of the octahedral high-spin complex, whereas low concentrations of HCl favour the low-spin planar complex. This behaviour contrasts with that found for $[Ni(cyclam)]^{2+}$ for which the addition of HCl increases the concentration of the planar species[65].

This behaviour could be due to the protonation of the tertiary amino nitrogen[17]. The resulting trialkylammonium group could then interact by hydrogen bonding with a chloride anion in such a way so as to force it to bind axially to the nickel(II) cation, thus stabilising the high spin octahedral species, Figure 1.3.5.2.

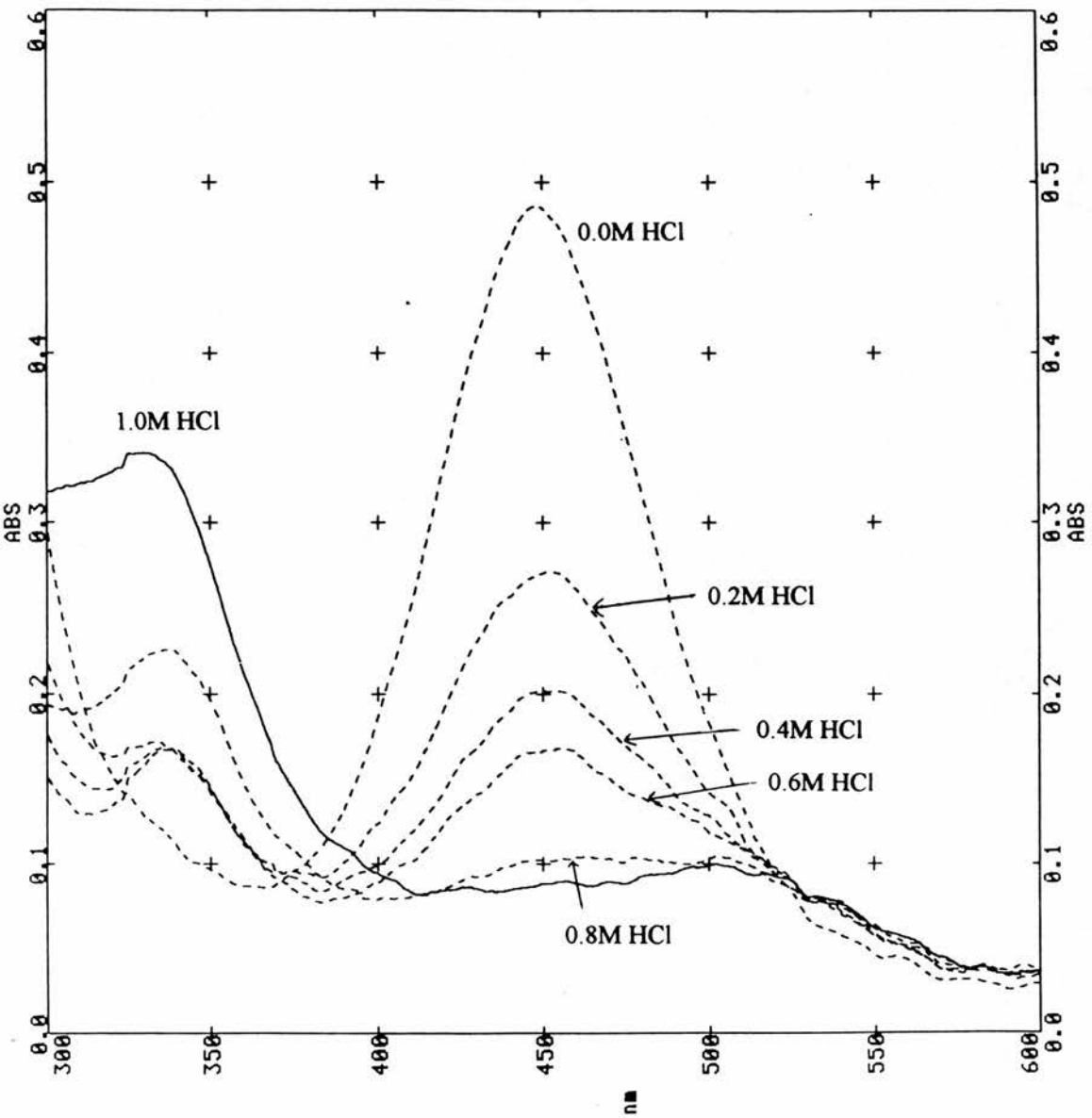

Figure 1.3.5.1. Square planar absorption of $[Ni(HATCOD)]^{2+}$ with varying concentrations of HCl. T = 25°C. [Ni(HATCOD)] = 0.01 mol dm^{-3}.

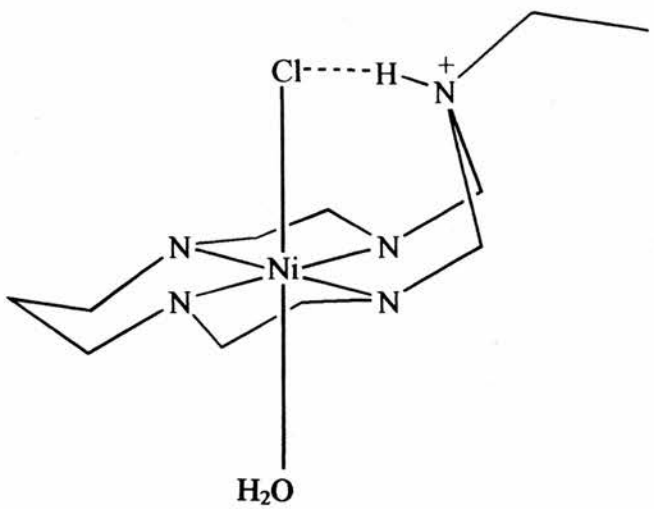

Figure 1.3.5.2. Suggested arrangement of octahedral $[Ni(L_{Et})]$ in aqueous solutions of HCl (> 1.0 mol dm^{-3}).

Such a species would require a rearrangement of the six membered chelate ring containing the ammonium group so that the ammonium proton would be in the correct orientation for interaction with the chloride anion. This rearrangement from the chair conformation in the solid state to a twist-boat conformation can be easily achieved by the $[Ni(L_{Et})]^{2+}$ complex. However, for other macrocyclic complexes such rearrangements may be more difficult. At a given concentration of acid the proportion of the square planar species depends upon the macrocyclic structure. Table 1.3.5.1 shows how the proportion of square planar to octahedral species varies with acid concentration for a series of nickel(II) macrocyclic complexes previously studied[17]. Values for $[Ni(L_{Et})]^{2+}$ are plotted in Figure 1.3.5.3.

Table 1.3.5.1. Percentage of the square planar species at 25°C for $[Ni(L)]^{2+}$ in aqueous hydrochloric acid solutions at 25°C.

[HCl] (mol dm^{-3})	Percentage of the square planar species at 25°C for complex; Ni(A)	Ni(HATCOD)	Ni(HATCEI)	$Ni(L_{Me})$	$Ni(L_{Et})$
0	70	96	63		71.4
0.1	37	94		28	*
0.5	11	66	19	9	*
1.0	6	29	6	4	7.5
2.0	5	8	< 3	< 3	

* See Figure 1.3.5.3.

The proportion of the square planar species at any given HCl concentration decreases in the order Ni(HATCOD) > $Ni(L_{Et})$ ≥ Ni(A) ≥ Ni(HATCEI) > $Ni(L_{Me})$. It is expected that the formation of the octahedral species should be affected by the Ni—N bond distance and the flexibility of the macrocyclic ligand. The Ni—N bond distance is longer in the octahedral complex and so its formation should be favoured by square planar species with longer Ni—N bond lengths. The complex Ni(HATCOD) is relatively inflexible and also has the shortest Ni—N bond length and this is reflected in its preference for square planar geometry.

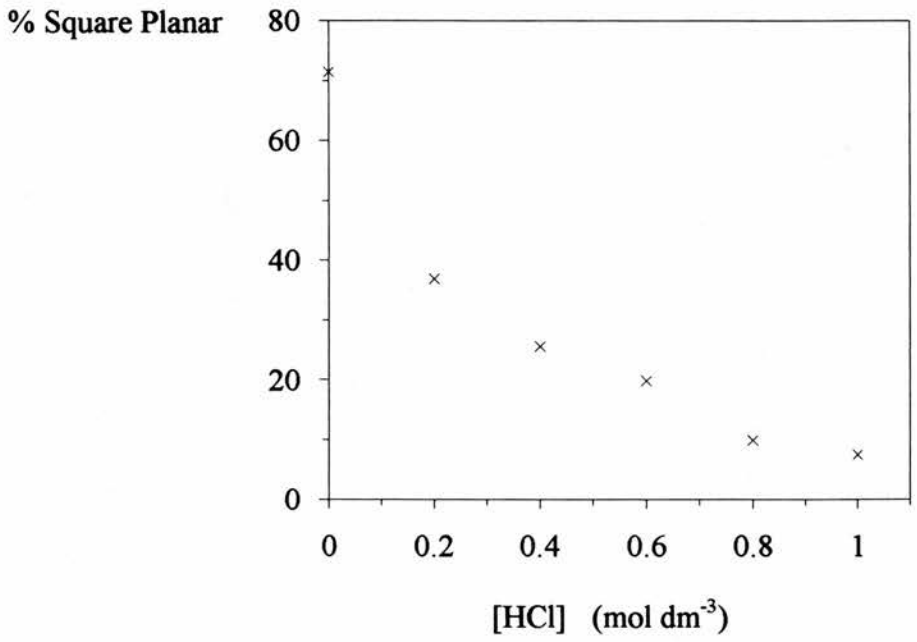

Figure 1.3.5.3. Percentage of the square planar species at 25°C for $[Ni(L_{Et})]^{2+}$ in aqueous hydrochloric acid solutions at 25°C.

1 F.G. Riddell and P. Murrray-Rust, *J. Chem. Soc., Chem. Commun.*, 1970, 1075

2 V.L. Goedken and S-M. Peng, *J. Chem. Soc., Chem. Commun.*, 1973, 62

3 N.W. Alcock and P.A. Tasker, *J. Chem. Soc., Chem. Commun.*, 1972, 1239

4 U. Thewalt and J. Weiss, *Zeitschrift Anorg. Chemie*, 1966, **348,** 238

5 U. Thewalt and C.E. Bugg, *Chemische Berichte*, 1972, **105,** 1614

6 I.I. Creaser, J.MacB. Harrowfield, A.J. Hertl, A.M. Sargeson, J. Springborg, R.J.Geue and M.R. Snow, *J. Am. Chem. Soc.*, 1977, **99,** 3181

7 I.I. Creaser, R.J.Geue, J.MacB. Harrowfield, A.J. Hertl, A.M. Sargeson, M.R. Snow and J. Springborg, *J. Am. Chem. Soc.*, 1982, **104,** 6016

8 M-P. Suh, W. Shin, D. Kim and S. Kim, *Inorg. Chem.*, 1984, **23,** 618

9 M-P. Suh and S-G. Kang, *Inorg. Chem.*, 1988, **27,** 2544

10 M-P. Suh, W. Shin, H. Kim and C.H. Koo, *Inorg. Chem.*, 1987, **26,** 1846

11 O. Barton and W.D. Ollis, *in Comprehensive Organic Chemistry*, 1979, **2,** 83

12 M-P. Suh and D.Kim, *Inorg. Chem.*, 1985, **24,** 3712

13 M. Shakir, A.K. Mohamed, S.P. Varkey, O.S.M. Nasman and Z.A. Siddiqi, *Polyhedron*, 1995, **14,** 1277

14 R.W. Hay, J.M. Armstrong and M.M. Hassan, *Trans. Met. Chem.*, 1992, **17,** 270

15 L. Ballester, M.C. Barral, A. Gutierrez, A. Monge, M.F. Perpinan, C. Ruiz-Valero, A.E. Sanchez-Pellaez, *Inorg. Chem.*, 1994, **33**, 2142

16 M-P. Suh, B.Y. Shim and T-S. Yoon, *Inorg. Chem.*, 1994, **33,** 5509

17 L. Fabbrizzi, A.M.M. Lanfredi, P. Pallavicini, A. Perotti, A. Taglietti and F. Ugozzoli, *J. Chem. Soc., Dalton Trans.*, 1991, 3263

18 T.V. Snopok, I.M. Maloshtan, B.A. Snopok, A.P. Filippov and Y.D. Lampeka, *Theoretical and Experimental Chemistry*, 1994, **30,** 39

19 Y.D. Lampeka, S.F. Lyuksyutov, B.A. Snopok, E.A. Tikhonov and I.M. Maloshtan, *Theoretical and Experimental Chemistry*, 1993, **29,** 348

20 S.A. Hudson and P.M. Maitlis, *Chem. Rev.*, 1993, **93,** 861

21 I.M. Maloshtan, S.V. Rosokha and Y.D. Lampeka, *Zh. Neorg. Khim*, 1994, **39,** 792

22 S.V. Rosokha and Y.D. Lampeka, *J. Chem. Soc., Chem. Commun.*, 1991, 1077

23 S.V. Rosokha, Y.D. Lampeka and I.M. Maloshtan, *J. Chem. Soc., Dalton Trans.*, 1993, 631

24 Y. Inouye, T. Kanamori, M. Sugiyama, T. Yoshida, T. Koike, M. Shionoya, K. Enomoto, K. Suehiro And E. Kimura, *Antiviral Chemistry and Therapy*, 1995, **6**, 337

25 S-G. Kang, S-K. Jung, J.K. Kweon and M-S. Kim, *Polyhedron*, 1993, **12,** 353

26 M-P. Suh and S-K. Kim, *Inorg. Chem.*, 1993, **32,** 3562

27 K.B. Yatsimirskii and Y.A. Lampeka, in *Physicochemistry of Metal Complexes with Macrocyclic Ligands*, Naukova Dumka, Kiev, 1985

28 G.A. Lawrance, T.M. Manning, B.W. Skelton and A.H. White, *J. Chem. Soc., Chem. Commun.*, 1988, 1344

29 M-P. Suh, J. Choi, S-G. Kang and W. Shin, *Inorg. Chem.*, 1989, **28,** 1763

30 M-P. Suh, S-G. Kang, V.L. Goedken and S-H. Park, *Inorg. Chem.*, 1991, **30,** 365

31 M-P. Suh, W. Shin, S-G. Kang, M.S. Lah and T-M. Chung, *Inorg. Chem.*, 1989, **28,** 1602

32 A. De Blas, G. De Santis, L. Fabbrizzi, M. Licchelli, A.M.M. Lanfredi, P. Morosini, P. Pallavicini and F. Ugozzili, *J. Chem. Soc., Dalton Trans.*, 1993, 1411

33 F. Abba, G. De Santis, L. Fabbrizzi, M. Licchelli, A.M.M. Lanfredi, P. Pallavicini, A. Poggi and F. Ugozzili, *Inorg. Chem.*, 1994, **33,** 1366

34 A. De Blas, G. De Santis, L. Fabbrizzi, M. Licchelli, C. Manano and P. Pallavicini, *Inorg. Chim. Acta,* 1992, **202,** 115

35 H.A. Boucher, G.A. Lawrance, P.A. Lay, A.M. Sargeson, A.M. Bond, D.F. Sangster and J.C. Sullivan, *J. Am. Chem. Soc.*, 1983, **105,** 4652

36 J. MacB. Harrowfield, A.J. Herlt, P.A. Lay. A.M. Sargeson, A.M. Bond, W.A. Mulac and J.C. Sullivan, *J. Am. Chem. Soc.*, 1983, **105,** 5503

37 R.J. Geue, T.W. Hambley, J. MacB. Harrowfield, A.M. Sargeson and M.R. Snow, *J. Am. Chem. Soc.*, 1984, **106,** 5478

38 P. Comba, N.F. Curtis, G.A. Lawrance, A.M. Sargeson, B.W. Skelton and A.H. White, *Inorg. Chem.*, 1986, **25,** 4260

39 P. Comba, N.F. Curtis, G.A. Lawrance, M.A. O'Leary, B.W. Skelton and A.H. White, *J. Chem. Soc., Dalton Trans.*, 1988, 497

40 P. Comba, N.F. Curtis, G.A. Lawrance, M.A. O'Leary, B.W. Skelton and A.H. White, *J. Chem. Soc., Dalton Trans.*, 1988, 2145

41 G.A. Lawrance, M. Maeder, M.A. O'Leary and F-H. Woon, *Polyhedron,* 1990, **9,** 2227

42 G.A. Lawrance, M. Martinez, B.W. Skelton and A.H. White, *J. Chem. Soc., Dalton Trans.*, 1992, 823

43 T.W. Hambley, G.A. Lawrance, M. Maeder and E.N. Wilkes, *J. Chem. Soc., Dalton Trans.*, 1992, 1283

44 T.W. Hambley, G.A. Lawrance, M. Martinez, B.W. Skelton and A.H. White, *J. Chem. Soc., Dalton Trans.*, 1992, 1643

45 G.A. Lawrance, M. Martinez, B.W. Skelton and A.H. White, *J. Chem. Soc., Dalton Trans.*, 1992, 1649

46 G.A. Lawrance and M.A. O'Leary, *Polyhedron,* 1987, **6,** 1291

47 A. Altomare, M.C. Burla, M. Camalli, M. Cascarano, C. Giacovazzo, A. Guagliardi and G. Polidori, *J. Appl. Crystallogr.*, in press

48 P.T. Beurskens, G. Admiraal, G. Beurskens, W.P. Bosman, R. de Gelder, R. Israel and J.M.M. Smits, *The DIRDIF-94 program system,* Technical Report of the Crystallography Laboratory, University of Nijmegen, The Netherlands., 1994.

49 Least squares:

Function minimised: $\sum \omega\left(|Fo| - |Fc|\right)^2$

where $w = \dfrac{1}{\sigma^2(Fo)} = \dfrac{4Fo^2}{\sigma^2(Fo^2)}$

$$\sigma^2(Fo^2) = \frac{S^2(C + R^2B) + (pFo^2)^2}{Lp^2}$$

S = Scan rate

C = Total integrated peak count

R = Ratio of scan time to background counting time

B = Total background count

Lp = Lorentz-polarization factor

p = p-factor

50 Standard deviation of an observation of unit weight:

$$\sqrt{\Sigma w\left(|Fo|-|Fc|\right)^2/(No-Nv)}$$

where: No = number of observations

Nv = number of variables

51 teXsan: Crystal Structure Analysis Package, Molecular Structure Corporation, 1985 and 1992

52 N.F. Curtis, ed. G.A. Melson, in *Coordination Chemistry of Macrocyclic Complexes,* Plenum, New York, 1979

53 T.C.W. Mak, O.W. Lau, M.F.C. Ladd and D.C. Povey, *Acta Crystallograph., Sect. B*, 1978, **34,** 1290

54 C. Mealli and E.C. Lingafelter, *J. Chem. Soc., Chem. Commun.*, 1970, 885

55 E.K. Barefield, D. Chueng, D.G. Van der Veer, *J. Chem. Soc., Chem. Commun.*, 1981, 302

56 R.W. Hay and M. Tozaffal Tarafder, *J. Chem. Soc., Dalton Trans.*, 1991, 823

57 B, Bosnich, R Mason, P.J. Pauling, G.B. Robertson and M.L. Tobe, *J. Chem. Soc., Chem. Commun.*, 1965, 97

58 F. Wagner and E.K. Barefield, *Inorg. Chem.*, 1976, **15,** 408

59 N.J. Jubran, G. Zinzburg H. Cohen, Y. Koresh and D. Meyerstein, *Inorg. Chem.*, 1985, **24,** 251

60 F. Wagner, M.T. Mocella, M.J. D'Aniello, A.H.J. Wang and E.K. Barefield, *J. Am. Chem. Soc.*, 1974, **96,** 2625

61 G.M. Freeman, E.K. Barefield and D.G. Derveer, *Inorg. Chem.*, 1984, **23,** 3092

62 G.A. Melson, *Coordination Chemistry of Macrocyclic Complexes*, Plenum Press, New York. 1979

63 L.Y. Tsymbal, S.V. Rosokha and Y.D. Lampeka, *J. Chem. Soc., Dalton Trans.*, 1995, 2633

64 R.W. Hay, B. Jeragh, G. Ferguson, B. Kaitner and B.L. Ruhl, *J. Chem. Soc., Dalton Trans.*, 1982, 1531

65 A. Anichini, L. Fabbrizzi, P. Paoletti and R.M. Clay, *Inorg. Chim. Acta,* 1977, **24**, L21

66 S-J. Kim, J-S. Choi, S-G. Kang, C-S. Kim and M-P Suh, *Bull. Korean Chem. Soc.*, 1995, **16,** 217

Chapter 2

Kinetic Studies of Binuclear Hexaaza Macrocycles

2.1 Introduction

Binuclear metal sites are common in many biomolecules and enzymes and have been the subject of several recent reviews[1,2]. The dioxygen transport protein hemocyanin and the monoxygenase tyrosinase are both binuclear copper proteins and many attempts have been made to prepare binuclear model complexes to mimic these systems.

Hemocyanin is a ubiquitous oxygen carrier protein for invertebrates and preliminary structural information[3,4] suggests that the metal containing active site of deoxy hemocyanin contains two coordinatively unsaturated Cu(I) centres each bound to the protein via histidine residues, Figure 2.1.1.

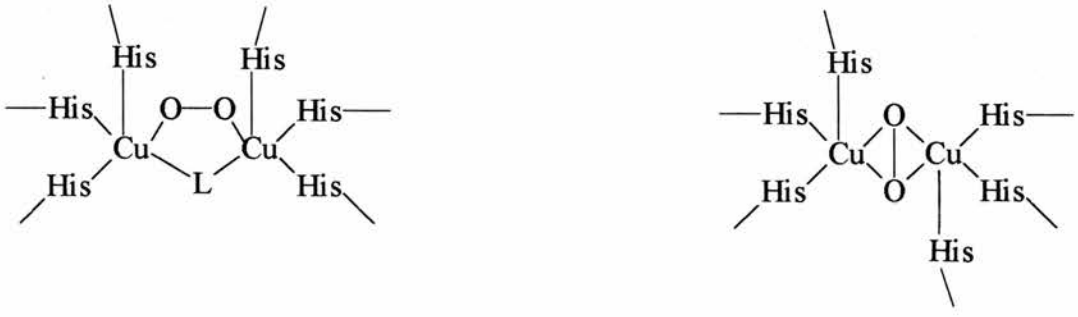

Figure 2.1.1. The active site of deoxyhemocyanin.

The active site of the oxyprotein[5] contains antiferromagnetically coupled binuclear copper(II) with a Cu—Cu distance of approximately 3.6 ± 0.2 Å. This is too long for a metal-metal bond and after studying several model systems it was postulated that the oxy form contains either *cis*-μ-η^1:η^1 or μ-η^2:η^2 coordinated dioxygen in the

peroxide oxidation state as a bridging ligand. In the *cis*-μ- η^1: η^1 model the Cu(II) centres are bridged by both dioxygen and hydroxo ligand to give a five membered ring, Figure 2.1.1. The alternative model contains an O_2^{2-} coordinated "side on" without an additional ligand and with a weaker O—O bond[6]. This latter model was only seriously considered after modeling studies with simple ligands produced such a complex[7,8], Figure 2.1.2.

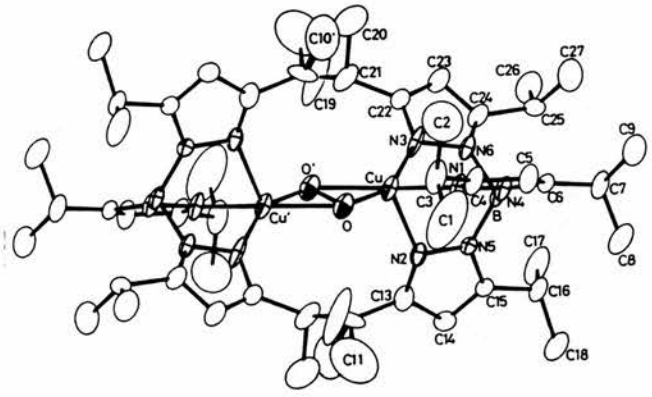

Figure 2.1.2. μ-η^2:η^2 peroxo binuclear Cu(II) complex.

Recently high resolution X-ray crystallographic studies[9] of oxy-hemocyanin from *Limulus polyphenus* have confirmed that the actual structure mirrors that found in the μ-η^2:η^2 model.

Tyrosinase is the oldest known monooxygenase. This dinuclear copper protein acts as both a creolase, performing *ortho* hydroxylation of monophenols to catechols, and as a catecholase oxidising the catechols to *o*-quinones[10]. It is thought that the active site of tyrosinase is very similar to that of oxyhemocyanin, the only difference being in the peripheral structure allowing access of the phenolic substrate to the dinuclear copper centre[11].

Copper is not the only metal found in binuclear enzymes. The enzyme methane monooxygenase from *Methylococcus capsulatus* contains a binuclear iron active site[12] and the enzyme manganese catalase from *Thermus thermophilus* has, as its name suggests, a binuclear manganese centre[13].

Efforts to functionally model binuclear enzymes have led to the development of a whole range of dinuclear complexes. Macrocyclic complexes in particular have been prepared in order to mimic such enzymes, especially since the isolation[14] of the binuclear copper(II) macrocyclic peptide ascidiacyclamide, Figure 2.1.3, from *Lissoclinum patella*.

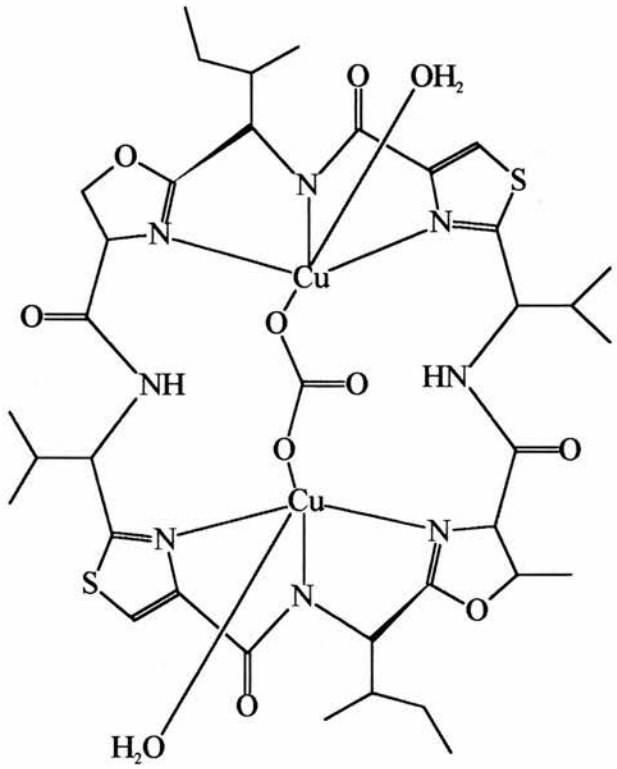

Figure 2.1.3. Ascidiacyclamide - a cyclic peptide from *Lissoclinum patella.*

Various synthetic strategies can be applied to the preparation of binuclear macrocyclic complexes or ligands that will form binuclear complexes. The most commonly used is the Schiff base condensation reaction between dialdehydes and diamines. The characteristics of the macrocycle can be altered extensively by using different diamines and dialdehydes as starting materials.

The earliest preparation of a Schiff base macrocycle was reported by Steinkopf *et al*[15] in 1939. The [2+2] condensation between 3,4-dibromothiophene-2,5-dicarbaldehyde and a series of diamines gives the cyclic product shown in Figure 2.1.4.

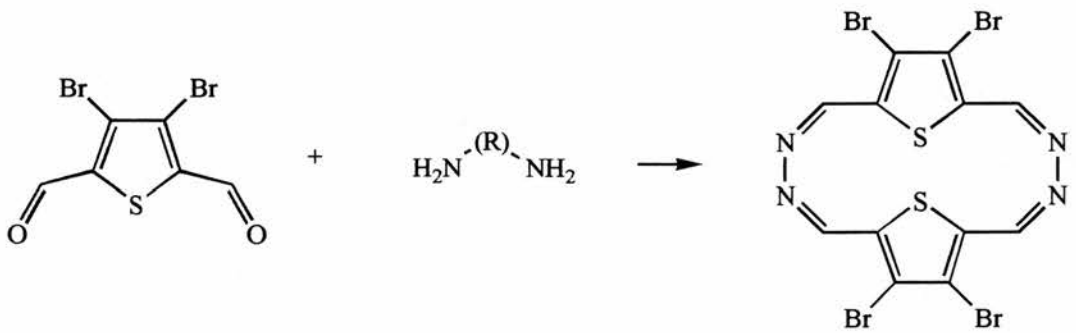

Figure 2.1.4. Steinkopf's Schiff base macrocycle.

More recent attempts[16] to repeat this procedure have cast doubt upon its authenticity since only polymeric condensation products were obtained. Early work suggested that a metal ion template around which the macrocyclic could form was a prerequisite in the synthesis of Schiff base macrcocycles. Some template reactions are shown in Table 2.1.1. Most use a large metal ion such as Ag^{I} or Ba^{II} to give [2+2] condensation

products. Using smaller templates can lead to [1+1] products[17]. Difficulties are encountered in isolating the free ligands and usually the only route to complexes of different metals is via transmetallation reactions.

However, attempts to synthesise Schiff base macrocycles without a template have been successful, thus removing the problem of isolating the free ligand from its complex with the template ion[18]. Table 2.1.2 lists many of the non-template Schiff base condensations between α,ω-diamines and dialdehydes resulting in macrocyclic products reported in the literature. Examples of the reaction using amines containing three primary amine groups are shown in Table 2.1.3.

Many Schiff base macrocycles containing secondary amines undergo ring contraction to form tri-cyclic ligands. This is due to the nucleophilic addition of the secondary amines across the adjacent imine bonds to form five or six membered rings. Initially it was claimed that the contraction was due to the macrocycle adjusting its cavity size to fit the template ion[19,20]. However, the same rearrangement was observed in ligands synthesised without a template ion[21,22,23,24]. The formation of the 1,3-aminal rings and the precipitation of the insoluble products is claimed to be the driving force for the macrocyclisation reaction[25]. Reduction of the Schiff base macrocycles or their polycyclic isomers with sodium borohydride or lithium aluminium hydride gives the polyamine mono-macrocycles[17, 25].

Binuclear complexes with most late row transition metals have been prepared for many of the Schiff base ligands and their reduced amine analogues. Homonuclear copper complexes have been most extensively studied because of their similarity to the natural systems. Heteronuclear complexes have also been reported[26] with Pb^{II} and

Table 2.1.1. Template Schiff base condensations to form macrocyclic imines.

Template	Di-carbonyl	Di-amine	Addition	Reference
Pb^{II}	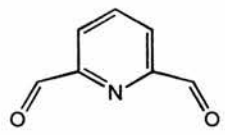	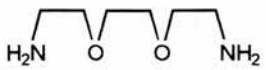	[2+2]	30
Ag^{I}	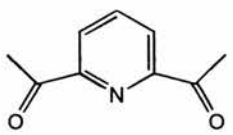	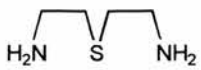	[2+2]	27
Ba^{II}	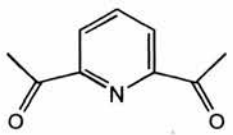	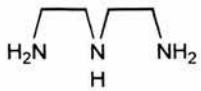	[2+2]	24
Ba^{II}, Pb^{II}	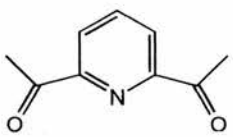	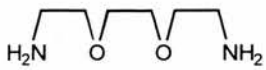	[2+2]	31, 28
Ba^{II}	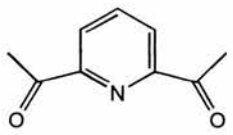	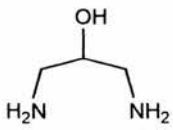	[2+2] [4+4]	32
Ba^{II}	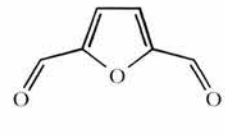		[2+2]	33, 20

Table 2.1.2. Non template Schiff base condensations to form macrocyclic imines.

Di-carbonyl	Di-amine	Reference
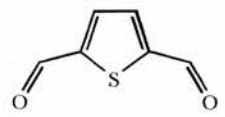	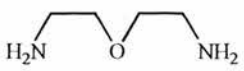	34, 23
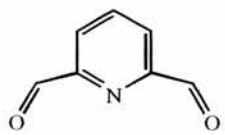	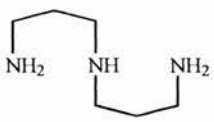	35
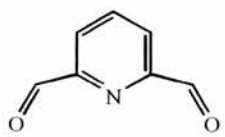	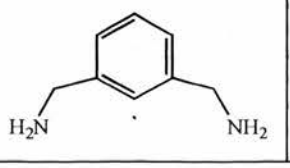 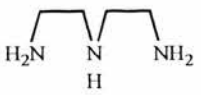	36
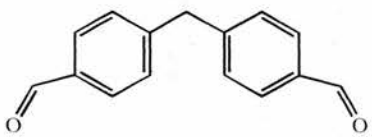	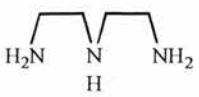	37
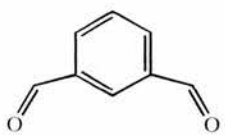		21,38, 39
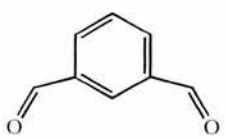	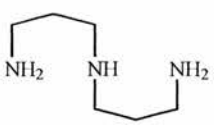	40
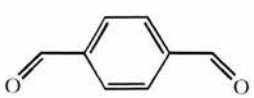	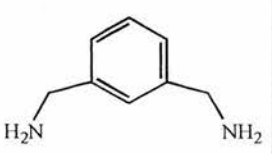 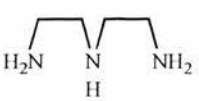	36

Table 2.1.2. (cont.)

Di-carbonyl	Di-amine	Reference
	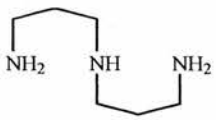	25, 41
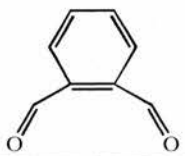	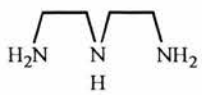	42
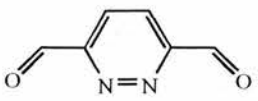	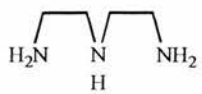	43
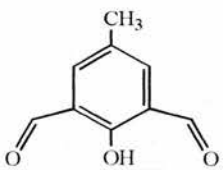	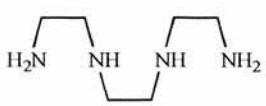	22
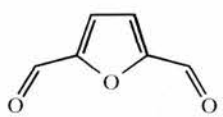	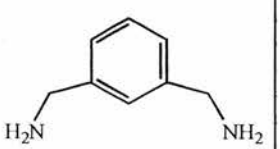 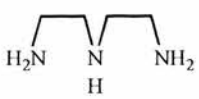	36
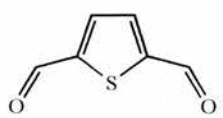	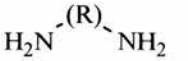 R $(CH_2)_n$ n = 3,4,5,6 $(CH_2)_nNH(CH_2)_n$ n=2,3 $(CH_2)_2O(CH_2)_2O(CH_2)_2$ $(CH_2)_2O(CH_2)_2O(CH_2)_2O(CH_2)_2$	23

Table 2.1.3. [2+3] Schiff base condensations to form bicyclic macrocycles.

Amine	Di-carbonyl	Addition	Reference
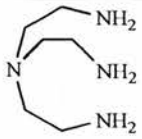	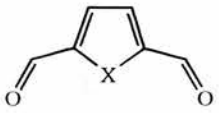	[2+3]	44, 45
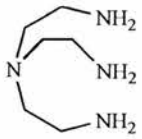	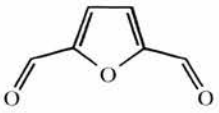	[2+3]	45,46
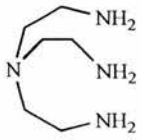		[2+3]	47
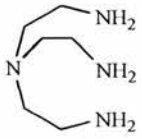	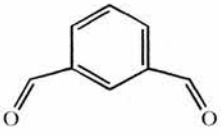	[2+3]	48

Mn^{II}. The metal-metal inter atomic distances are listed for several complexes in Table 2.1.4. These metal-metal distances are within the range required for forming complexes with bridging ligands. Examples of bridged complexes have been reported with imidazole[27,28], μ-hydroxy[28], thiocyanate[29] and azide bridging ligands.

Table 2.1.4. Metal-metal distances for several binuclear macrocyclic complexes.

Complex	M-M distance (Å)	Reference
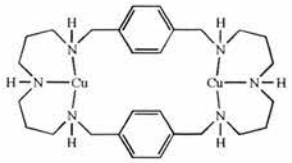	8.40 Å	41
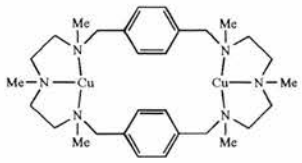	6.945 Å	49
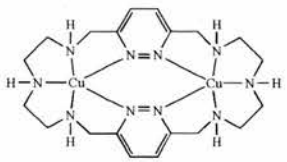	3.924 Å	43
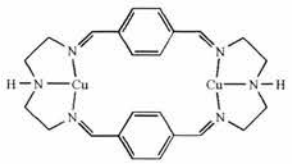	8.50 Å	50
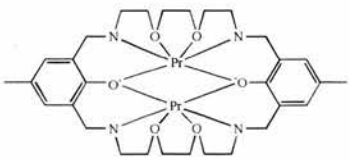	4.047 Å	51
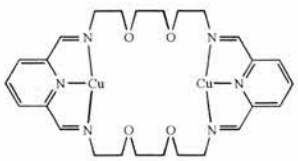	6.02 Å	52
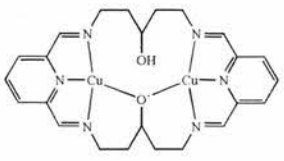	4.82 Å	53

Nomenclature

In view of the complex nature of the IUPAC nomenclature for the binuclear ligands and complexes discussed in this chapter a trivial nomenclature has been adopted. For example, the ligand below is given the IUPAC name as shown.

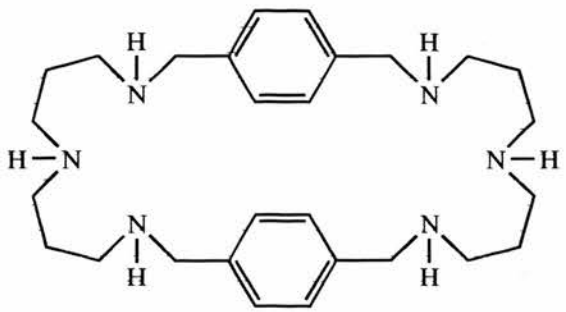

3,7,11,18,22,26-hexaazatricyclo-[26.2.2.213,16]-tetratriaconta-1(31),13(33),14,16(34),28(32),29-hexaene

However, since the connectivity across the aromatic ring is *para* and the amines are bridged by propyl groups this ligand is termed ***para*-propyl-amine** (PPA). The binuclear metal complex would be $[M_2(PPA)]^{x+}$.

The complex below, having *meta* linkage across the aromatic ring and ethyl bridges between the adjacent amines would be termed ***meta*-ethyl-amine** (MEA).

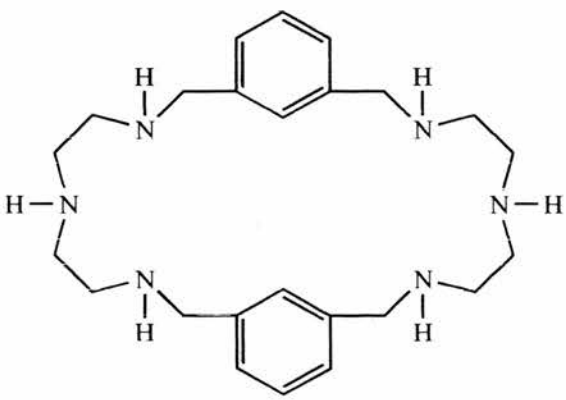

3,6,9,17,20,23-hexaazatricyclo-[23.3.1.1^{11,15}]triaconta-1(28),11(30),12,14,25(29),26-hexaene

2.2 Experimental.

2.2.1 Synthesis

All reagents, except the dialdehydes, were obtained from the Aldrich Chemical Company and used without further purification. The dialdehydes were used as obtained from Avocado Research Chemicals Ltd. The ligands and complexes of MEA and MPA were synthesised by Dr. T. Clifford, University of St. Andrews.

Preparation of the macrocyclic Schiff base, PPA

The macrocyclic Schiff base was prepared according to the method of Pietraszkiewicz and Gasiorowski[25]. *p*-phthalaldehyde (2.68 g, 0.02 mol) was dissolved in dry THF and 1,7-diamino-4-azaheptane (2.62 g, 0.02 mol) dissolved in THF added dropwise. The mixture was stirred at 0°C for 4 days and the white precipitate was filtered off. The compound was sufficiently pure for the next step to be carried out directly. (Yield 4.02 g, 87 %)

Reduction of the Schiff base to yield 3,7,11,18,22,26-hexaazatricyclo-[26.2.2.2^{13,16}]tetratriaconta-1(31),13(33),14,16(34),28(32),29-hexaene, PPA

To a vigorously stirred solution of the macrocyclic Schiff base (5 g, 0.011 mol) in methanol an excess of sodium borohydride was slowly added. The mixture was stirred

overnight until effervescence ceased. A small quantity of water (10 ml) was added to destroy any unreacted sodium borohydride. The mixture was then filtered and the filtrate evaporated to give a brown residue which was then dissolved in water. The aqueous solution was extracted with dichloromethane and the organic layer separated. Removal of the dichloromethane gave the free ligand as a colourless oil which was not further purified. Addition of concentrated hydrochloric acid dropwise to a methanol solution of the amine gave the hydrochloride salt. The hydrochloride salt was recrystallized from water:methanol to give colourless crystals which were dried in *vacuo*. (Yield (of free base) 2.67 g, 52 %), M.W. 466.71 g mol^{-1}, (Found: C, 46.69; H, 8.43; N, 10.49 %. Calculated for $C_{28}H_{46}N_6 \cdot 6HCl \cdot H_2O \cdot 3MeOH$: C, 46.57; H, 8.32; N, 10.51 %)

Preparation of $[Cu_2(PPA)Cl_4]$

The free ligand (2.35 g, 0.005 mol) was dissolved in ethanol (50 cm^3) and added to an ethanolic solution of $CuCl_2$ (1.70 g, 0.01 mol). The solution was allowed to stand for 1 hour after which time the green precipitate was filtered off. A second crop was obtained by reducing the volume of the filtrate on a rotary evaporator. The product was recrystallized from methanol and dried *in vacuo*. (Yield 1.82 g, 49.5 %), M.W. 735.62 g mol^{-1}, (Found: C, 44.78; H, 6.35; N, 11.01 %. Calculated for $C_{28}H_{46}N_6Cl_4Cu_2$: C, 45.72; H, 6.30; N, 11.42 %); λ_{max} = 680 nm ε = 271 dm^3 mol^{-1} cm^{-1} (H_2O) I.R./cm^{-1}; ν(N-H); 3254; ν(C-H) 2894; δ(N-H) 1632; 1544, (KBr)

Preparation of $[Cu_2(PPA)Cl_4]$ by a template reaction

This method is similar to that for the preparation of binuclear cryptands reported by Qin *et al*[54]. 1,7-diamino-4-azaheptane (1.31 g, 10 mmol) and *p*-phthalaldehyde (1.34 g, 10 mmol) were added to a solution of $CuCl_2 \cdot 2H_2O$ (1.71 g, 10 mmol) in a 1:3 acetonitrile:ethanol mixed solvent under nitrogen. The green solution was heated at 60°C for 1 hour to produce a blue solution. The solvent was removed on a rotary evaporator and the solid re-dissolved in methanol. An equimolar quantity of sodium borohydride was slowly added to the solution and when effervescence had ceased (overnight) a small quantity of water was added to ensure destruction of the sodium borohydride. The mixture was filtered and the filtrate reduced in volume on a rotary evaporator to yield a green microcrystalline product. This was recrystallized from methanol, filtered off and dried *in vacuo*. (Yield 2.72 g, 34 %), M.W. 807.68 g mol^{-1} (Found: C, 41.24; H, 6.92; N, 10.01 %. Calculated for $C_{28}H_{46}N_6Cl_4Cu_2 \cdot 4H_2O$: C, 41.64; H, 6.74; N, 10.41 %)

Preparation of $[Ni_2(PPA)Cl_4]$

The free ligand (2.35 g, 0.005 mol) was dissolved in ethanol and added to a methanolic solution of $NiCl_2 \cdot 6H_2O$ (2.38 g, 0.01 mol) The pale green product precipitated immediately and was filtered off after standing for 15 minutes. The product was recrystallized from methanol and dried *in vacuo*. (Yield 2.95 g, 42 %),

MW = 703.25 g mol^{-1}, (Found: C, 44.86; H, 5.99; N, 10.88 %. Calculated for $C_{28}H_{46}N_6Ni_2Cl_4 \cdot 2H_2O$, C, 44.51; H, 5.87; N, 11.12 %)

Preparation of the macrocyclic Schiff base, PEA

Chen and Martell's method[36] was used to prepare this ligand. *p*-phthalaldehyde (1.34 g, 0.01 mol) was dissolved in dry acetonitrile and a solution of 1,5-diamino-3-azapentane (1.03 g, 0.01 mol) in acetonitrile was slowly added. After stirring for 5 hours the solvent was removed on a rotary evaporator to give a yellow oil. The crude product was used for the reduction to form the free base. (Yield 1.87 g, 91 %)

Reduction of the macrocyclic Schiff base to yield 3,6,9,16,19,22-hexa-azatricyclo[22.2.2.$2^{11,14}$]triaconta-1(27),11(29),12,14(30),24(28),25-hexaene, PEA

The Schiff base produced above was (4.15 g, 8.96 mmol) was dissolved in ethanol (100 cm^3) and cooled in an ice bath. Sodium borohydride (6 g) was added in small quantities and the mixture was left stirring until effervescence ceased (overnight). The mixture was then acidified with HCl to pH 2 and ethanol added to precipitate a white solid which was filtered off and dried in *vacuo*. This solid was then redissolved in water and basified with sodium hydroxide. The product was then extracted with dichloromethane and dried over anhydrous sodium sulphate. After removal of the

solvent the white solid was recrystallized from toluene yielding white needles. (Yield 3.42 g, 82%) M.W. 410.6 g mol^{-1}, (Found; C, 70.21; H, 9.35; N, 20.44 %. Calculated for $C_{24}H_{38}N_6$; C, 70.20; H, 9.33; N, 20.47 %); I.R./cm^{-1}; ν(N-H); 3293, 3227; ν(C-H) 2873, 2800; δ(N-H) 1503; 1434, (KBr)

Preparation of $[Cu_2(PEA)Cl_4]\cdot 3H_2O\cdot MeOH$

To an ethanolic solution (20 cm^3) of copper(II) chloride hydrate (0.832 g, 4.88 mmol) was added to a refluxing solution of the PEA free base (1.0 g, 2.44 mmol) in ethanol (20 cm^3). Upon cooling a fine green precipitate was formed which was filtered off and washed with ethanol and dried in *vacuo*. This product was recrystallized from aqueous methanol. (Yield 1.65 g, 88%) M.W. 765.6 g mol^{-1}, (Found; C, 39.10; H, 5.52; N, 11.06 %. Calculated for $C_{25}H_{48}N_6Cu_2Cl_4O_4$; C, 39.22; H, 6.32; N, 10.98 %); λ_{max} = 617 nm ε = 238 $dm^3\ mol^{-1}\ cm^{-1}$ (H_2O) I.R./cm^{-1}; ν(N-H); 3182; ν(C-H) 2879; δ(N-H) 1617; 1520, 1451, 1065, 1019 (KBr)

Preparation of the macrocyclic Schiff base 3,7,11,19,23,27-hexaazatricyclo-[27.3.1.1^{13,17}]tetratriaconta-1(32),2,11,13,15,17(34),18,27,29(33),30-decaene, MPA

The procedure was essentially as described by Llobet *et al*[40]. To a solution of *m*-phthalaldehyde (1.34 g, 0.01 mol) in acetonitrile was slowly added a solution of 1,7-diamino-4-azaheptane (1.31 g, 0.01 mol) in acetonitrile. The mixture was stirred for 5 hours and then the solvent was removed using a rotary evaporator to give a colourless oil. This was washed with ether and dried *in vacuo*. The crude product was used to prepare the free base hexaaza macrocycle. (Yield 3.91 g, 84 %)

Preparation of 3,7,11,19,23,27-hexaazatricyclo-[27.3.1.1^{13,17}]tetratriaconta-1(32),13,15,17(34),29(33),30-hexaaene, MPA

This uses the same procedure as for the sodium borohydride reduction of the macrocyclic Schiff base to form PPA hexaamine. However, unlike the PPA analogue the free base of MPA does not form a crystalline solid, but yields a viscous oil. (Yield 82 %) (Found; C, 65.87; H, 11.06; N, 16.41 %. Calculated for $C_{28}H_{46}N_6 \cdot 2.5H_2O$; C, 65.72; H, 10.04; N, 16.42 %)

Preparation of $[Cu_2(MPA)Cl_2](CuCl_4)\cdot 2H_20\cdot EtOH$

Copper(II) chloride hydrate (0.738 g, 4.33 mmol) was dissolved in ethanol (20 cm^3) and added dropwise to a refluxing solution of the MPA free base (1.01 g, 2.16 mmol) in ethanol (20 cm^3). The resulting pale green precipitate was filtered off and washed with ethanol, then ether and dried in *vacuo*. (Yield 0.79 g, 38%) (Found; C, 38.07; H, 5.53; N, 9.00 %. Calculated for $C_{30}H_{56}N_6Cu_3Cl_6$; C, 37.84; H, 5.93; N, 8.83 %); λ_{max} 430, 732 nm ε = 226, 433 $dm^3\ mol^{-1}\ cm^{-1}$ (H_2O) I.R./cm^{-1}; ν(N-H); 3181; ν(C-H) 2939, 2875; δ(N-H) 1612; 1590, 1447, (KBr)

Preparation of the macrocyclic Schiff base 3,6,9,17,20,23-hexaazatricyclo-[23.3.1.1^{11,15}]triaconta-1(28),2,9,11(30),12,14,16,23,25(29),26-decaene, MEA

The procedure followed by Menif and Martell[38] was used to prepare this ligand. To a solution of *m*-phthalaldehyde (1.34 g, 0.01 mol) in acetonitrile was slowly added a solution of 1,5-diamino-3-azapentane (1.03 g, 0.01 mol) in acetonitrile. The mixture was stirred for 5 hours and then the solvent was removed using a rotary evaporator to give a colourless oil. This was washed with ether and dried *in vacuo*.

Preparation of 3,6,9,17,20,23-hexaazatricyclo[23.3.1.1^{11,15}]triaconta-1(28),11(30),12,14,25(29),26-hexaene, MEA

This uses the same procedure as for the sodium borohydride reduction of the macrocyclic Schiff base to form PPA hexaamine. This ligand was isolated as the hydrobromide salt. (Found; C, 29.57; H, 3.67; N, 8.35; Br, 48.83 %. Calculated for $C_{24}H_{54}N_6Br_6O_5$; C, 29.23; H, 5.52; N, 8.52; Br, 48.62 %)

Preparation of $[Cu_2(MEA)Cl_2](Cu_2Cl_4)_{0.33}\cdot 0.167EtOH$

Copper chloride dihydrate (0.993 g, 4.82 mmol) was dissolved in ethanol (20 cm^3) and was added dropwise to a refluxing solution of the MEA free base (1.20 g, 2.93 mmol) in ethanol (20 cm^3). The fine green precipitate was filtered off and washed with ethanol, ether and then dried in *vacuo*. (Yield 1.70 g, 75%) (Found; C, 37.49; H, 5.07; N, 10.78 %. Calculated for $C_{24}H_{38}N_6Cu_2\cdot(Cu_2Cl_4)_{1/3}\cdot(EtOH)_{1/6}$; C, 37.60; H, 5.06; N, 10.81 %); λ_{max} 437, 692 nm ε = 116, 304 dm^3 mol^{-1} cm^{-1} (H_2O) I.R./cm^{-1}; ν(N-H); 3186; ν(C-H) 2944, 2875; δ(N-H) 1614; 1448, (KBr)

2.2.2 Physical Measurements

The acid catalysed dissociation of the Cu(II) complex of PEA was studied using hydrochloric acid solutions (Volucon standard concentrate) adjusted to I = 0.1M with NaCl. All reactions were monitored spectrophotometrically at 630 nm using a Hi-Tech SF-51 stopped-flow spectrophotometer. Pseudo first order conditions were maintained by using at least ten-fold excess of acid. Observed rate constants were calculated from the experimental data using a Hewlett Packard Series 300 micro-computer. Rapid scan spectrophotometry was performed using a Spectrascan rotating monochromator accessory with the Hi-Tech SF-51 stopped flow instrument. Temperature was controlled using a Heto thermostated circulating water bath.

2.2 Results and Discussion.

2.2.1 Synthesis

The non-template reaction of *bis*-(3-aminopropyl)amine with *p*-phthalaldehyde in THF solution gives high yields of the macrocyclic diene. This diene is in equilibrium with the tetra-imine, Figure 2.2.1.1, and results from the nucleophilic addition of the two secondary amine functions across adjacent imine bonds in the tetra-imine. The structure is consistent with the ^{1}H n.m.r. and has been confirmed by X-ray crystallography. The diimine is reduced to form the tri-cyclic PPA ligand in good yield.

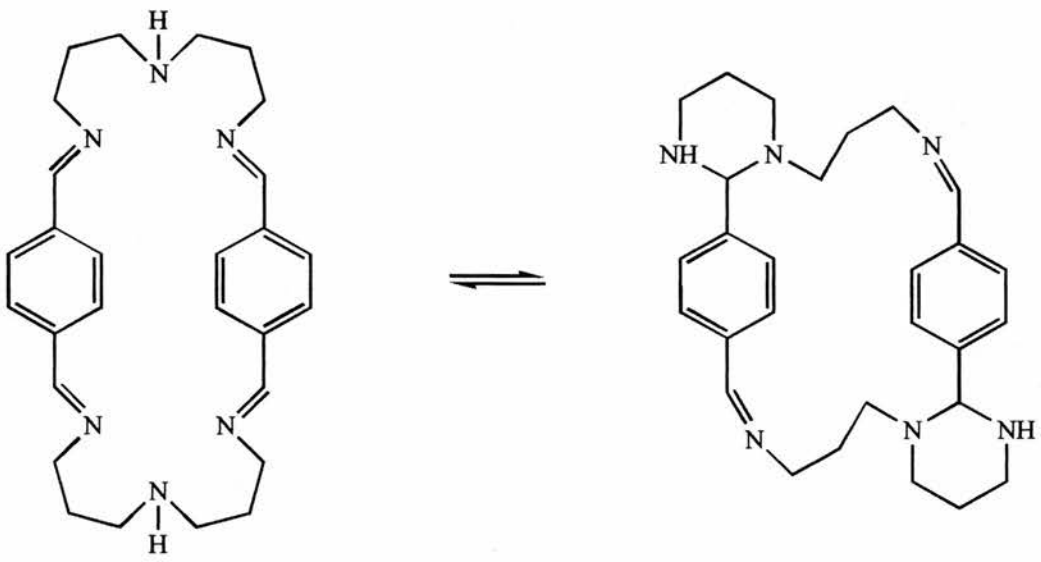

Figure 2.2.1.1 Macrocyclic tetra-imine and diene products from the condensation of *bis*-(3-aminopropyl)amine with *p*-phthalaldehyde.

The reaction also works well if *bis*-(2-aminoethyl)amine is substituted for *bis*-(3-aminopropyl)amine and acetonitrile is used as solvent instead of THF. The resulting Schiff base does not undergo intramolecular nucleophilic addition of the two secondary amines across two imine bonds as does the *para*-propyl Schiff base. The formation of five membered diaza rings is not favored in this system.

Using *meta*-phthalaldehyde (isophthalaldehyde) with *bis*-(2-aminoethyl)amine produces the *meta*-ethyl Schiff base which forms significant amounts of the diaza ring structure in addition to the tetra-imine. The reaction between *meta*-phthalaldehyde and *bis*-(3-aminopropyl)amine also gives good yields of the *meta*-propyl Schiff base. No evidence was found for the formation of diaza rings in this ligand.

Attempts at the non-template Schiff base [2+2] condensation between *ortho*-terephthalaldehyde and the two amines were unsuccessful. However, Shakir *et al*[42] have recently reported the successful synthesis of metal complexes of the *ortho*-ethyl Schiff base ligands. Copper(II) and nickel(II) ions were used as templates for the [2+2] condensation reactions in methanolic solution.

All of the Schiff base macrocycles undergo reduction with sodium borohydride to form their corresponding hexa-amine analogues.

2.3.2 Acid Catalysed Dissociation Kinetics of Cu_2PEA

All dissociation reactions demonstrate simple pseudo first order kinetics with no evidence for concurrent reactions. Time lapse rapid scanning spectrophotometric measurements, Figure 2.3.2.1, confirm this point showing a simple first order decay of the *d—d* transition at *ca.* 640 nm. This result suggests that both metal centres within the molecule act independently of each other and both have identical dissociation rates. The observed first order rate constants (k_{obs}) obtained over a range of temperature are listed in Table 2.3.2.1.

Table 2.3.2.1. k_{obs} for the acid catalysed dissociation of Cu_2PEA

[H+] (10^3)	19.7°C	24.4°C	29.3°C	34.1°C	38.9°C	43.9°C
49.1	0.739	1.144	1.720	2.710	3.950	6.280
36.8	0.731	1.113	1.680	2.560	3.750	5.620
24.5	0.645	1.014	1.560	2.370	3.370	5.090
12.3	0.547	0.891	1.350	1.950	2.940	4.160
4.91	0.438	0.653	0.978	1.400	2.040	2.830
3.68	0.389	0.581	0.832	1.210	1.680	2.330
2.45	0.290	0.453	0.614	0.923	1.230	1.750
1.23	0.164	0.261	0.337	0.455	0.621	0.774
0.49	0.053	0.100	0.120	0.167	0.217	0.322

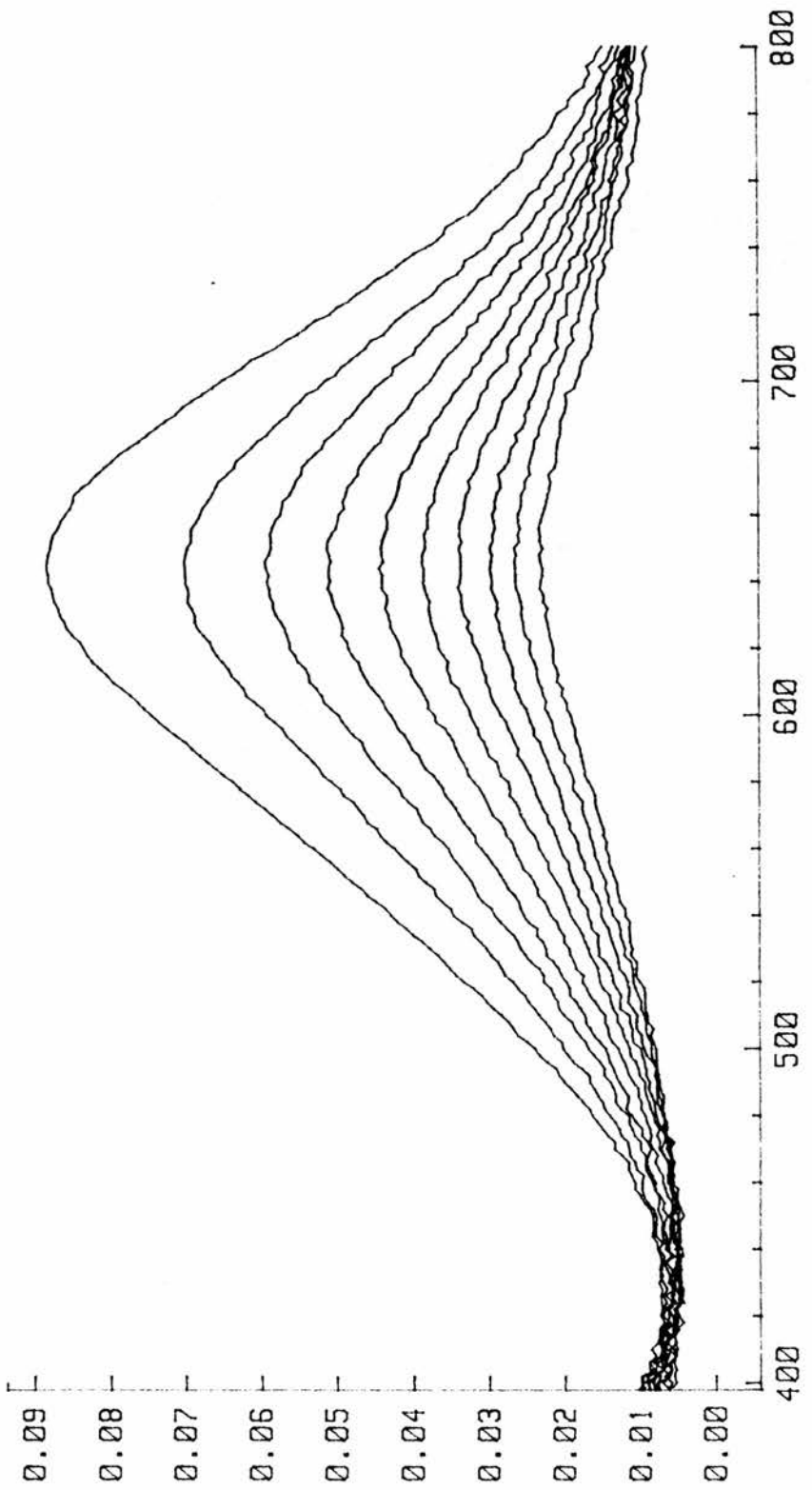

Figure 2.3.2.1 Absorbance changes during the acid catalysed demetallation of Cu(PEA).

$T = 24.4°C$, $[H^+] = 2.45 \times 10^{-3}$ mol dm^{-3}, $\Delta t = 0.3$ secs.

A plot of k_{obs} versus $[H^+]$ at 25°C is shown in Figure 2.3.2.2. At each temperature there is initially a linear dependence of k_{obs} on $[H^+]$, but at higher hydrogen ion concentrations the rate of reaction becomes independent of $[H^+]$. The linear part of the plot at low acidities intercepts the origin indicating the absence of a solvolytic pathway resulting in metal dissociation.

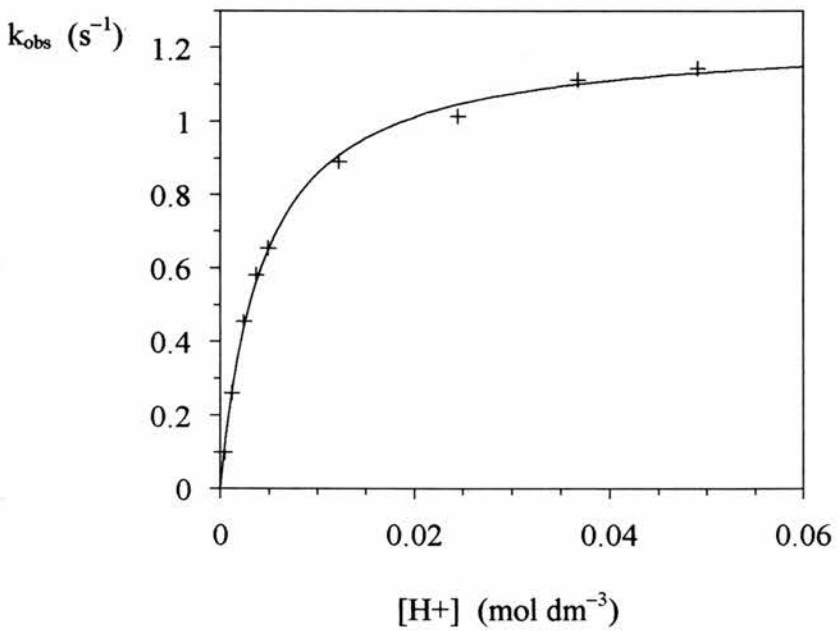

Figure 2.3.2.2. k_{obs} versus $[H^+]$ at 24.4°C for the acid catalysed dissociation of Cu_2PEA

Figure 2.3.2.3 shows how the rate of reaction increases with increasing temperature and H^+ concentration.

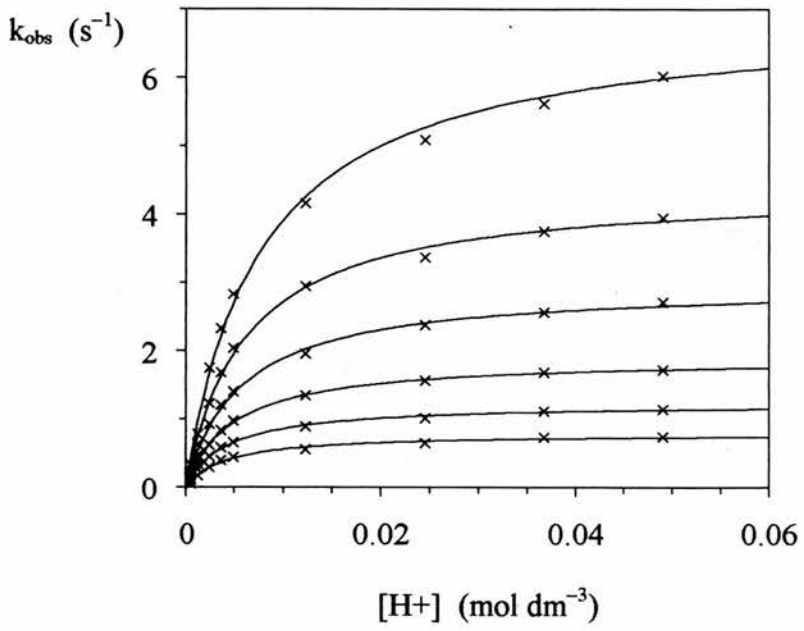

Figure 2.3.2.3. k_{obs} versus $[H^+]$ at 19.7, 24.4, 29.3, 34.1, 38.9 and 43.9°C for the acid catalysed dissociation of Cu_2PEA

Since the metal centres appear to dissociate independently the dissociation can be represented by the reaction scheme where CuN_3 represents the binding site for one copper;

Scheme 2.3.2.1. Mechanism of acid catalysed Cu(II) dissociation from Cu_2PEA.

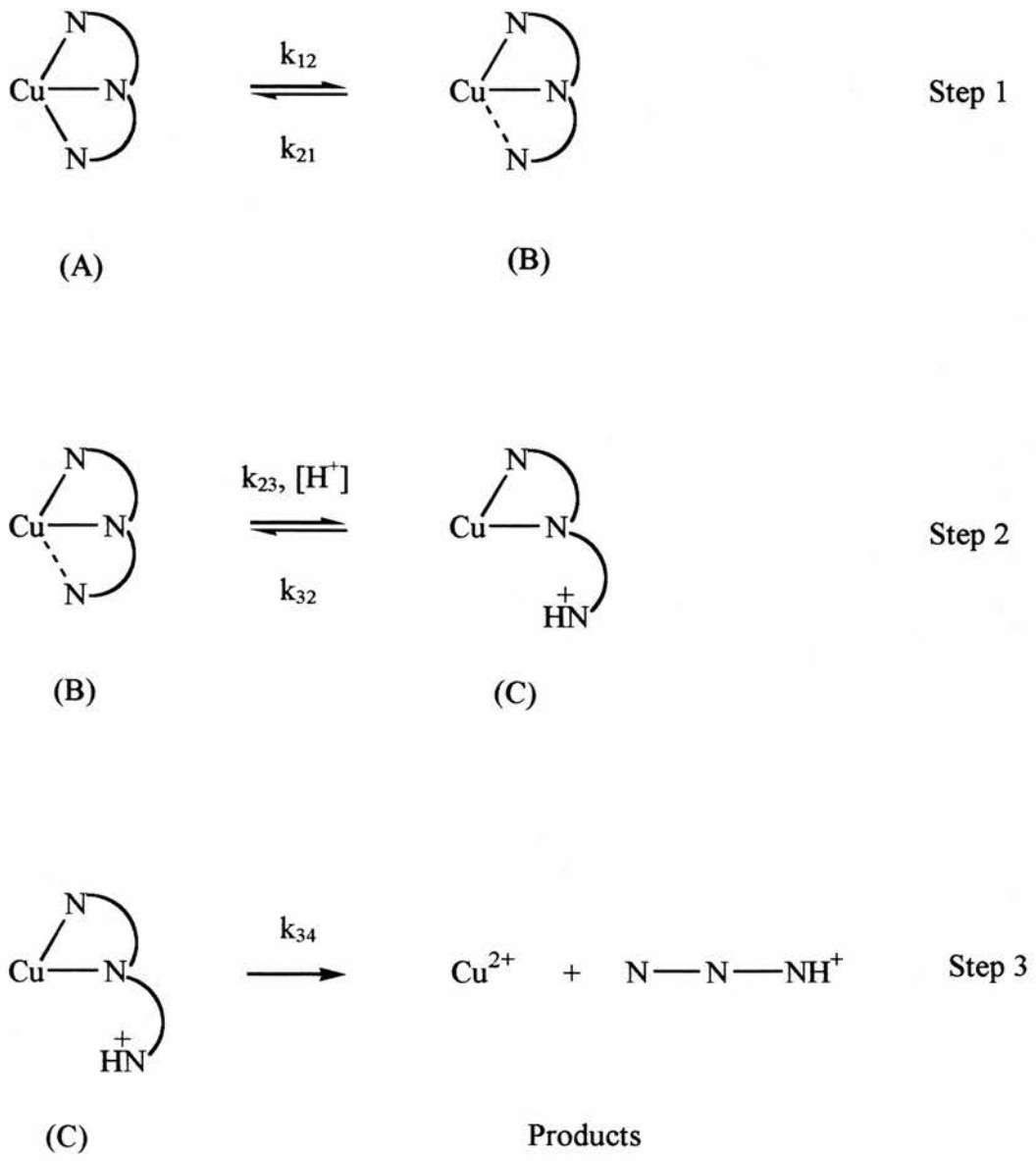

In step 1 of the proposed pathway one nitrogen donor is dissociated from the metal ion without its replacement by a solvent molecule. However the chelate ring has not been broken sufficiently to move the nitrogen atom out of the inner coordination

sphere of the metal ion. This activated species is susceptible to protonation (step 2) after which the complex rapidly dissociates (step 3).

If it is assumed that the intermediate (B) is present in a small "steady state" concentration, k_{32} can be neglected and if k_{23} is rapid then the observed rate of the reaction is given by;

$$V = k_{obs}[A] = k_{23}[B][H^+]$$

Since,

$$\frac{dB}{dt} = 0 \ ,$$

$$k_{12}[A] = k_{21}[B] + k_{23}[B][H^+]$$

and therefore

$$[B] = \frac{k_{12}[A]}{(k_{21} + k_{23}[H^+])}$$

the rate equation can then be rearranged to;

$$k_{obs}[A] = \frac{k_{23}[H^+]k_{12}[A]}{\left(k_{21} + k_{23}[H^+]\right)}$$

$$k_{obs} = \frac{k_{12}k_{23}[H^+]}{\left(k_{21} + k_{23}[H^+]\right)}$$

Since, $K = \frac{k_{12}}{k_{21}}$,

$$k_{obs} = \frac{k_{23}K[H^+]}{\left(1 + \frac{k_{23}[H^+]}{k_{21}}\right)}$$

This can be rearranged to give the final rate expression;

$$k_{obs} = \frac{k_{23}K[H^+]}{\left(1 + \frac{k_{23}K[H^+]}{k_{12}}\right)}$$

A plot of k_{obs}^{-1} versus $[H^+]^{-1}$ is linear. Using the Statmost curve fitting algorithms values for k_{12}, $k_{23}K$ and k_{23}/k_{21} were obtained for each temperature and are summarised in Table 2.3.2.2.

Table 2.3.2.2. Rate and Equilibrium Constants for the Acid Catalysed Dissociation of Cu_2PEA.

T (°C)	T (K)	k_{12} (s^{-1})	$k_{23}K$ (M^{-1} s^{-1})	k_{23}/k_{21} (M^{-1})
19.7	292.8	0.79	182.6	231.2
24.4	297.5	1.23	281.2	229.1
29.3	302.4	1.90	381.0	200.6
34.1	307.2	2.97	513.4	173.0
38.9	312.0	4.38	711.0	162.7
43.9	317.0	6.97	892.0	128.2

Arrhenius and Eyring plots, Figures 2.3.2.4 and 2.3.2.5 respectively, were used to determine the activation energy (E_A = 68.35 ± 1.10 kJ mol^{-1}), the enthalpy of activation ($\Delta H^{\ddagger}$ = 65.85 ± 1.07 kJ mol^{-1}) and the entropy of activation ($\Delta S^{\ddagger}$ = –22.36 ± 3.50 J K^{-1} mol^{-1}) from the temperature dependence of k_{12}.

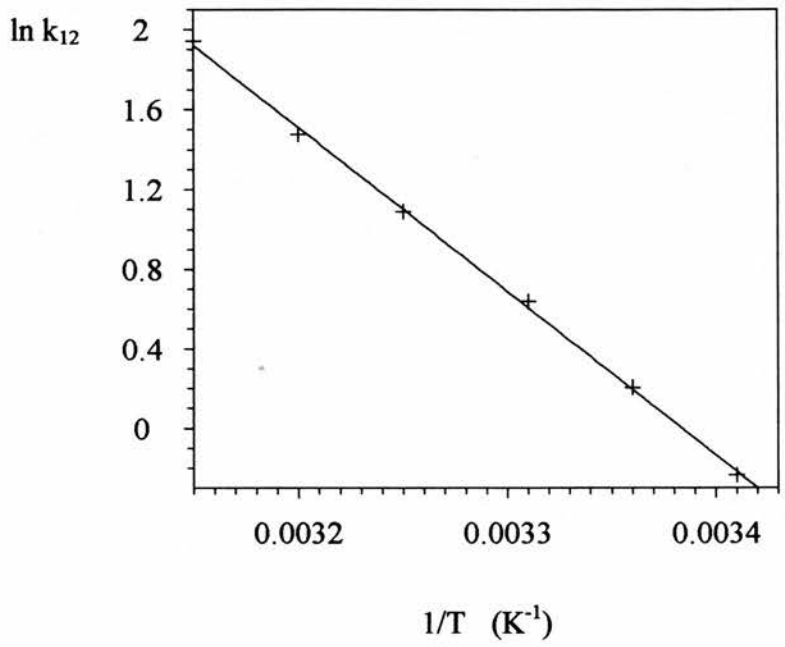

Figure 2.3.2.4. Arrhenius plot of $\ln(k_{12})$ versus 1/T.

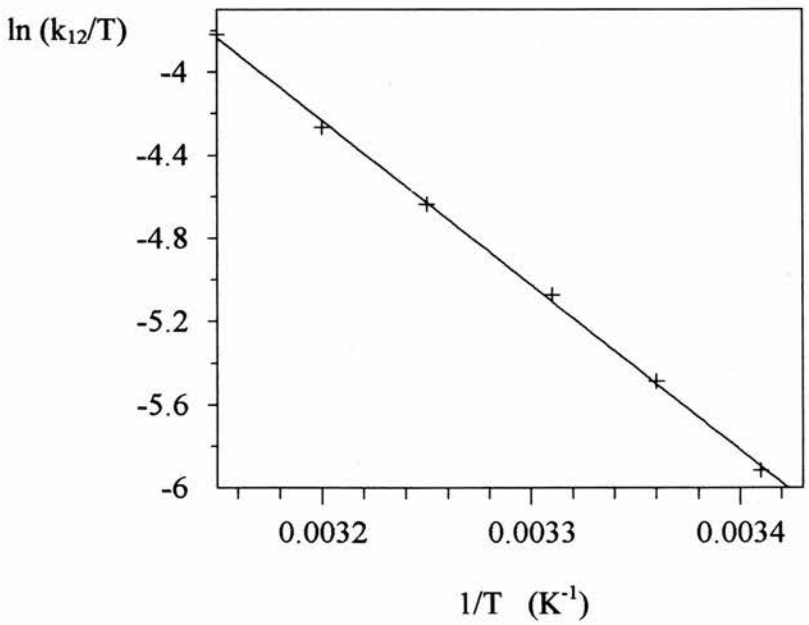

Figure 2.3.2.5. Eyring plot of $\ln(k_{12}/T)$ versus 1/T.

Comparison of these values with those found for similar systems reported in the literature (Table 2.3.2.3) shows that the closest correlation is with the linear triamine complexes.

Table 2.3.2.3. Thermodynamic parameters for the demetallation of several copper(II) amine complexes.

Complex	k_{12} (s^{-1})	$\Delta H^{\ddagger}$ ($kJmol^{-1}$)	$\Delta S^{\ddagger}$ ($JK^{-1}mol^{-1}$)	k_{23}/k_{21} (M^{-1})	Reference
$[Cu_2PEA)]^{2+}$	1.3	65.9	22.4	229	*This work*
$([9]aneN_3)Cu^{II}$		34	–68		55
$([10]aneN_3)Cu^{II}$			–78		56
$([11]aneN_3)Cu^{II}$		45	–79		56
$([12]aneN_3)Cu^{II}$		21	–57		56
$([13]aneN_3)Cu^{II}$		63	–19		56
$[Cu(ethylenediamine)]^{2+}$	150	65	21	12	57
$[Cu(1,3\text{-propanediamine})]^{2+}$	73	57	12		57
$[Cu(N\text{-}(2\text{-aminoethyl})\text{-}1,3\text{-propanediamine})]^{2+}$	3.5	62	–17	71	57
$[Cu(N,N'\text{-}(3\text{-aminopropyl})\text{-}1,2\text{-ethylenediamine})]^{2+}$	9.7	43	–58	28	57

2.3.3 Acid Catalysed Dissociation Kinetics of Cu_2MPA and Cu_2PPA.

The complex Cu_2MPA dissociates completely in < 0.001M HCl solution. However, unlike the dissociation reaction for Cu_2PEA the dissociation of Cu_2MPA proceeds via two consecutive reactions. Monitoring the reaction at a fixed wavelength of 270 nm clearly shows the two reactions, Figure 2.3.3.1. The time interval scanning technique using the Hi-Tech spectrascan accessory shows that the initial scan does not coincide with subsequent scans which show clean isosbestic points indicating first order behaviour. The first reaction is too fast to be observed fully using the spectrascan technique. Both reactions follow pseudo first order kinetics and display a non-linear dependence on $[H^+]$. Figure 2.3.3.2 shows the relationship between $[H^+]$ and k_{1obs} at 25°C and Figure 2.3.3.3 the relationship with k_{2obs} at 25°C.

Figure 2.3.3.1. The acid catalysed dissociation of $Cu_2(MPA)$

T = 25°C, λ = 270 nm, $[H^+] = 2.5 \times 10^{-3}$ mol dm^{-3}, $[Cu_2(MPA)] = 1.1 \times 10^{-4}$ mol dm^{-3}.

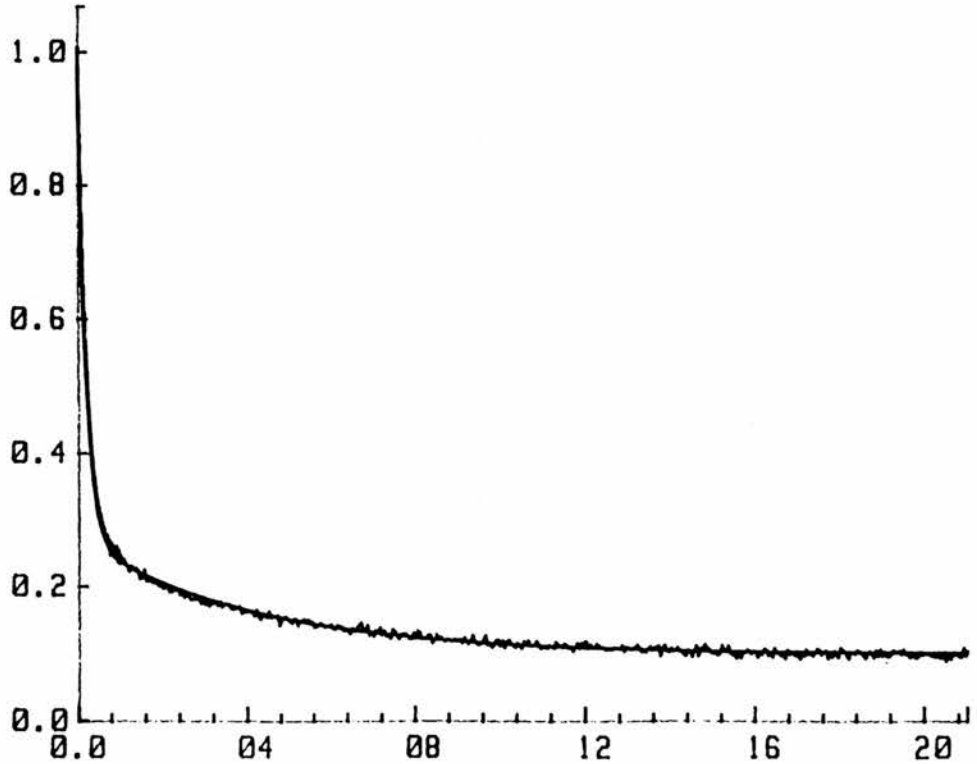

Figure 2.3.3.2. k_{1obs} versus $[H^+]$ at 25°C for the acid catalysed dissociation of Cu_2MPA.

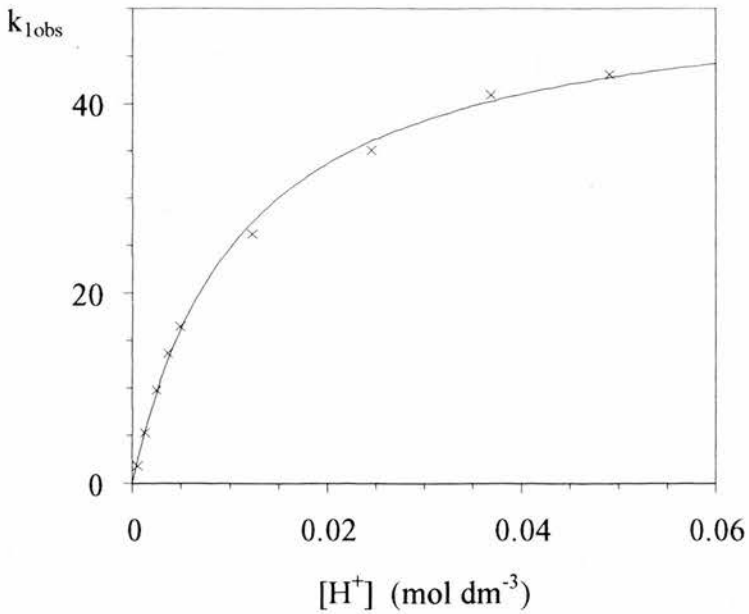

Figure 2.3.3.3. k_{2obs} versus $[H^+]$ at 25°C for the acid catalysed dissociation of Cu_2MPA.

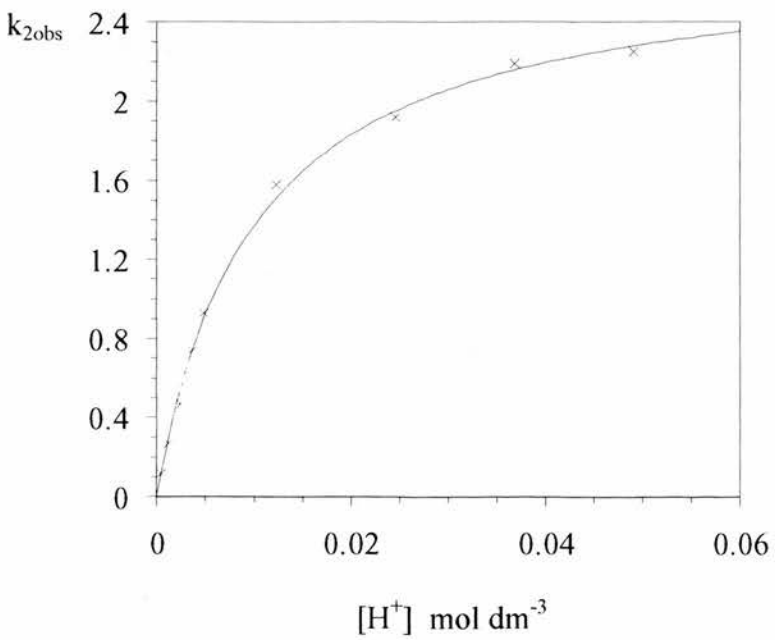

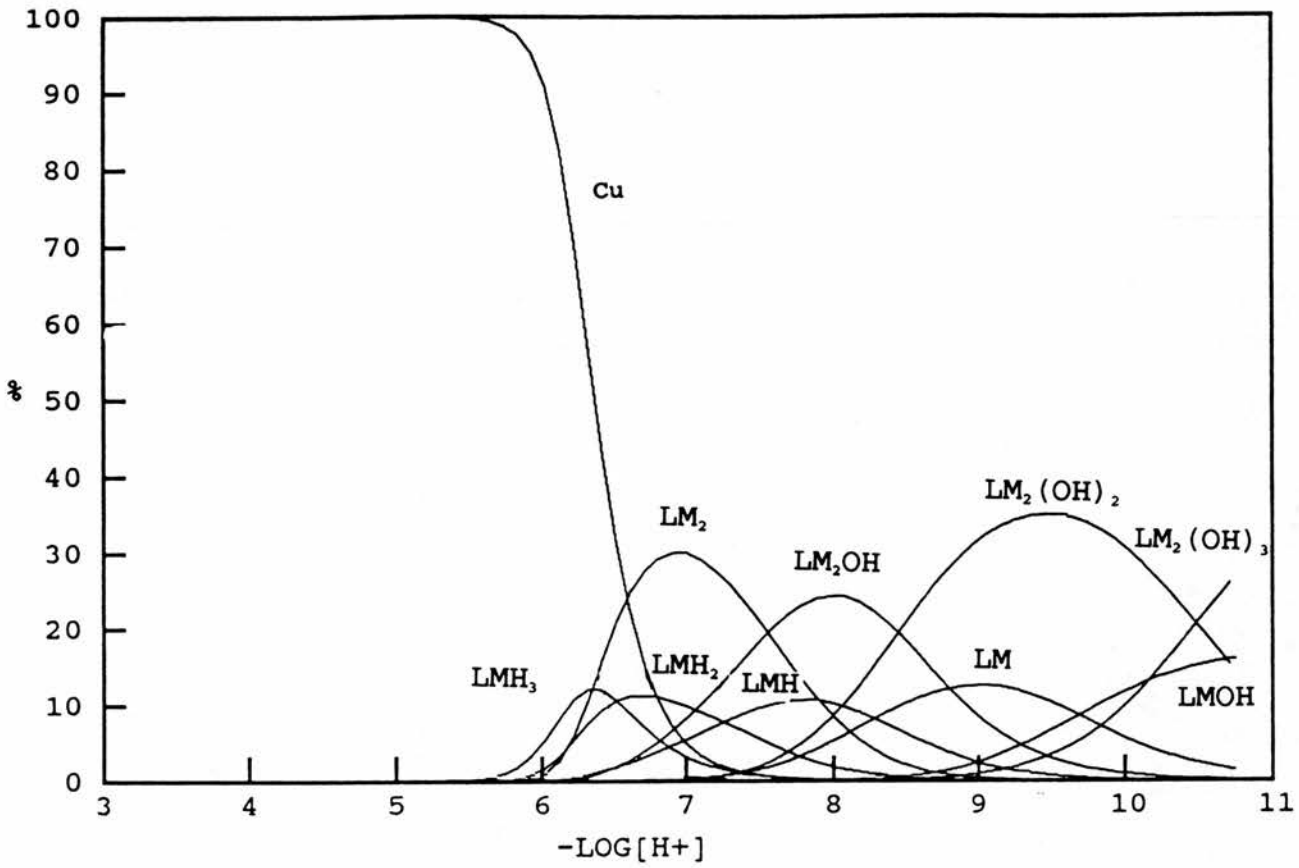

Figure 2.3.3.4. Speciation curves for copper(II) complexes of MPA

The initial pH of the complex in aqueous solution (5.5×10^{-3}) is 6.6. Potentiometric studies of the copper(II) complexes[58] have shown that several species are present at this pH. The speciation diagram for copper(II) complexes of MPA, Figure 2.3.3.4, shows that at pH 6.6 four species are present in appreciable quantities. These are the Cu(II) ion, the binuclear complex, the tri-protonated mononuclear complex and the di-protonated mononuclear complex. It is not unreasonable to expect that these complexes will undergo acid catalysed metal dissociation by different mechanisms.

The large absorption change at 270 nm for the first reaction compared with the second reaction suggests that the initial process could be the dissociation of the binuclear species. This is supported by the fact that when the initial pH of the complex solution is buffered at a lower pH the relative absorption change for the first reaction compared to the second is reduced and when the pH is increased the relative absorption change is higher. This reflects the changing concentration of the binuclear species compared to the mononuclear species. Fitting the data to the model;

$$k_{obs} = \frac{kK[H^+]}{1+K[H^+]}$$

gives values of $k = 52.5 \pm 6.2\ s^{-1}$ and $K = 89.3 \pm 9.4\ dm^3\ mol^{-1}$ for the first stage and $k = 2.74 \pm 0.61\ s^{-1}$ and $K = 100.7 \pm 3.1\ dm^3\ mol^{-1}$ for the second stage of the reaction. The binuclear copper(II) complex of the *para*-propyl ligand dissociates rapidly in acidic solution. The dissociation reaction is too rapid to be observed using the spectrascan stopped flow apparatus. Fixed wavelength measurements of the dissociation show that there is a complicated reaction mechanism. At low acid concentrations the dissociation demonstrates biphasic kinetics with the first of the two consecutive reactions having a linear dependence on $[H^+]$ and the second reaction demonstrating saturation kinetics as $[H^+]$ increases. A plot of $k_{(1)obs}$ *versus* $[H^+]$ gives a first order rate constant of $k = (1.54 \pm 0.21) \times 10^3\ dm^3\ mol^{-1}\ s^{-1}$. Using the saturation kinetic model as for the dissociation of Cu_2(MPA) gives values of $k = 33.3 \pm 3.4\ s^{-1}$ and $K = 515.2 \pm 31.1\ dm^3\ mol^{-1}$

2.4 References

1 Z. Tyeklar and K.D. Karlin, *Acc. Chem. Res.*, 1989, **22,** 241

2 T.N. Sorrell, *Tetrahedron,* 1989, **45,** 3

3 K.A. Magnus, H. Ton-That and J.E. Carpenter, *Chem. Rev.*, 1994, **94,** 727

4 W.P.J Gaykema, W.G.J. Hol, J.M. Vereijken, N.M. Soeter, H.J. Bak and J.J. Beintema, *Nature,* 1984, **309,** 23

5 H. Tin-That and K.A. Magnus, *Journal of Inorganic Biochemistry,* 1993, **51,** 65

6 N. Kitajima and Y. Moro-oka, *J. Chem. Soc., Dalton Trans.*, 1993, 2665

7 N. Kitajima, T. Koda, S. Hashimoto, T. Kitagawa and Y. Moro-oka, *J. Chem. Soc., Chem. Comm.*, 1988, 151

8 N. Kitajima, K. Fujisawa, Y. Moro-oka and K. Toriumi, *J. Am. Chem. Soc.*, 1989, **111,** 8975

9 K.A. Magnus, B. Hazes, H. Ton-That, C. Bonaventura, J. Bonaventura and W.G.J. Hol, *Proteins-Structure, Function and Genetics,* 1994, **19,** 302

10 E.I. Solomon, M.J. Baldwin and M.D. Lowery, *Chem. Rev.*, 1992, **92,** 521

11 D.E. Wilcox, A.G. Porras, Y.T. Wang, K. Lerch, M.E. Winkler and E.I. Solomon, *J. Am. Chem. Soc.*, 1985, **107,** 4015

12 A.C. Rosenzweig and S.J. Lippard, *Acc. Chem. Res.*, 1994, **27,** 229

13 A. Ivancich, V.V. Barynin and J.L. Zimmermann, *Biochemistry,* 1995, **34,** 6628

14 A.L. Vandenbrenk, K.A. Byriel, D.P. Fairlie, L.R. Gahan, G.R. Hanson, C.J. Hawkins, A. Jones, C.H.L. Kennard, B. Moubaraki and K.S. Murray, *Inorg. Chem.*, 1994, **33,** 3549

15 W. Steinkopf, R. Leitsmann, A.H. Muller and H. Wilhelm, *Leibigs Ann. Chem.*, 1939, **541,** 260

16 M. Meth-Cohn, *Quarterly Reports on Sulphur Chemistry,* 1970, **5,** 129

17 D.E. Fenton, B.P. Murphy, A.J. Leong, L.F. Lindoy, A. Bashall and M. McPartlin, *J. Chem. Soc., Dalton Trans.*, 1987, 2543

18 P.G. Owston, R. Peters, E. Ramsammy, P.A. Tasker and J. Trotter, *J. Chem. Soc., Chem. Comm.*, 1980, 1218

19 M.G.B. Drew, J. Nelson and S.M. Nelson, *J. Chem. Soc., Dalton Trans.*, 1981, 1678

20 H. Adams, N.A. Bailey, D.E. Fenton, R.J. Good, R. Moody and O.C. Rodriguez de Barbarin, *J. Chem. Soc., Dalton Trans.*, 1987, 207

21 R. Menif, A.E. Martell, P.J Squattrito and A. Clearfield, *Inorg. Chem.*, 1990, **29,** 4723

22 K. Motoda, H. Sakiyama, N. Matsumoto, H. Okawa and S. Kida, *Bull. Chem. Soc. Jpn.*, 1992, **65,** 1176

23 N.A. Bailey, M.M. Eddy, D.E. Fenton, S. Moss, A. Mukhopadhyay and G. Jones, *J. Chem. Soc., Dalton Trans.*, 1984, 2281

24 S.M. Nelson, *Pure Appl. Chem.*, 1980, **52,** 2461

25 M. Pietraszkiewicz and R. Gasiorowski, *Chem. Ber.*, 1990, **123,** 405

26 J. Nelson, B.P. Murphy, M.G.B. Drew, P.C. Yates and S.M. Nelson, *J. Chem. Soc., Dalton Trans.*, 1988, 1001

27 M.G.B. Drew, C. Cairns, A. Lavery and S.M. Nelson, *J. Chem. Soc., Chem. Comm.*, 1980, 1122

28 M.G.B. Drew, M. McCann and S.M. Nelson, *J. Chem. Soc., Dalton Trans.*, 1981, 1868

29 C. Harding, D. McDowell, J. Nelson, S. Raghunathan, C. Stephenson, M.G.B. Drew and P.C. Yates, *J. Chem. Soc., Dalton Trans.*, 1990, 2521

30 M.G.B. Drew, A. Rodgers, M. McCann and S.M. Nelson, *J. Chem. Soc., Chem. Comm.*, 1978, 415

31 S.M. Nelson, C.V. Knox, M. McCann and M.G.B. Drew, *J. Chem. Soc., Dalton Trans.*, 1981, 1669

32 S. Brooker, V. McKee, W.B. Shepard and L.K. Pannell, *J. Chem. Soc., Dalton Trans.*, 1987, 2555

33 S.M. Nelson, F. Esho, A. Lavery and M.B.G. Drew, *J. Am. Chem. Soc.*, 1983, **105,** 5693

34 N.A. Bailey, M.M. Eddy, D.E. Fenton, G. Jones, S. Moss and A. Mukhopadhyay, *J. Chem. Soc., Chem. Comm.*, 1981, 628

35 N.W. Alcock, R.G. Kingston, P. Moore and C. Pierpont, *J. Chem. Soc., Dalton Trans.*, 1984, 1937

36 D. Chen and A.E. Martell, *Tetrahedron,* 1991, **47,** 6895

37 J. Jazwinski, J-M. Lehn, R. Meric, J-P. Vigneron, M. Cesario, J. Guilhem and C. Pascard, *Tetrahedron Letters,* 1987, **28,** 3489

38 R. Menif and A.E. Martell, *J. Chem. Soc., Chem. Comm.*, 1989, 1521

39 R. Menif, A.E. Martell, P.J Squattrito and A. Clearfield, *Inorg. Chem.*, 1991, **30,** 1428

40 A. Llobet, J. Reibenspies and A.E. Martell, *Inorg. Chem.*, 1994, **33,** 5946

41 C.J. McKenzie, H. Toftlund, M. Pietraszkiewicz, S. Stojek and K. Slowinski, *Inorg. Chim. Acta,* 1993, **210,** 143

42 M. Shakir, O.S.M. Nasman and S.P. Varkey, *Polyhedron,* 1996, **15,** 309

43 M. Kumar, V.J. Aran, P. Navarro, A. Ramos-Gallardo and A. Vegas, *Tetrahedron Letters,* 1994, **35,** 5723

44 D. MacDowell and J. Nelson, *Tetrahedron Letters,* 1988, **29,** 385

45 V. McKee, M.J.R. Dorrity, J.F. Malone, D. Marrs and J. Nelson, *J. Chem. Soc., Chem. Comm.*, 1992, 383

46 D. McDowell, J. Nelson and V. McKee, *Polyhedron,* 1989, **8,** 1143

47 M.G.B. Drew, D. McDowell and J. Nelson, *Polyhedron,* 1988, **7,** 2229

48 V. McKee, W.T. Robinson, D. McDowell and J. Nelson, *Tetrahedron Letters,* 1989, **30,** 7453

49 C. Bazzicalupi, A. Bencini, A. Bianchi, V. Fusi, C. Giorgi, P. Paoletti, A. Stefani and B. Valtancoli, *Inorg. Chem.*, 1995, **34,** 552

50 T.W. Hambley, D.T. Richens and R.W. Hay, *14th International Symposium on Macrocyclic Chemistry. Absract SF37*

51 K.D. Matthews, I.A. Kahwa and D.J. Williams, *Inorg. Chem.*, 1994, **33,** 1382

52 M.G.B. Drew, M. McCann and S.M. Nelson, *J. Chem. Soc., Chem. Comm.*, 1979, 481

53 N.A. Bailey, D.E. Fenton, R. Moody, O.C. Rodriguez de Barbarin, I Nina, J.M. Latour, D. Limosin and V. McKee, *J. Chem. Soc., Dalton Trans.*, 1987, 2519

54 L. Qin, M. McCann and J. Nelson, *Journal of Inorganic Biochemistry,* 1993, **51,** 633

55 L.J. Murphy and L.J. Zompa, *Inorg. Chem.*, 1979, **18,** 3278

56 P.G. Graham and D.C. Weatherburn, *Aus. J. Chem.*, 1981, **34,** 291

57 D.C. Weatherburn, *Aus. J. Chem.*, 1983, **36,** 433

58 T. Clifford, *Ph.D. Thesis,* University of St. Andrews, 1996

Chapter 3

Studies of Cobalt(III) Complexes of [15]aneN$_4$

3.1 Introduction.

3.1.1 Tetraaza Macrocyclic Complexes.

For many years the importance of macrocyclic complexes in industrial, pharmacological and analytical chemistry has been appreciated, and more recently their use as models for their natural counterparts such as porphyrins and corrins has become more widespread. Consequently, investigations into the coordination chemistry of these complexes continues to be of interest. Although much of this work is centred on substituted and/or unsaturated nitrogen macrocyclic ligands, probably the best approach to understanding the coordination chemistry of these complexes is to study the behaviour of the saturated, unsubstituted tetraaza macrocycles.

Ring size is the single structural parameter that is uniquely characteristic of all macrocyclic ligands. By comparing the chemical and physical properties of these ligands with varying ring size a further understanding of macrocyclic coordination chemistry may be obtained.

It is the relative sizes of the ligand cavity and the ionic radius of the coordinating metal ion that must be considered when attempting to rationalise the chemistry of these complexes. The nature of the fit between the metal ion and the macrocycle cavity will determine the ligand field strength of the secondary amine donor atoms. Complexes in which the tetradentate chelation site fits the metal ion particularly well will have normal ligand field strengths. Those that have large cavity sizes produce weak ligand field strengths and those with a small cavity relative to the metal ionic radius, will produce unusually high strengths. If the cavity size is still smaller the

ligand may fail to encompass the metal ion and it will have to fold in order to chelate in a tetradentate manner. Occasionally the metal ion may fail to coordinate in a planar fashion with the four secondary amines and will form a complex analogous to the "sitting-a-top" complex in porphyrins[1].

Studies of the octahedral cobalt(III) complexes of the five macrocycles [12]aneN$_4$, [13]aneN$_4$, [14]aneN$_4$, [15]aneN$_4$ and [16]aneN$_4$ have shown how the relationship between the metal ionic radii and the cavity size affects the structures of the complexes. [Co([12]aneN$_4$)Cl$_2$]$^+$ exists only as the *cis-* isomer[2], Figure 3.1.1.1, because the metal is too large to fit within the small hole size of the 12-membered ring. The complexes [Co([13]aneN$_4$)]$^{3+}$ and [Co([14]aneN$_4$)]$^{3+}$ give complexes with both *cis-* and *trans-* geometry, whereas [Co([15]aneN$_4$)]$^{3+}$ and [Co([16]aneN$_4$)]$^{3+}$ give only *trans*-isomers[3].

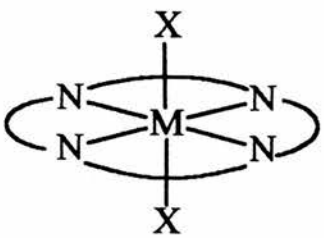

[M([15-16]aneN$_4$)X$_2$]$^{x+}$

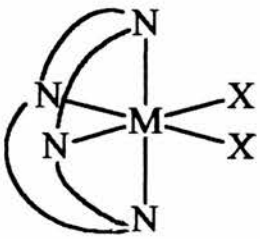

[M([12]aneN$_4$)X$_2$]$^{x+}$

Figure 3.1.1.1 *cis-* and *trans-* configurations of cyclic tetradentate ligands

Various physical techniques have been developed to differentiate between *cis-* and *trans-* isomers of macrocyclic complexes. Poon[4] demonstrated the usefulness of infra-red spectroscopy. It was shown that for four known *cis-* and *trans-* pairs of $[Co([14]aneN_4)X_2]Y$ the most consistent variations in the spectra occurred in the 800-910 cm^{-1} region. Complexes with a *trans-* configuration displayed two bands near 900 cm^{-1} and one band near 810 cm^{-1}, whereas those with a *cis-* configuration displayed at least five bands evenly spread between 800 and 910 cm^{-1}. Similar observations were made in the infra-red spectra of other macrocyclic complexes, with generally not more than three peaks in this region for the *trans-* complexes and at least five evenly arranged but less intense peaks in the spectra of *cis-* complexes.

3.1.2 Cobalt(III) Complexes of 1,4,8,12-tetraazacyclopentadecane

Most work on the chemistry of cobalt(III) complexes with unsubstituted, saturated tetraaza macrocycles has been concerned with complexes of $[12]aneN_4$ and $[14]aneN_4$. Obviously the ability of these complexes to form *cis-* or *trans-* isomers will affect their coordination chemistry; $[Co([12]aneN_4)]^{3+}$ forms only *cis-* complexes and $[Co([14]aneN_4)]^{3+}$ can form both *cis-* and *trans-* complexes. No evidence exists to suggest that $[Co([15]aneN_4)]^{3+}$ forms anything other than *trans-* complexes with monodentate anions.

1,4,8,12-tetraazacyclopentadecane ($[15]aneN_4$) is a hygroscopic solid[5] with a melting point of 99°C ± 1°C. The free base crystallises as white needles and is soluble in most

polar solvents. The ligand forms octahedral complexes with cobalt(III) and two monodentate anions. Six diastereoisomers can occur due to the existence of four chiral *sec*-NH centres and the ability of the chelate rings to adopt twist boat or chair structures[6], Figure 3.1.2.1.

The three six membered chelate rings may assume either twist (T) or chair (C) conformations, whereas the five membered ring may be either *gauche* (g) or *eclipsed* (e). The most stable conformation for the six membered ring is the chair form and for the five membered ring it is the *gauche* form. Of the six isomers it would appear that the *trans*-IV isomer should be the most stable and recent studies[5] show this to be so. Other studies[3] have described the isolation of two isomers of the complex *trans*-[Co([15]aneN$_4$)Cl$_2$]$^+$; isomer I and isomer II. These two isomers exhibit different physical properties including variations in colour, infrared spectra, electronic spectra, ^{13}C n.m.r. spectra and solubilities. The ^{13}C n.m.r. spectrum of isomer I displays eleven peaks which correspond to a molecule with eleven different carbon environments. This result indicates that the complex has no symmetry and therefore a point group C_1, identifying the isomer as *trans*-I. Isomer II can be prepared directly from *cis*-[Co([15]aneN$_4$)CO$_3$]$^+$, without N-H bond rupture, which indicates that the conformation is the same as that for the *cis*-complex. Since only those isomers which have two diagonal protons on the same side of the plane can fold readily to give the *cis*- configuration isomer II must be either *trans*- I, *trans*- IV, *trans*- V or *trans*- VI. Consideration of the symmetry indicated by the ^{13}C n.m.r. suggests that the isomer has the configuration of isomer IV.

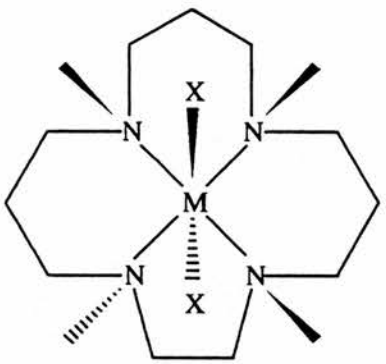

trans I

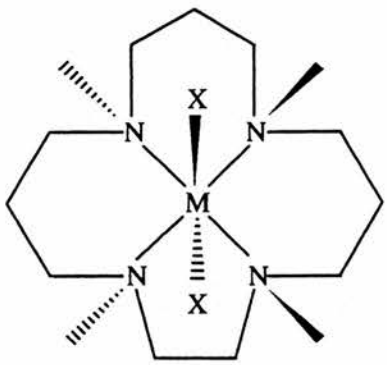

trans II

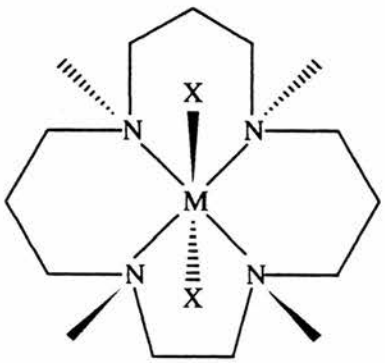

trans III

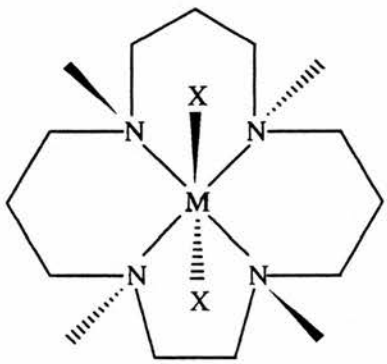

trans IV

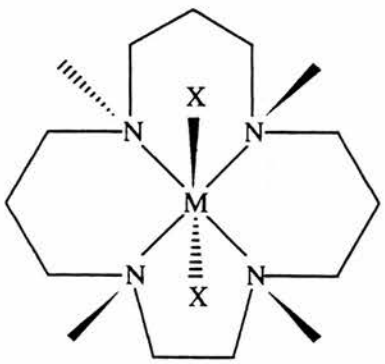

trans V

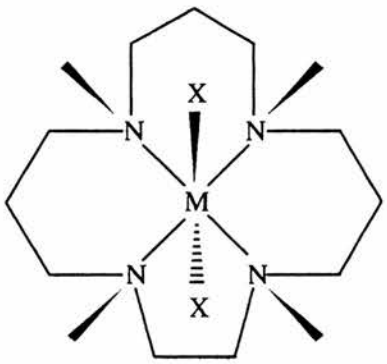

trans VI

Figure 3.1.2.1. The six diastereoisomers of $[Co([15]aneN_4)X_2]^{3+}$.

3.1.3 Kinetic Studies of the Acid Catalysed Aquation of [Co([15]aneN$_4$)Cl$_2$]$^+$.

Ligand substitution reactions of cobalt(III) complexes have been thoroughly investigated and their kinetic behaviour exemplifies the dissociative interchange mechanism[7]. This mechanistic assignment was based on the direct proportionality between the rate and equilibrium constants for cobalt(III) hydrolyses and the small positive values found for the volumes of activation[8]. However, different mechanistic pathways have been proposed for certain classes of cobalt(III) complexes, in particular cobalt(III) complexes with an equatorially bound tetraaza macrocyclic ligand have been shown to undergo a dissociative pathway in ligand substitution reactions. A large number of studies[9] have shown that in these systems the reaction rate varied as the leaving group was changed and that steric crowding of the reaction site accelerates the reaction rate. Both observations are consistent with a wholly dissociative mechanism.

Hung and Busch[10] studied the kinetics of the acid catalysed aquation reactions of a series of unsubstituted, saturated tetraaza macrocycles, [Co(MAC)Cl$_2$]$^+$, of varying ring size. In all cases the first step involves the replacement of a chloride by water. During this step it was found that there was full retention of configuration. The rates of the first aquation step for the *trans*- isomers can be arranged in the sequence [16]aneN$_4$ > [15]aneN$_4$ (isomer II) > [15]aneN$_4$ (isomer I) > [13]aneN$_4$ > [14]aneN$_4$. The two isomers of *trans*-[Co([15]aneN$_4$)Cl$_2$]$^+$ display different behaviour. Isomer I, the most stable isomer, undergoes two successive aquation reactions to form the diaqua complex, [(1) and (2) below].

$$trans\text{-}[Co(L)Cl_2]^+ + H_2O \rightleftharpoons trans\text{-}[Co(L)Cl(H_2O)]^{2+} + Cl^- \quad (1)$$

$$trans\text{-}[Co(L)Cl(H_2O)]^{2+} + H_2O \rightleftharpoons trans\text{-}[Co(L)(H_2O)_2]^{3+} + Cl^- \quad (2)$$

Isomer II first aquates to form the chloroaqua complex (step 3) and then isomerises (step 4) to form the configuration with the greatest stability (isomer I). This then undergoes a second aquation (step 5) to form the same diaqua complex as the aquation of isomer I.

$$trans(II)\text{-}[Co(L)Cl_2]^+ + H_2O \rightleftharpoons trans(II)\text{-}[Co(L)Cl(H_2O)]^{2+} + Cl^- \quad (3)$$

$$trans(II)\text{-}[Co(L)Cl(H_2O)]^{2+} \rightleftharpoons trans(I)\text{-}[Co(L)Cl(H_2O)]^{2+} \quad (4)$$

$$trans(I)\text{-}[Co(L)Cl(H_2O)]^{2+} + H_2O \rightleftharpoons trans(I)\text{-}[Co(L)(H_2O)_2]^{3+} + Cl^- \quad (5)$$

It was intended to confirm the results of Hung and Busch by studying the kinetics of the aquation reaction by conventional and stopped-flow visible spectrophotometry and by conductivity measurements.

3.1.4 Acid catalysed aquation of the $[Co([15]aneN_4)CO_3]^+$

As stated earlier, 15- and 16- membered macrocycles may experience steric crowding in the *cis*- configuration and therefore are more disposed toward *trans*- isomers with monodentate anions. However, with chelating bidentate ligands the macrocycle is forced to adopt a folded conformation around the metal centre because the bidentate ligand has to bind to two metal coordination sites which are *cis*- to each other. For example, all carbonato complexes have a *cis*- conformation.

There have been several studies[11,12,13] of the acid catalysed decarboxylation of cobalt macrocycle carbonato complexes. These have included cobalt carbonato complexes of $[12]aneN_4$, $[14]aneN_4$ and (5,7,7,12,14,14-hexamethyl-1,4,8,11-tetraazacyclotetradecane-4,11-diene), but have not included any 15- or 16- membered macrocycles. Many factors influence the rates of decarboxylation of which the two most important are probably the degree of strain in the folded macrocyclic ligand and the steric effects of the macrocycle at the fifth and sixth coordination sites of the metal.

The smaller the ring size the greater the degree of strain in the complex. This strain should be released on formation of a dissociative transition state leading to more rapid decarboxylation.

The rates for the three ligands so far studied support some of these ideas. $[Co([12]aneN_4)CO_3]^+$ has the fastest rate, followed by $[Co(trans\text{-}[14]diene)CO_3]^+$ both of which are approximately eight times faster than the rate for $[Co([14]aneN_4)CO_3]^+$. As expected the most strained complex has the fastest

decarboxylation rate. However, [Co(*trans*-[14]diene)CO_3]$^+$ is almost as fast which suggests that the ligand either does not sterically protect the carbonate ligand or that the diene is more strained than the corresponding unsubstituted, saturated macrocycle. The rate of acid catalysed decarboxylation of [Co([15]aneN$_4$)CO_3]$^+$ and [Co([16]aneN$_4$)CO_3]$^+$ is expected to be slower than for the smaller macrocycles.

3.2 Experimental

3.2.1 Synthesis

All materials were reagent grade and were purchased from the Aldrich.

Synthesis of [15]aneN$_4$ (1,4,8,12-tetra-azacyclopentadecane).

1,4,8,12-tetra-azacyclopentadecane was synthesised using a slightly modified version of Barefield's procedure[14]. Nickel(II) chloride hexahydrate (10.2 g, 0.043 mol) was dissolved in water (150 cm^3). To this solution was added N,N'-bis(3-aminopropyl)-1,3-propanediamine (8 g, 0.043 mol), with stirring, followed by 30-40% aqueous glyoxal solution (10 cm^3). The blue solution was then heated to 60-80°C for 2-3 hours during which time the solution changed to a brown-red colour. The solution was then transferred to a hydrogenation bottle along with 20 g of freshly prepared Raney nickel. After flushing the vessel with nitrogen the hydrogenation apparatus was heated to 70°C under 3.5 atmospheres of hydrogen until hydrogen uptake ceased. The violet solution was then filtered to remove the catalyst before it was cooled in an ice bath. To the cool solution sodium thiocyanate (5.2 g, 0.065 mol) dissolved in 25cm^3 of water was added. The purple precipitate was collected by filtration and was then dissolved in 75 cm^3 of water. To this, with appropriate precautions, sodium cyanide (5 g, 0.1 mol) was added and the solution refluxed for 1 hour. When cool, 5 g of sodium hydroxide was added and the solution was then extracted several times with dichloromethane. The extracts were combined and dried over anhydrous sodium

sulphate. After filtering to remove the sodium sulphate the dichloromethane was removed on a rotary evaporator to leave the product. This white powder was recrystallized from hexane to form white needle like crystals and the dried in *vacuo*. (Yield = 4.85 g, 52 %), M.W. 214.35 g mol^{-1}, m.p. 100°C; ν cm^{-1}, ν(N-H) 3242, 3270, 3283; N.M.R.; δ_H($CDCl_3$) 1.71 (6 H, quintet), 1.95 (4 H), 2.75 (16 H, multiplet)

Synthesis of 1,4,8,12-tetra-azacyclopentadecane tetrahydrochloride hemihydrate.

The hydrochloride salt of the ligand was prepared by adding an excess of concentrated hydrochloric acid to a saturated aqueous solution of 1,4,8,12-tetra-azacyclopentadecane (1.07 g, 5 mmol). The salt precipitated upon addition of the acid and was collected by filtration. Further purification was deemed unnecessary. (Yield = 1.64 g, 91 %), M.W. 360.20 g mol^{-1}, (Found: C, 35.54; H, 8.64; N, 15.12 %. Calculated for $C_{11}H_{30}N_4Cl_4 \cdot 0.5H_2O$: C, 34.93; H, 8.53; N, 14.81 %); m.p. 220-222°C; ν cm^{-1}, ν(N-H) 3242, 3270, 3283

Synthesis of [Co([15]aneN$_4$)Cl$_2$]ClO$_4$ (Isomer II) by aerial oxidation.

The preparation was essentially as reported by Islam and Uddin[15]. Cobalt(II) chloride

hexahydrate (1.42 g, 0.006 mol) and the ligand (1,4,8,12-tetra-azacyclopentadecane) (1.28 g, 0.006 mol) were dissolved in methanol (100 cm^3) to give a dark brown solution. Air, which had been passed through a solution of potassium hydroxide, was bubbled through this solution for 2 hours and then concentrated hydrochloric acid was added dropwise until the brown solution turned green (approx. 4 cm^3). Air was passed through the solution until its volume had been reduced to about 50 cm^3 and then 25 cm^3 of water was added. The volume of the solution was then reduced to *ca.* 30 cm^3 on a rotary evaporator. Perchloric acid (2 cm^3) was added to precipitate green crystals and which were filtered off. The product was recrystallised from hot hydrochloric acid, washed with iso-propanol and dried in *vacuo*.

This method gave low yields and occasionally the colour change associated with the aerial oxidation step did not occur.

This procedure gave only isomer II. A similar method was used to produce isomer I. (Yield = 0.53 g, 20 %), M.W. 443.64 g mol^{-1}, λ_{max} = 646, 486, 413 nm (ε = 25, 35, 51 dm^3 mol^{-1} cm^{-1}); ν cm^{-1}, ν(N-H) 3228 cm^{-1}; 1653, 1467, 1094, 624

Synthesis of [Co([15]aneN$_4$)Cl$_2$]ClO$_4$ (Isomer I) by aerial oxidation.

1,4,8,12-tetra-azacyclopentadecane (1.0 g, 4 mmol) was dissolved in methanol (60 cm^3) and an equimolar quantity of cobalt(II) chloride hexahydrate (0.95 g, 4 mmol). This solution was heated on a steam bath for 10 minutes and then concentrated hydrochloric acid (*ca.* 1 cm^3) was added dropwise until the purple

solution turned green. Air, which had been passed through a solution of potassium hydroxide, was then bubbled through the solution for two hours. The resultant brown solution was reduced in volume on a rotary evaporator to *ca.* 25 cm^3 and the product precipitated as the perchlorate salt by the addition of an excess of perchloric acid. A small quantity of the green isomer II was separated by recrystallising from acetonitrile. (Yield = 1.04 g, 39 %), M.W. 443.64 g mol^{-1}, (Found: C, 29.77; H, 5.70; N, 12.31 %. Calculated for $C_{11}H_{26}N_4Cl_3CoO_4$: C, 29.78; H, 5.91; N, 12.63 %); λ_{max} = 655, 513, 419 nm (ε = 51.5, 75.8, 122 dm^3 mol^{-1} cm^{-1}); ν cm^{-1}, ν(N-H) 3225, 1653, 1465, 1095, 623

Synthesis of [Co([15]aneN$_4$)Cl$_2$]ClO$_4$ (Isomer II) using Hydrogen Peroxide as the Oxidising Agent.

Cobalt(II) chloride hexahydrate (1.42 g, 0.006 mol) and the ligand (1,4,8,12-tetra-azacyclopentadecane) (1.28 g, 0.006 mol) were dissolved in methanol (100 cm^3) to give a dark brown solution. An excess of hydrogen peroxide was added and the solution was stirred at room temperature for 30 minutes. The volume of the solution was reduced to *ca.* 10 cm^3 on a rotary evaporator and then concentrated hydrochloric acid (*ca.* 2 cm^3) was added dropwise until the solution turned from purple to green. Sodium perchlorate (1.5 g 0.01 mol) was added to precipitate the product which was isolated by filtration and purified as described above.

This method gave higher yields than the aerial oxidation route. However, it produced

a greater proportion of isomer I which had to be separated from isomer II. This was done by washing with acetonitrile to remove isomer I which is considerably more soluble in the solvent than isomer II. (Yield; Isomer II, 1.14 g, 43 %; Isomer II, 0.35 g, 13 %), M.W. 443.64 g mol^{-1}

Synthesis of [Co([15]aneN$_4$)Cl$_2$]ClO$_4$ (Isomer II) from Na$_3$[Co(CO$_3$)$_3$]·3H$_2$O.

The hydrochloride salt of 1,4,8,12-tetra-azacyclopentadecane (1 g, 4 mmol) was ground into a fine powder with an equimolar quantity of sodium *tris*-carbonatocobaltate(III) trihydrate[16] (Na$_3$[Co(CO$_3$)$_3$]·3H$_2$O) (1.45 g, 4 mmol). To this powder water (4 cm^3) was added and the resulting green paste slowly changed colour to give a purple product. Upon completion of this reaction concentrated hydrochloric acid was added to give a green product which was recrystallised from methanol. However this product was deliquescent and it was found that a more stable product could be obtained in the form of the perchlorate salt by addition of an excess of sodium perchlorate to the methanolic solution. The precipitate was filtered, washed with cold methanol then diethyl ether and dried in *vacuo*. This method produced exclusively isomer II. (Yield 2.05 g, 77 %), M.W. 443.64 g mol^{-1}, (Found: C, 30.01; H, 5.48; N,12.87 %. Calculated for C$_{11}$H$_{26}$N$_4$Cl$_3$CoO$_4$: C, 29.78; H, 5.91; N, 12.63 %)

Synthesis of $[Co([15]aneN_4)CO_3]ClO_4$

The procedure for the synthesis of this product was initially the same as for the synthesis of $[Co([15]aneN_4)Cl_2]ClO_4$ using sodium *tris*-carbonatocobaltate(III) trihydrate. The hydrochloride salt of 1,4,8,12-tetra-azacyclopentadecane (1 g, 4 mmol) was ground into a fine powder with an equimolar quantity of sodium tris-carbonatocobaltate(III) trihydrate ($Na_3[Co(CO_3)_3]\cdot 3H_2O$) (1.45 g, 4 mmol). To this powder water (4 cm^3) was added and the resulting green paste slowly changed colour to give a purple product. The purple product was dissolved in ethanol (50 cm^3) and filtered. Sodium perchlorate (0.8 g, 6.5 mmol) was added to the filtrate and the purple perchlorate salt precipitated by the dropwise addition of petroleum ether. The product was further purified by recrystallisation from methanol and was dried in *vacuo*. (Yield 1.54 g, 89 %), M.W. 432.75 g mol^{-1}, (Found: C, 32.2 ; H, 5.8 ; N, 12.8 %. Calculated for $C_{12}H_{26}N_4ClCoO_7$: C, 33.3; H, 6.0; N, 12.9 %) λ_{max} 528, 369 nm (ε = 156, 216 $dm^3\ mol^{-1}\ cm^{-1}$) ν(N-H), 3237; ν(CO), 1657, 1615, 827, 753

3.2.2 Physical Measurements

Ultra-Violet/Visible Spectroscopy

UV/Visible spectra were measured using either a Philips PU 8720, a Perkin Elmer Lambda 5 or a Perkin Elmer Lambda 14P scanning spectrophotometer. The Perkin Elmer instruments were electronically thermostated using a Peltier electronic

thermostat whereas the Philips instrument was thermostated using a Heto circulating water bath. All samples were measured in a 1 cm quartz cell.

Infra-Red Spectroscopy

Infra-red spectra were measured with a Perkin Elmer 1710 Fourier Transform Infra-Red spectrometer. Samples were run as KBr discs and their infra-red spectra (4400-400cm^{-1}) were plotted.

Stopped Flow Kinetics and Equilibria Measurements

All stopped flow spectrophotometry was carried out using a High Tech SU 51 stopped flow spectrophotometer which had thermostatically controlled reactant reservoir and reaction chamber. Solutions of hydrochloric acid were made up from Volucon standard concentrate.

Conductivity Measurements

Conductivity measurements were performed using an AGB 1000 conductivity meter outputing to a chart recorder.

3.3 Results and Discussion.

3.3.1 Synthesis

The synthesis of the macrocycle 1,4,8,12-tetraazacyclopentadecane and its tetrahydrochloride salt by literature methods were successful. The preparation of cobalt(III) complexes using the methods of Busch *et al*[17] gave poor yields and alternative methods of synthesis were investigated. The low yield could be due to an acid catalysed demetallation reaction occurring during the oxidation step. It was found that increasing the quantity of acid added and the time allowed for oxidation both decreased the yield of *trans*-$[Co([15]aneN_4)Cl_2]^+$, Figure 3.3.1.1. Infra red spectra of the product showed that the protonated ligand was present in the complex. The use of hydrogen peroxide as an oxidising agent gave good yields of isomer I but also significant quantities of isomer II. Separation of the two isomers was not difficult because of the greater solubility of isomer I in acetonitrile compared with isomer II. Preparation of isomer II using sodium *tris*-carbonatocobaltate(III) trihydrate ($Na_3[Co(CO_3)_3]\cdot 3H_2O$) to prepare the *cis*-$[Co([15]aneN_4)CO_3]^+$ intermediate followed by acid hydrolysis significantly increased yields of isomer II. Additionally the reaction produced exclusively isomer II. The isolation of *cis*-$[Co([15]aneN_4)CO_3]^+$ using the same method was also successful. It appears that sodium *tris*-carbonatocobaltate(III) trihydrate is a versatile intermediate for the preparation of cobalt(III) complexes of this type.

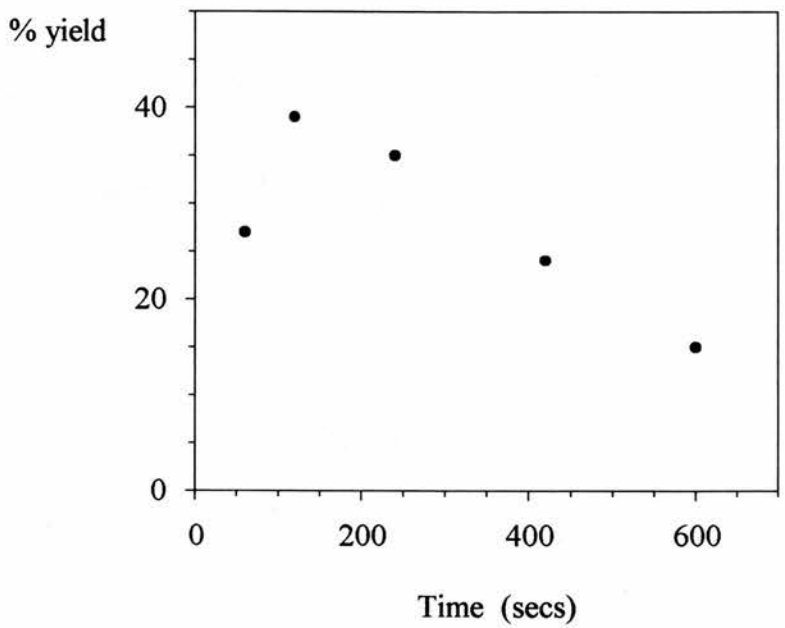

Figure 3.3.1.1. Yield *versus* time allowed for aerial oxidation for the preparation of *trans*-[Co([15]aneN$_4$)Cl$_2$]$^+$.

Aqueous solutions of the complexes were stable for several days. Perchlorate salts of the *trans*-cobalt(III) complexes were susceptible to reduction in the solid state and therefore freshly prepared samples were always used for kinetic studies.

3.3.2 Acid Catalysed Decarboxylation of *cis*-[Co([15]aneN$_4$)(CO$_3$)]$^+$

As stated earlier, there have been several studies of the acid catalysed decarboxylation of cobalt(III) carbonato complexes of macrocyclic tetra-amines[6,10,11] and many studies of the decarboxylation of non-cyclic amine complexes[18,19,20]. These investigations have established that the cobalt(III) complexes all undergo acid catalysed aquation *via* a common mechanism involving opening of the carbonato chelate ring followed by a rapid decarboxylation of the monodentate carbonato intermediate.

$$cis\text{-}[Co(L)(CO_3)]^+ + H_2O \xrightarrow{k_0} cis\text{-}[Co(L)(OH)(HCO_3)]^+ \quad (1)$$

$$cis\text{-}[Co(L)(CO_3)]^+ + H_3O^+ \xrightarrow{k_H} cis\text{-}[Co(L)(H_2O)(HCO_3)]^{2+} \quad (2)$$

$$cis\text{-}[Co(L)(H_2O)(HCO_3)]^{2+} \xrightarrow{k_1} cis\text{-}[Co(L)(OH)(H_2O)]^{2+} + CO_2 \quad (3)$$

$$cis\text{-}[Co(L)(OH)(H_2O)]^{2+} + H_3O^+ \overset{K_2}{\rightleftharpoons} cis\text{-}[Co(L)(H_2O)_2]^{3+} + H_2O \quad (4)$$

The conversion of the monodentate bicarbonato species (step 3) to the hydroxy-aqua species is fast and not rate determining. The ring opening step is found to be catalysed by both water (step 1) and acid (step 2) and the rate expression for the two parallel reactions is given by;

$$k_{obs} = k_0 + k_H[H^+] \quad (5)$$

where k_0 is the rate constant for the solvolytic pathway and k_H is the rate constant for the acid catalysed pathway.

If the tetraamine is a large ring macrocycle (> 13 membered ring) capable of forming stable *trans*-complexes then the decarboxylation reaction is followed by a *cis* ⟶ *trans* isomerisation which can be observed kinetically.

$$cis\text{-}[Co(L)(H_2O)_2]^{3+} \xrightarrow{k_i} trans\text{-}[Co(L)(H_2O)_2]^{3+} \qquad (6)$$

There is a large variation in the rate constant for the acid catalysed aquation (k_H) as a function of the structure of the inert amine. This variation, of up to six orders of magnitude, has been attributed to several factors including sterically induced strain within the carbonato chelate ring caused by the N_4 ligand and the electron donating ability of the N_4 ligand.

Previous studies of the acid catalysed decarboxylation of cobalt(III) macrocyclic complexes have concentrated on 14 membered rings. One investigation has dealt with the cobalt(III) complex of the 12-membered ring 1,4,7,10-tetra-azacyclododecane (cyclen)[11]. In order to gain further insights into the above relationships the acid catalysed aquation of *cis*-$[Co([15]aneN_4)(CO_3)]^+$ has been studied.

Figure 3.3.2.1 shows the time interval scan for the reaction between 7.21×10^{-4} mol dm^{-3} $[Co([15]aneN_4)(CO_3)]^+$ and 0.5 mol dm^{-3} $[HNO_3]$ at 35°C and constant ionic strength (I = 1.0 mol dm^{-3}). The spectra, taken every two minutes as the reaction proceeded, show that the reaction is not of a simple pseudo-first order

Figure 3.3.2.1. The time interval scan for the reaction between 7.21×10^{-4} mol dm^{-3} $[Co([15]aneN_4)(CO_3)]^+$ and 0.5 mol dm^{-3} $[HNO_3]^+$ at 35°C. $\Delta t = 5$ mins. Final spectrum = 60 mins

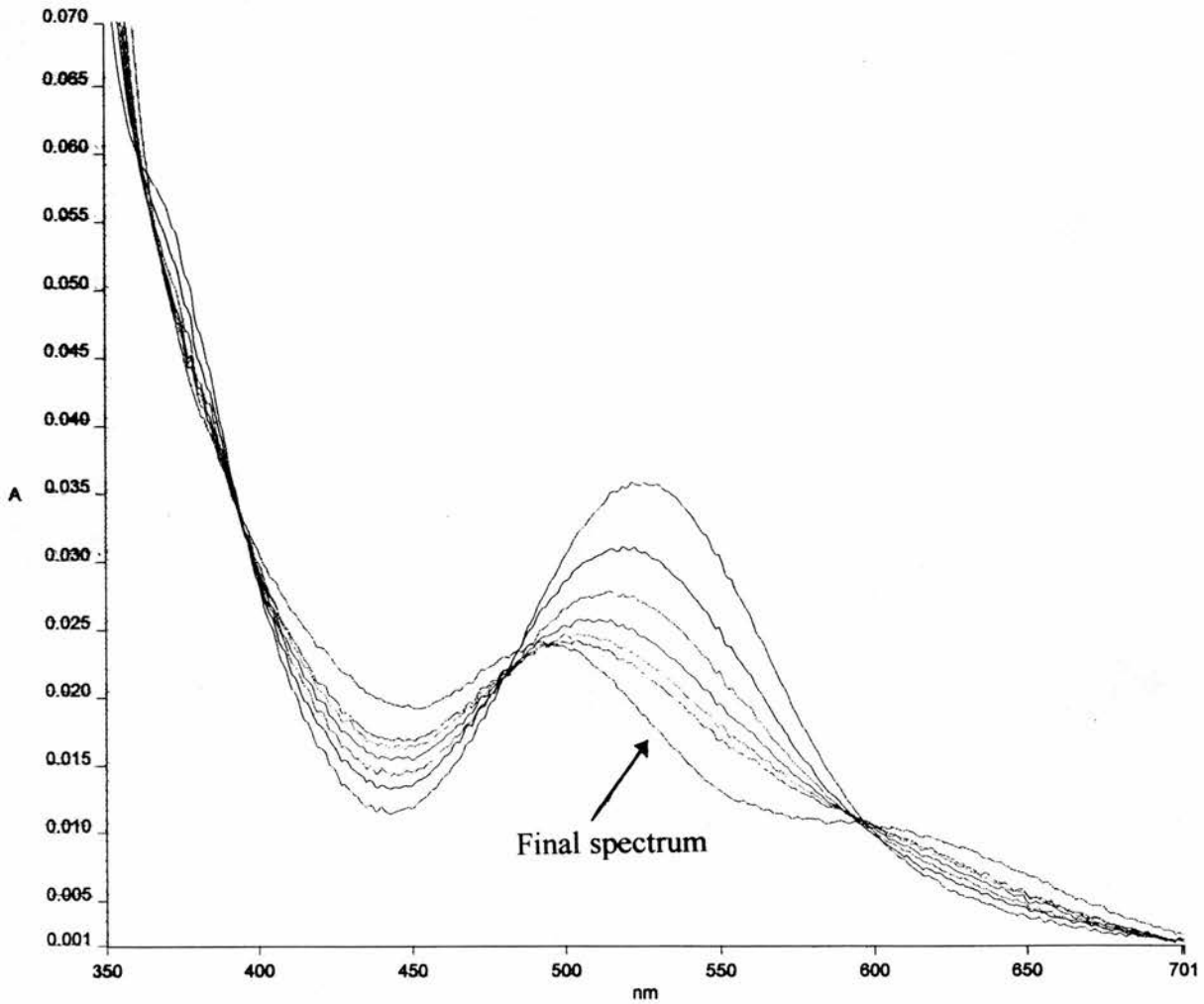

nature. This can be seen by plotting the absorbance *versus* time at a fixed wavelength (540 nm) as shown in Figure 3.3.2.2. The decrease in absorbance at 540 nm does not follow a simple exponential decay.

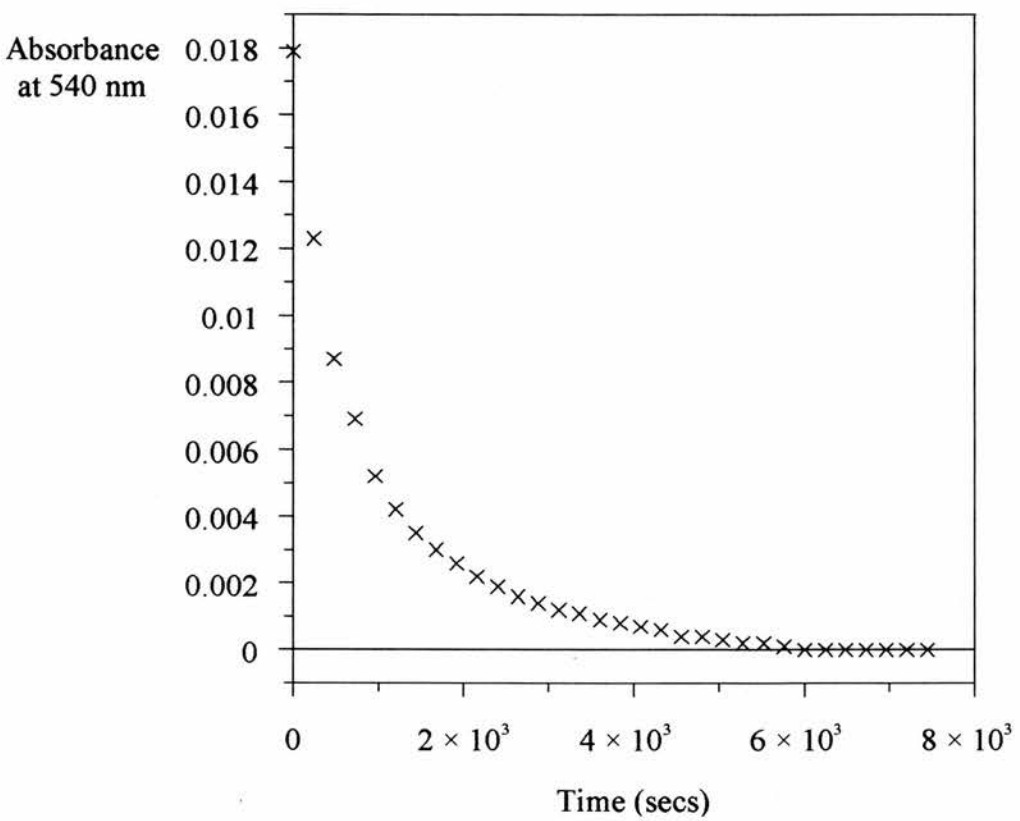

Figure 3.3.2.2. Absorbance at 540 nm *versus* time for the acid catalysed aquation of $[Co([15]aneN_4)(CO_3)]^+$ $[H^+] = 0.5$ mol dm^{-3}, I = 1.0 mol dm^{-3}, T = 35°C

Plots of $\log(A_t - A_\infty)$ *versus* time were not linear over the full time scale. Good fits were obtained for two consecutive exponential decays. By splitting the time interval

scans into two stages it can be seen that the reaction consists of two first order steps. The first stage of the reaction is shown in Figure 3.3.2.3. The initial spectrum is that of *cis*-[Co([15]aneN$_4$)(CO$_3$)]$^+$ with bands at 369 nm and 528 nm. As the reaction proceeds the band at 528 nm decreases in intensity and moves to slightly lower wavelengths (*ca.* 518 nm) while the band at 369 nm disappears. These changes are accompanied by isosbestic points at 397, 477 and 587 nm. The time interval scans for the second stage of the reaction are shown in Figure 3.3.2.4. During this step the band at 518 nm shifts to a lower wavelength of *ca.* 490 nm and decreases slightly in intensity. A new band of low intensity appears at 610 nm. These changes are accompanied by clean isosbestic points at 367, 406, 491 and 598 nm indicating the presence of only two uniquely absorbing species.

By monitoring the reaction at 485 nm, a wavelength midway between two of the isosbestic points for each consecutive reaction, a decrease in absorbance should be observed as the first stage proceeds and then as the second stage occurs the absorbance should increase. Figure 3.3.2.5, a plot of absorbance at 485 nm *versus* time, shows this to be the case.

Figure 3.3.2.3. The time interval scan for the first stage of the reaction between 7.21×10^{-4} mol dm^{-3} [Co([15]aneN$_4$)(CO$_3$)]$^+$ and 0.5 mol dm^{-3} [HNO$_3$] at 35°C. $\Delta t = 2$ mins. (I = 1.0 mol dm^{-3}).

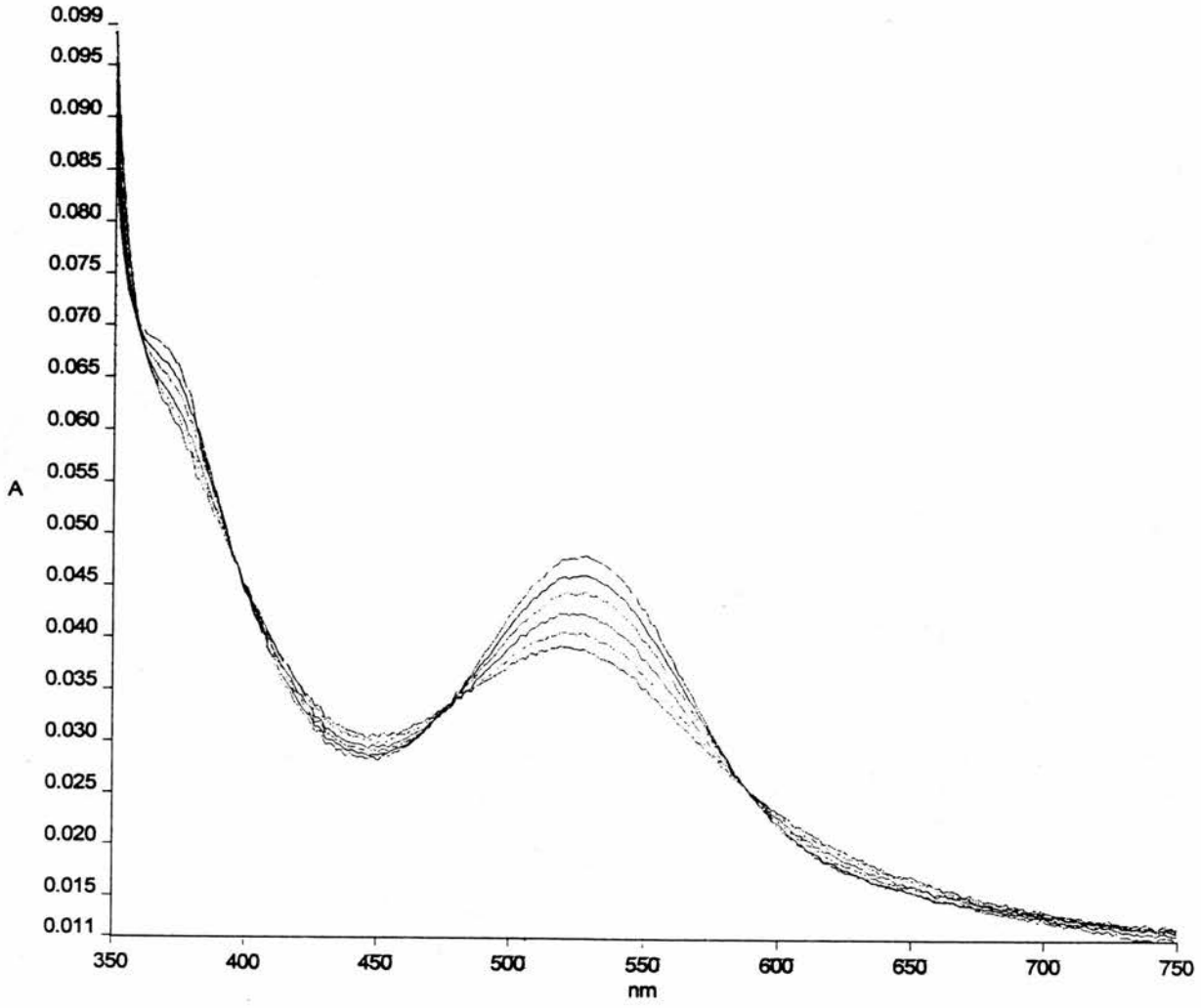

Figure 3.3.2.4. The time interval scan for the second stage of the reaction between 7.21×10^{-4} mol dm^{-3} [Co([15]aneN$_4$)(CO$_3$)]$^+$ and 0.5 mol dm^{-3} [HNO$_3$] at 35°C. $\Delta t = 2$ mins. (I = 1.0 mol dm^{-3}).

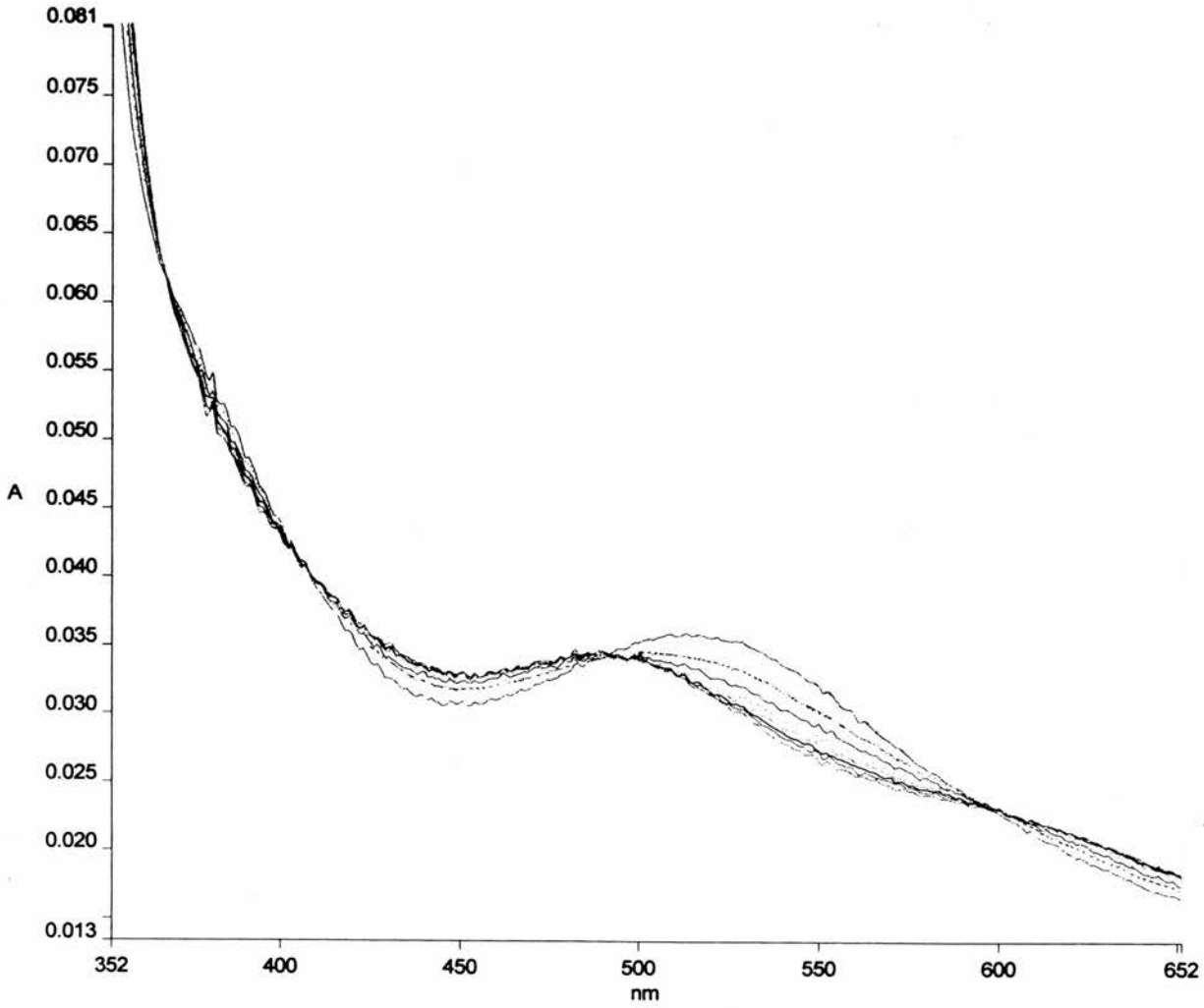

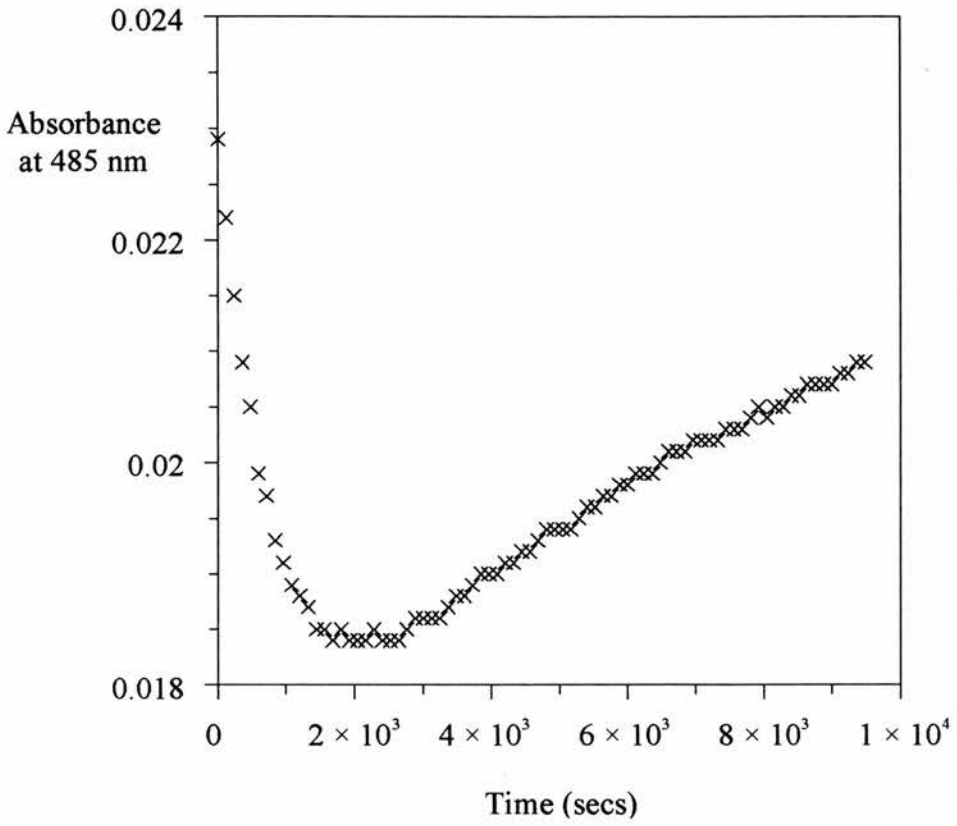

Figure 3.3.2.5. Absorbance at 484 nm *versus* time for the acid catalysed aquation of $[Co([15]aneN_4)(CO_3)]^+$ $[H^+] = 0.5$ mol dm^{-3}, I = 1.0 mol dm^{-3}, T = 30°C

The data obtained at 485 and 540 nm was treated in a manner analogous to the treatment of radioactive decay where a daughter species is generated whose decay half life is longer than that of the parent (Appendix 1). Good fits to the data were obtained with this model. Values for k_{1obs} and k_{2obs} were obtained for acid strengths of $0.1 > [H^+] > 1.0$ mol dm^{-3} and at temperatures of 15, 25, 30, 35, 40 and 45 °C. The results are summarised Table 3.3.2.1.

Table 3.3.2.1. Values of k_{1obs} for the acid catalysed aquation of $[Co([15]aneN_4)(CO_3)]^+$. I = 1.0 mol dm^{-3}

[H$^+$]	Temperature (°C)					
	15	25	30	35	40	45
	10^3 k_{1obs} (s^{-1})					
0.05	0.02	0.25	0.29	0.47	1.10	1.93
0.125	0.07	0.34	0.43	0.90	1.53	2.85
0.25	0.14	0.49	0.78	1.20	2.22	4.16
0.375	0.20	0.63	1.21	2.18	3.31	5.38
0.5	0.27	0.74	1.53	2.40	3.69	5.42

The first stage of the reaction involves the conversion of *cis*-$[Co([15]aneN_4)(CO_3)]^+$ with λ_{max} of 369 and 528 nm (ε = 216, 156 dm^3 mol^{-1} cm^{-1}) to a product with λ_{max} of 518 nm. This product appears to be *cis*-$[Co([15]aneN_4)(H_2O)_2]^{3+}$. Attempts to synthesise *cis*-$[Co([15]aneN_4)(H_2O)_2]^{3+}$ to characterise the intermediate were unsuccessful. However, a comparison of the spectral changes for the aquation of *cis*-$[Co([15]aneN_4)(CO_3)]^+$ with those for the aquation of the analogous complexes *cis*-$[Co(cyclam)(CO_3)]^+$ and *cis*-$[Co(tet\ b)(CO_3)]^+$ suggest that the diaqua complex is indeed the intermediate, Table 3.3.2.2.

Table 3.3.2.2. Comparison of λ_{max} and ε changes for the aquation of three Co(III) carbonato complexes.

	cis-$[Co(cyclam)X]^{n+}$		*cis*-$[Co([15]aneN_4)X]^{n+}$		*β-cis*-$[Co(tetb)X]^{n+}$	
	λ_{max} (nm)	ε ($M^{-1}cm^{-1}$)	λ_{max} (nm)	ε ($M^{-1}cm^{-1}$)	λ_{max} (nm)	ε ($M^{-1}cm^{-1}$)
$X_n = CO_3$	365	140	369	182	380	180
	520	164	528	138	551	184
$X_n = (H_2O)_2$	367	99	518		383	133
	506	110			534	91

The bands at 520 and 551 nm for *cis*-$[Co(cyclam)X]^{n+}$ and *cis*-β[Co(tet *b*)$X]^{n+}$ both move to shorter wavelengths and decrease in intensity upon conversion to the *cis*-diaqua species. This is also found to be the case for $[Co([15]aneN_4)(CO_3)]^+$ as the initial step of the aquation reaction occurs a similar decrease in absorption is also observed at *ca.* 365 nm. Previous kinetic studies have also found that the initial product of aquation is the *cis*-diaqua complex. Dasgupta[12] observed that step 3 in the decarboxylation of the cyclam complex is very rapid (k_1 is large) and this would also be expected to be the case for the present system.

Plots of k_{1obs} *versus* the concentration of HNO_3 are linear and display small positive intercepts. The rate expression is of the form $k_{1obs} = k_0 + k_H[H^+]$. The values of k_H and k_0 obtained are listed in Table 3.3.2.3.

Table 3.3.2.3. Calculated values of k_0 and k_H for the water and acid catalysed carbonato ring opening of $[Co([15]aneN_4)(CO_3)]^+$. I = 1.0 mol dm^{-3}.

Temperature (°C)	$10^3\, k_H$ (dm^3 mol^{-1} s^{-1})	$10^4\, k_0$ (s^{-1})
15	0.55 ± 0.01	0.02 ± 0.04
25	1.10 ± 0.04	1.2 ± 0.4
30	2.85 ± 1.17	1.1 ± 0.4
35	4.46 ± 0.52	2.7 ± 1.6
40	6.54 ± 0.46	8.0 ± 1.4
45	10.1 ± 1.3	10.8 ± 4.0

Values of k_0 are subject to large errors. The uncertainty in k_0 arises from the rather small intercept in a large linear extrapolation. More reliable k_0 values could be obtained by studying the reaction at lower H^+ concentrations where the errors are smaller. Using Arrhenius (ln k_H *versus* 1/T) and Eyring (ln (k_H/T) *versus* 1/T) plots, values of the activation energy (E_a), 164 ± 18.7 kJ mol^{-1}, enthalpy of activation ($\Delta H^{\ddagger}$) 161.6 ± 18.7 kJ mol^{-1} and the entropy of activation ($\Delta S_{298}^{\ddagger}$) 211 ± 62 J K^{-1} mol^{-1} can be obtained for the water catalysed ring opening reaction (k_0). Table 3.3.2.4 compares these values with those found for similar Co(III) carbonato complexes.

Table 3.3.2.4. Rate and Activation Parameters for Water Catalysed Ring Opening Reactions at 25 °C.

Complex Ion	$10^4 k_0$ (mol dm^{-3} s^{-1})	$\Delta H^{\ddagger}$ (kJ mol^{-1})	$\Delta S_{298}^{\ddagger}$ (J K^{-1} mol^{-1})	I (mol dm^{-3})	Ref.
$(NH_3)_4$	1.3 ± 0.2	50 ± 4	−155 ± 79	0.5	21
$(en)_2$	1.2 ± 0.2	75 ± 13	−63 ± 38	0.5	22
$(pn)_2$	1.0 ± 0.2	75 ± 13	−63 ± 38	0.5	22
tren	1.7 ± 0.2	63 ± 8	−105 ± 21	0.5	18
$(py)_4$	(1.3 ± 0.1) × 10^{-6}	139 ± 3	109 ± 6	1.0	23
cis-$(en)(H_2O)_2$	710	169 ± 34	300 ± 122	1.0	24
trans-Me_2[14]diene	0.75	115 ± 28	65 ± 89	0.5	25
$[15]aneN_4$	1.2 ± 0.3	162 ± 19	211 ± 62	1.0	This work

The values of k_0 vary over four orders of magnitude. The activation parameters for these and other related complexes demonstrate a good isokinetic relationship, Figure 3.3.2.6, supporting a common mechanism for the reactions.

Figure 3.3.2.6. $\Delta S_{298}^{\ddagger}$ *versus* $\Delta H^{\ddagger}$ for the water catalysed ring opening step in the decarboxylation of various Co(III) carbonato complexes.

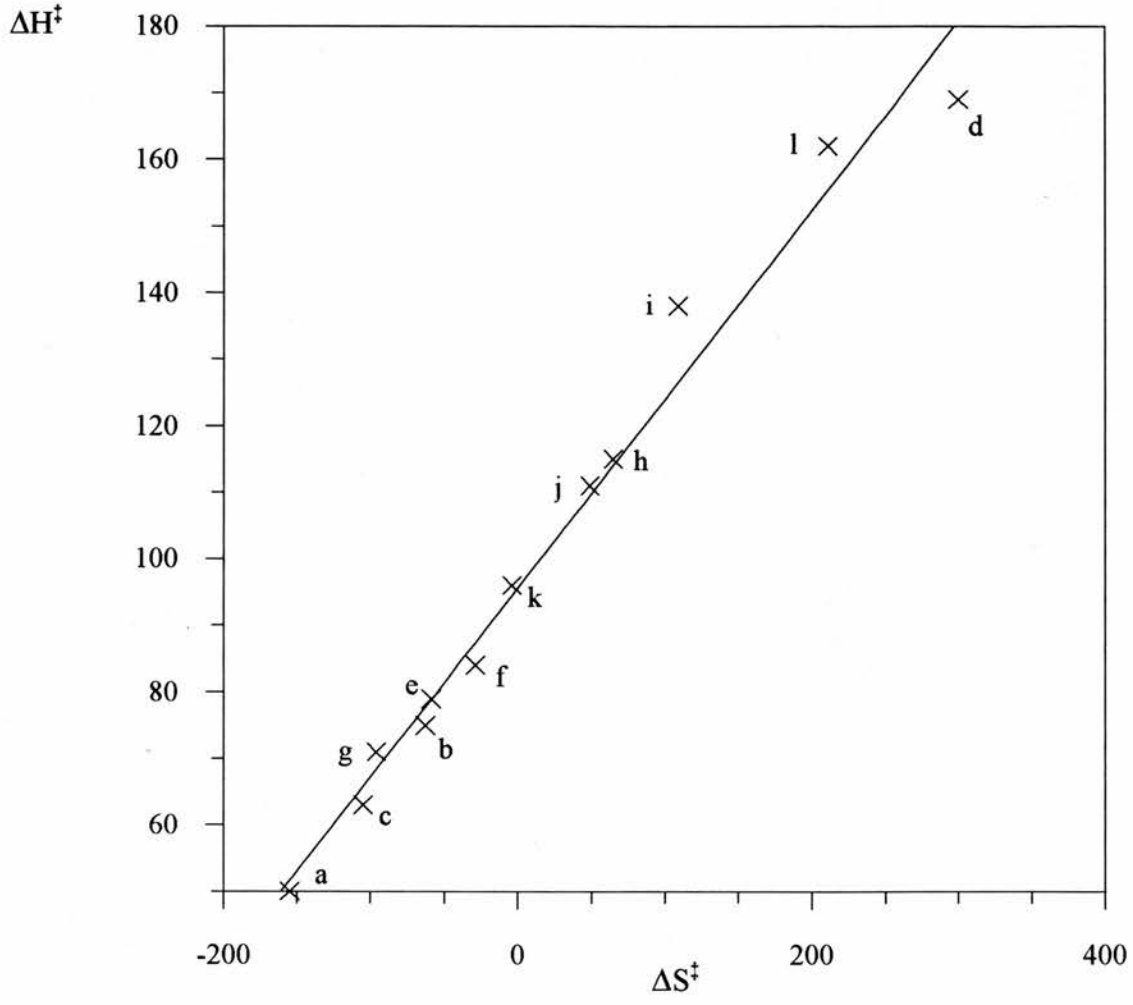

		Ref			Ref
a	$[Co(NH_3)_4CO_3]^+$	21	g	β-$[Co(trien)CO_3]^+$	18
b	$[Co(en)_2CO_3]^+$	22	h	$[Co(Me_2[14]dieneN_4)CO_3]^+$	25
c	$[Co(tren)CO_3]^+$	18	i	$[Co(py)_4CO_3]^+$	23
d	*cis*-$[Co(en)(H_2O)_2CO_3]^+$	24	j	*cis*-$[Co(py)_2(H_2O)_2CO_3]^+$	26
e	*trans*-$[Co(en)(NH_3)_2CO_3]^+$	18	k	*cis*-$[Co(py)_2(CO_3)_2]^-$	27
f	α-$[Co(trien)CO_3]^+$	18	l	$[Co([15]aneN_4)CO_3]^+$	

The activation parameters for the acid catalysed ring opening step (k_H) were also determined. An Arrhenius plot gives an activation energy of 73.5 ± 1.7 kJ mol^{-1} and an Eyring plot the enthalpy of activation ($\Delta H^{\ddagger}$) of 71.0 ± 1.7 kJ mol^{-1} and the entropy of activation ($\Delta S_{298}^{\ddagger}$) of –60.6 ± 5.7 J K^{-1} mol^{-1}.

The enthalpy and entropy of activation and values of k_H are compared with those determined for other similar carbonato complexes in Table 3.3.2.5. The variation of k_H is approximately six orders of magnitude. Values of k_H for the macrocyclic complexes are all about three orders of magnitude smaller than those for the simple tetraamines ($(NH_3)_4$, $(en)_2$, $(pn)_2$). Within the group of macrocyclic complexes studied the cobalt(III)carbonato complex of *trans*-Me$_2$[14]diene aquates at the fastest rate followed by *trans*-Me$_6$[14]diene, [12]aneN$_4$ (cyclen) and then [15]aneN$_4$. Co([15]aneN$_4$)CO$_3^+$ undergoes acid catalysed ring opening some four times faster than Co([14]aneN$_4$)CO$_3^+$.

Table 3.3.2.5. Rate Constants and Activation Parameters for the Acid Catalysed Ring Opening Reaction at 25 °C.

Complex Ion	k_H (mol dm^{-3} s^{-1})	$\Delta H^{\ddagger}$ (kJ mol^{-1})	$\Delta S_{298}^{\ddagger}$ (J K^{-1} mol^{-1})	I (mol dm^{-3})	Ref.
$(NH_3)_4$	1.5 ± 0.1	64 ± 4	−26 ± 16	0.5	21
$(en)_2$	0.6 ± 0.05	59 ± 13	−54 ± 38	0.5	22
$(pn)_2$	0.5 ± 0.05	59 ± 13	−54 ± 38	0.5	22
tren	2.0 ± 0.05	46 ± 4	−84 ± 17	0.5	22
$(py)_4$	$(8.0 \pm 0.5) \times 10^{-6}$	97 ± 4	−17 ± 13	5.0	23
trans-Me_6[14]diene	8×10^{-3}	71 ± 21	−42 ± 71	0.25	13
trans-Me_2[14]diene	1.5×10^{-2}	81 ± 1	−6 ± 2	0.5	25
[12]$aneN_4$ (cyclen)	7.0×10^{-3}	100.4	+51	0.5	11
[14]$aneN_4$ (cyclam)	1.3×10^{-3}	86 ± 2	−11 ± 5	0.5	12
[15]$aneN_4$	5.5×10^{-3}	71 ± 2	−61 ± 6	1.0	This work

The non-participating ligands and the charge on the metal ion effect the strength of the Co—O bond which in turn will determine the value of k_H. A plot of $\Delta H^{\ddagger}$ *versus* $\Delta S_{298}^{\ddagger}$, Figure 3.3.2.7, gives an isokinetic plot with considerable scatter.

Figure 3.3.2.7. $\Delta S_{298}^{\ddagger}$ *versus* $\Delta H^{\ddagger}$ for the acid catalysed ring opening step in the decarboxylation of various Co(III) carbonato complexes.

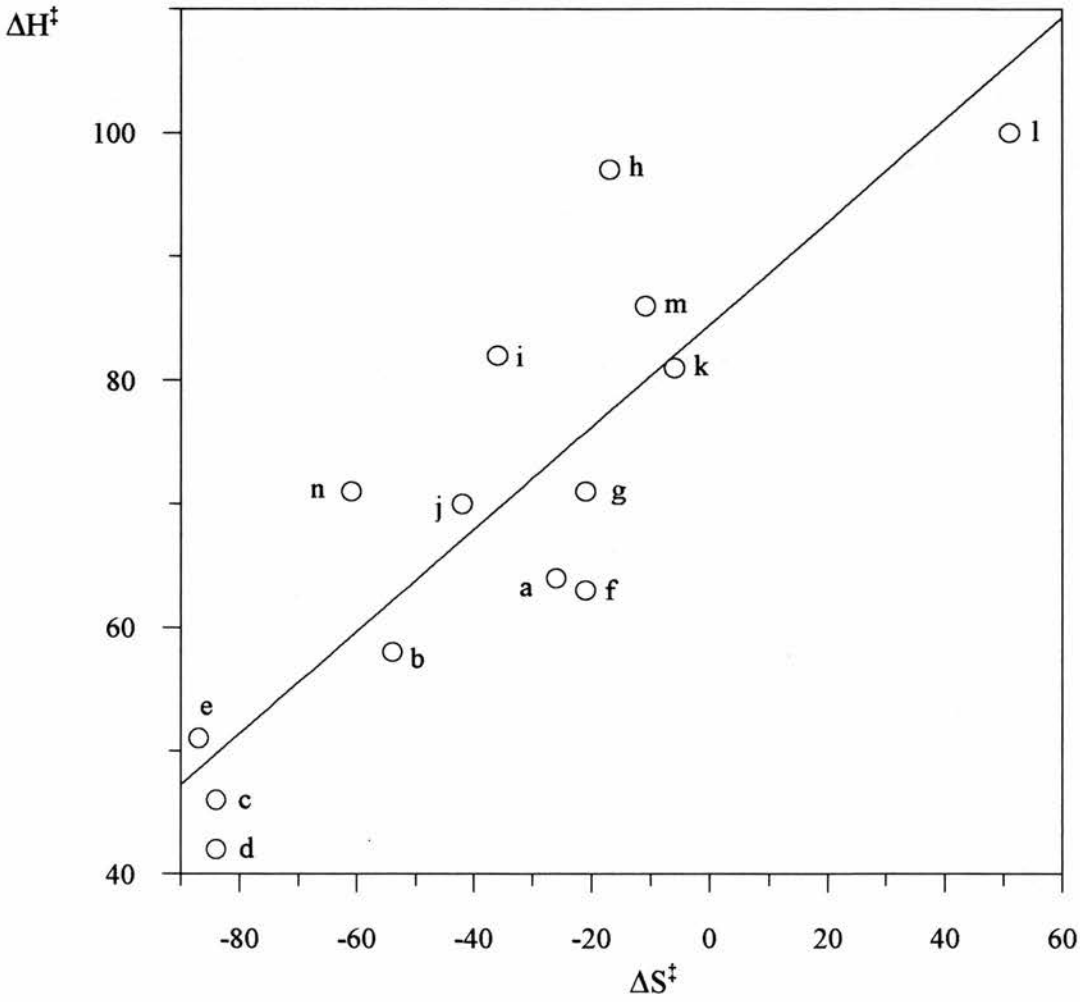

		Ref			Ref
a	$[Co(NH_3)_4CO_3]^+$	21	h	$[Co(py)_4CO_3]^+$	23
b	$[Co(en)_2CO_3]^+$	22	i	*cis*-$[Co(py)_2(H_2O)_2CO_3]^+$	26
c	$[Co(tren)CO_3]^+$	18	j	$[Co(Me_6[14]dieneN_4)CO_3]^+$	13
d	*trans*-$[Co(en)(NH_3)_2CO_3]^+$	18	k	$[Co(Me_2[14]dieneN_4)CO_3]^+$	25
e	*cis*-$[Co(en)(H_2O)_2CO_3]^+$	24	l	$[Co(cyclen)CO_3]^+$	11
f	α-$[Co(trien)CO_3]^+$	18	m	$[Co(cyclam)CO_3]^+$	12
g	β-$[Co(trien)CO_3]^+$	18	n	$[Co([15]aneN_4)CO_3]^+$	

Francis and Jordan[28] have proposed that there is a correlation between the rate constant k_H and the average pK_a of the amine ligands in the $[Co(III)N_4CO_3]^+$ complexes. The average pK_a of the amine ligand can be used as a very rough measure of the basicity and hence electron donating ability of the nitrogen atoms. As the electron donating ability decreases an increase in the residual positive charge on the cobalt atom would be expected to lead to a stronger Co—O bond. Therefore the more acidic the amine ligands the stronger the Co—O bonds. Table 3.3.2.6 lists the average pK_a values of some of the amine ligands compared previously.

Table 3.3.2.6. Average pK_a values for N containing ligands.

Ligand	Average pK_a of ligand	k_H (mol dm^{-3} s^{-1})
NH_3	9.3	1.5
en	8.6	0.6
pn	8.5	0.5
[15]aneN$_4$	7.6	5.5×10^{-3}
[14]aneN$_4$	6.7	1.3×10^{-3}
[12]aneN$_4$	6.0	7.0×10^{-3}
py	5.3	8.0×10^{-6}

There does appear to be some correlation between average pK_a and k_H for the basic ligands but any correlation is lost for the more acidic ligands.

One complication is that k_H is the product of a rate constant and an equilibrium constant so contrasting variations in these parameters may occur. To account for the dependence of k_H on the concentration of H^+ three mechanisms can be considered, Scheme 3.3.2.1.

Mechanism A involves a slow concerted H^+ catalysed dechelation followed by a rapid loss of the monodentate bicarbonate. Mechanisms B and C both involve a rapid pre-equilibrium protonation step followed by a slow rate determining chelate ring opening step. However, in mechanism B a water molecule participates in the rate determining ring opening step whereas in mechanism C the rate determining step does not involve a solvent molecule and is just a rearrangement of the bidentate carbonato group to the monodentate bicarbonato group.

In mechanism A, a rate determining proton transfer step is involved which gives rise to a normal kinetic isotope effect and therefore $k_{D2O} / k_{H2O} < 1$. For mechanisms B and C, $k_{D2O} / k_{H2O} > 1$ since D_2O is less basic than H_2O and therefore the substrate will be able to compete more effectively with the solvent for the deuterion in D_2O than for the proton in H_2O. In other words, the conjugate acid intermediate will be present at higher equilibrium concentrations in D_2O since the dissociation of weak acids is generally smaller in the heavier solvent[29]. If the conjugate acid intermediate gives the product in a second rate determining step which is not subject to an isotope effect, as in mechanism C since k_{C1} is not subject to an isotope effect, the observed rate will demonstrate maximum enhancement. If however the intermediate is converted to

Scheme 3.3.2.1. Possible mechanisms for the acid catalysed carbonato chelate ring opening step.

Mechanism A

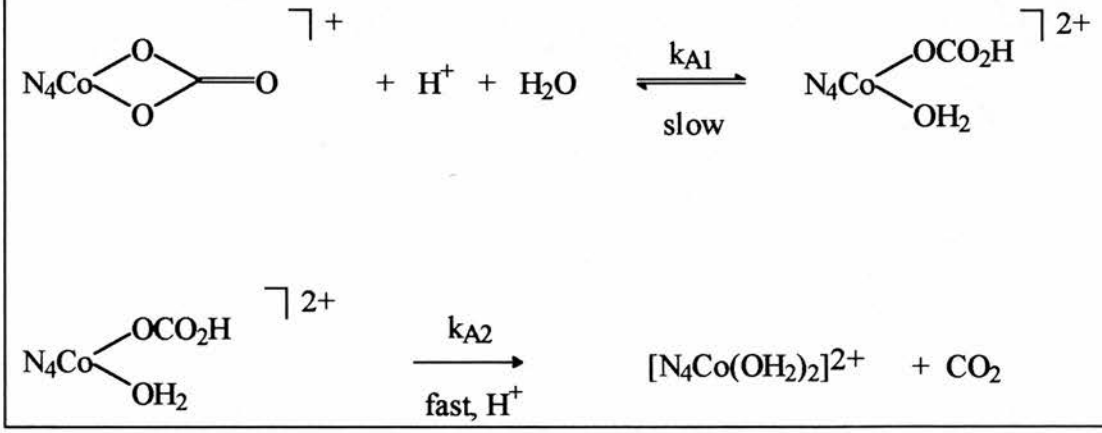

Mechanism B

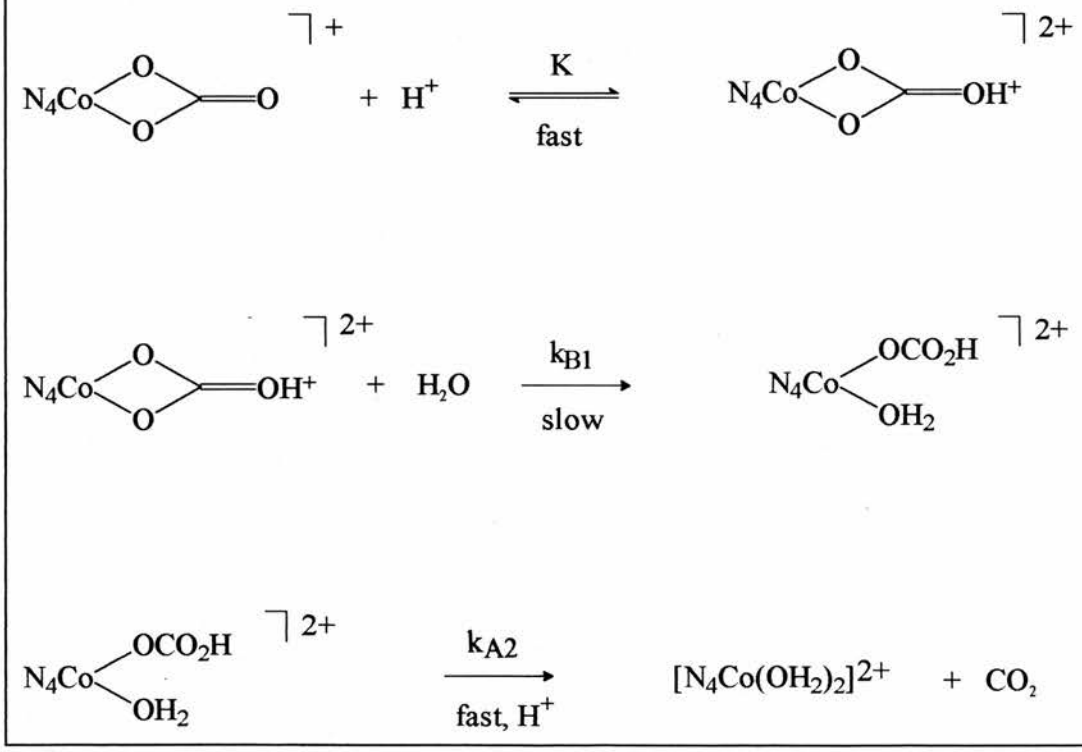

Mechanism C

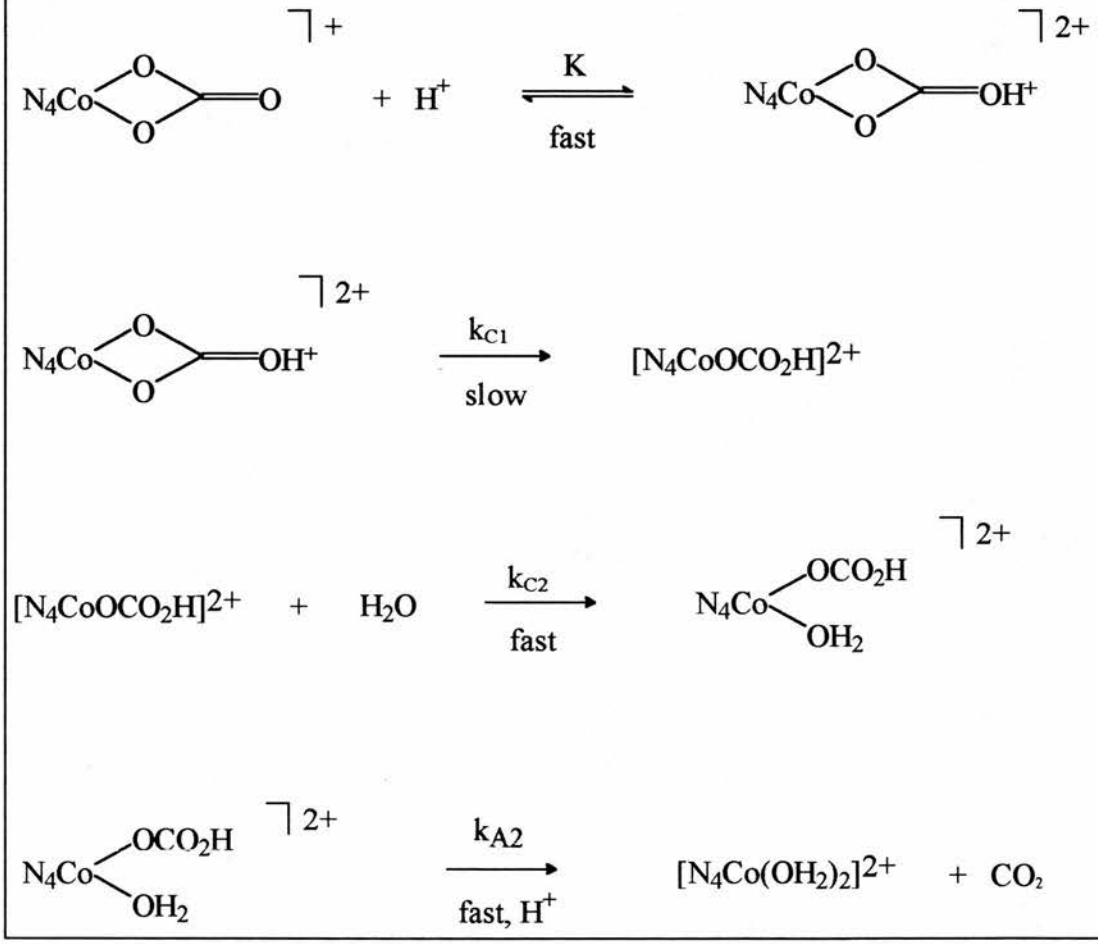
+
K
fast
2+
2+
k_{C1}
slow
$[N_4CoOCO_2H]^{2+}$
$[N_4CoOCO_2H]^{2+}$ + H_2O
k_{C2}
fast
2+
2+
k_{A2}
fast, H^+
$[N_4Co(OH_2)_2]^{2+}$ + CO_2

product by a rate determining step which is subject to a retarding isotope effect, as in the case of mechanism B, the observed rate depends upon the relative magnitudes of the two effects. In the case of mechanism B the value of $k_{B1}(D_2O/ H_2O)$ will be somewhat less than unity, but $K(D_2O/ H_2O)$ is much greater. Since $k_{obs} = k_{B1}K[H^+][H_2O]$, k_{obs} increases in D_2O but not to such an extent as for mechanism C where $k_{obs} = k_{C1}K[H^+][H_2O]$ and k_{C1} is subjected to no retarding isotope effect.

The results of a solvent deuterium isotope effect study on the rate of decarboxylation of *cis*-$[Co([15]aneN_4)CO_3]^+$ are shown in Table 3.3.2.7.

Table 3.3.2.7. Solvent deuterium isotope effects for the acid catalysed decarboxylation of *cis*-$[Co([15]aneN_4)CO_3]^+$ at 25°C.

DCl/D_2O solvent		
[DCl] (mol dm^{-3})	k_{obs} (s^{-1})	$10^3\ k_{obs}/[H^+]$ ($dm^3\ mol^{-1}\ s^{-1}$)
0.51	1.73×10^{-3}	3.39
HCl/H_2O solvent		
[HCl] (mol dm^{-3})	k_{obs} (s^{-1})	$10^3\ k_{obs}/[H^+]$ ($dm^3\ mol^{-1}\ s^{-1}$)
0.5	7.20×10^{-4}	1.44

The contribution of the k_0 term to k_{obs} at these relatively high acidities is small and therefore no attempt has been made to correct for its contribution. For solutions in $[H^+]$ of *ca.* 0.5 mol dm^{-3} the value of k_{D2O}/k_{H2O} for *cis*-$[Co([15]aneN_4)CO_3]^+$ at 25°C is 2.35. This compares well with values found in previous studies of similar systems of 2.3 for *cis*-$[Co(en)_2CO_3]^+$ [30], 2.6 for *cis*-$[Co(Me_2[14]diene)CO_3]^+$ [25] and 2.05 for *cis*-$[Co(cyclen)CO_3]^+$ [11]. All of these values fall within the range 1.9 to 2.6 considered typical[31] for reactions proceeding via an A-1 mechanism (mechanism C). These values are somewhat larger than the values of 1.3 to 1.4 which are typical for A-2 type mechanisms (mechanism B).

The evidence appears to suggest that the acid catalysed dechelation of the bidentate carbonate complex *cis*-$[Co([15]aneN_4)CO_3]^+$ proceeds via a mechanism of type C involving a rapid preequilibrium followed by a slow rate determining chelate ring opening step.

Presuming k_{C2} and k_{B2} are both very rapid equation 5 can be modified to;

$$k_{obs} = \frac{k_0 + k_{C1}K_3[H^+]}{1 + K_3[H^+]}$$

since;

$$K_3 = \frac{[CoN_4(CO_3H)^{n+}]}{[H^+][CoN_4(CO_3)^{n+1}]}$$

and

$$\frac{d[CoN_4(CO_3H)(H_2O)^{(n+1)+}]}{dt} = k_H([CoN_4(CO_3)^{n+}] + [CoN_4(CO_3H)^{(n+1)+}])$$

$$= k_{C1}[CoN_4(CO_3H)^{(n+1)+}] = k_{C1}K_3[CoN_4(CO_3)^{n+}][H^+]$$

so;

$$k_H = \frac{k_{C1}K_3[H^+]}{(1 + K_3[H^+])}$$

This can be further simplified to

$$k_H = k_{C1}K_3[H^+]$$

since K_3 for the protonation of a carbonyl group is known to be very small[30]. If this were not the case a plot of k_{obs} *versus* $[H^+]$ would not be linear. Although non-linear plots have been observed[18,30,32] these effects are due to an enhanced ring opening reaction which is faster than the rate of decarboxylation. As a result, the decarboxylation step, which is acid independent, becomes rate limiting at higher acid concentrations.

The two constants k_{C1} and K_3 may well behave differently towards stereochemical and electronic effects thus complicating the interpretation of k_H. Furthermore, the complex nature of k_H could to some extent account for the large scatter of the isokinetic plot, Figure 3.3.2.7, since the activation parameters will also be composite quantities,

i.e. $\Delta H_H^{\ddagger} = \Delta H_3° + \Delta H_{C1}^{\ddagger}$ and $\Delta S_H^{\ddagger} = \Delta S_3° + \Delta S_{C1}^{\ddagger}$.

The second stage of the reaction involves the conversion of *cis*-$[Co([15]aneN_4)(H_2O)_2]^{3+}$ to a product with λ_{max} at *ca.* 490 nm and a second less intense band at 610 nm. This spectrum corresponds to that expected for *trans*-$[Co([15]aneN_4)(H_2O)_2]^{3+}$. The rate of the isomerisation appears to be independent of the acidity over the narrow range studied. Values of k_i over a temperature range are given in Table 3.3.2.8 along with the standard deviations (σ).

Table 3.3.2.8. k_i for the acid catalysed aquation of $[Co([15]aneN_4)(CO_3)]^+$.

$I = 1.0$ mol dm^{-3}

Temperature (°C)	k_i (s^{-1})	σ
15	2.48×10^{-6}	1.62×10^{-6}
25	4.88×10^{-6}	2.16×10^{-6}
30	2.58×10^{-4}	1.36×10^{-4}
35	3.92×10^{-4}	1.26×10^{-4}
40	5.65×10^{-4}	2.25×10^{-4}
45	1.24×10^{-3}	7.10×10^{-4}

Previous studies[13,33] of the *cis-trans* isomerisation of macrocyclic Co(III) complexes have revealed that the mechanism of isomerisation is complex.

3.3.3 Aquation of *trans* I-$[Co([15]aneN_4)Cl_2]^+$

The two isomers of *trans*-$[Co([15]aneN_4)Cl_2]^+$ reported by Hung and Busch[3] were readily isolated and characterised. The acid catalysed aquation kinetics have been studied and the results compared to literature values[10]. In nitric acid solution the two isomers display different aquation kinetics. Busch claims that isomer I aquates to form the chloroaqua complex *trans*-$[Co([15]aneN_4)(H_2O)Cl]^{2+}$ with isosbestic points at 630, 562 and 468 nm. This species exhibits bands in the electronic spectrum at 625, 500 and 408 nm. The first aquation is followed by a second aquation to form the diaqua species *trans*-$[Co([15]aneN_4)(H_2O)_2]^{2+}$ and this reaction is characterised by isosbestic points at 400 and 460 nm. The rate constant k_1 for the first aquation step was reported to be 1.16×10^{-3} s^{-1} at 25°C and $[HNO_3] = 0.1$ mol dm^{-3}.

The present study of the aquation of isomer I gives slightly different results from those of Busch and Hung. Figure 3.3.3.1 shows the time interval scan for the aquation of *trans*-$[Co([15]aneN_4)Cl_2]^+$. The initial scan displays bands at 420, 505 and 655 nm which match those expected for unreacted *trans*(I)-$[Co([15]aneN_4)Cl_2]^+$ as found by Busch. The reaction proceeds with six isosbestic points in the visible region at 368, 432, 465, 522, 557 and 634 nm to give a product with bands at 406, 500 and 636 nm. This spectrum is similar to that of the *trans*-$[Co([15]aneN_4)(H_2O)Cl]^{2+}$ product of the first aquation step quoted by Busch except that the $^1E_g \leftarrow {}^1A_{1g}$ band is at a slightly lower energy. Three additional isosbestic points are observed in the visible region at 522, 432 and 368 nm. The second much slower stage of the reaction is accompanied by somewhat smaller changes in the visible region. The earlier work found isosbestic

Figure 3.3.3.1. Time interval scan for the first stage of the aquation of $[Co([15]aneN_4)Cl_2]^+$.

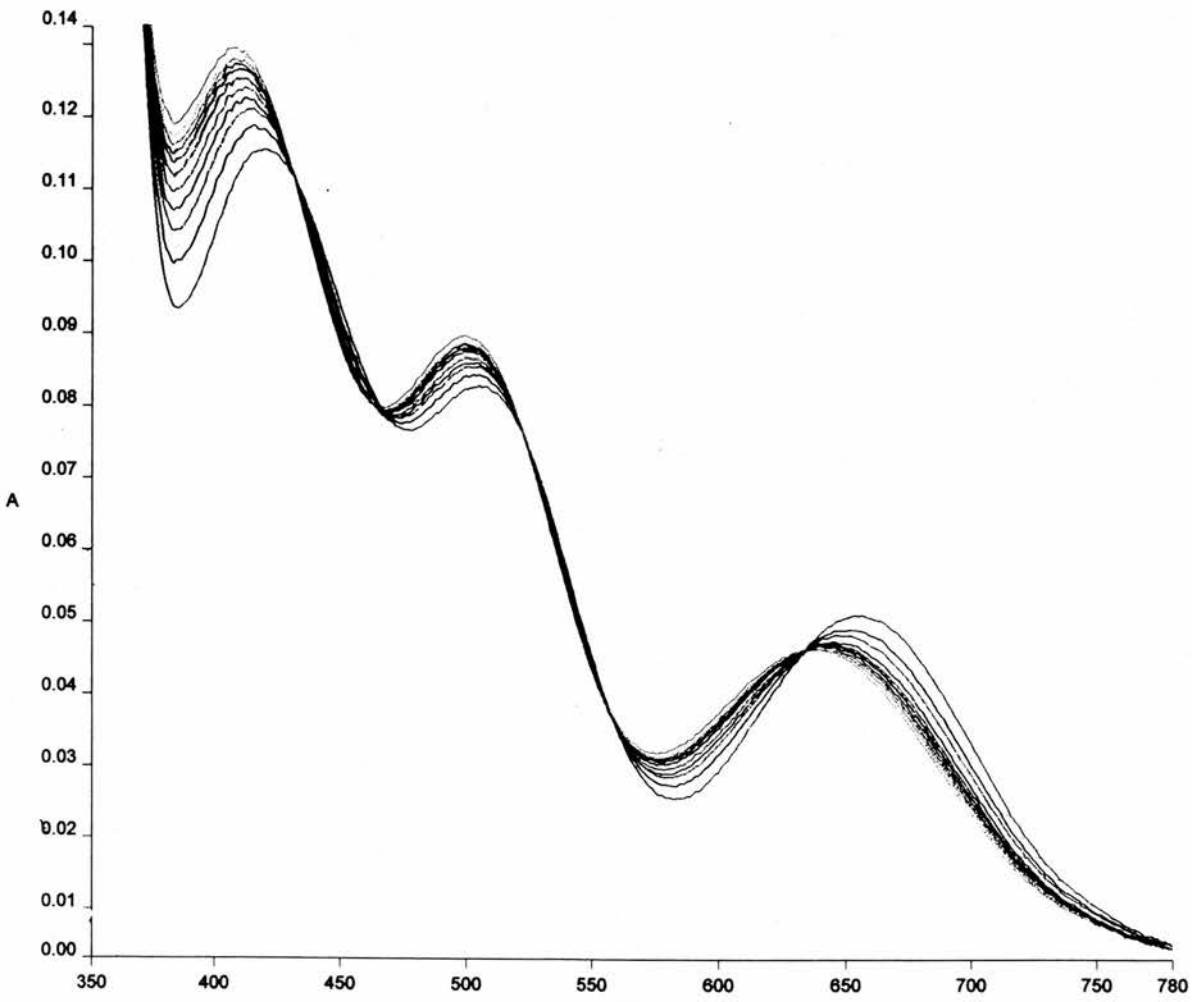

Δt = 180 secs., T = 30°C, $[HNO_3]$ = 0.1 mol dm^{-3}

points for the second aquation step at 400 nm and 460 nm. The time interval scan for the second stage of the reaction is shown in Figure 3.3.3.2. Isosbestic points can be observed at 398, 453, 489, 546 and 612 nm. However, the spectral changes are quite small. By measuring absorption with respect to time at 398 nm and 612 nm the second reaction should not be observed and the rate constant calculated for the reaction from a plot of ln $[A]_t$ *versus* time gives the rate constant for the first stage of the reaction. By measuring absorption with respect to time at 368 nm only the second reaction will be observed. The observed rate constants for the two steps at 25 °C are $k_{1obs} = 0.97 \times 10^{-3}$ s^{-1} and $k_{2obs} = 4.68 \times 10^{-5}$ s^{-1}. These values compare well with the value determined by Busch and Hung for $k_{1obs} = 1.16 \times 10^{-3}$ s^{-1}. However, they did not report a value for k_{2obs}.

The reaction was also monitored by measuring changes in conductivity. A plot of conductivity *versus* time is shown in Figure 3.3.3.3. Clearly this plot indicates that the reaction is not of a simple first order process. A good fit of this data is obtained if it is treated as two consecutive pseudo first order reactions which gives the observed rate constants of $k_{1obs} = 1.03 \times 10^{-3}$ s^{-1} and $k_{2obs} = 5.75 \times 10^{-5}$ s^{-1}. These rate constants are in good agreement with those determined spectrophotometrically despite the fact that the conductivity measurements were not carried out at the same ionic strength.

Figure 3.3.3.2. Time interval scans for the second stage of the aquation of $[Co([15]aneN_4)Cl(H_2O)]^{2+}$.

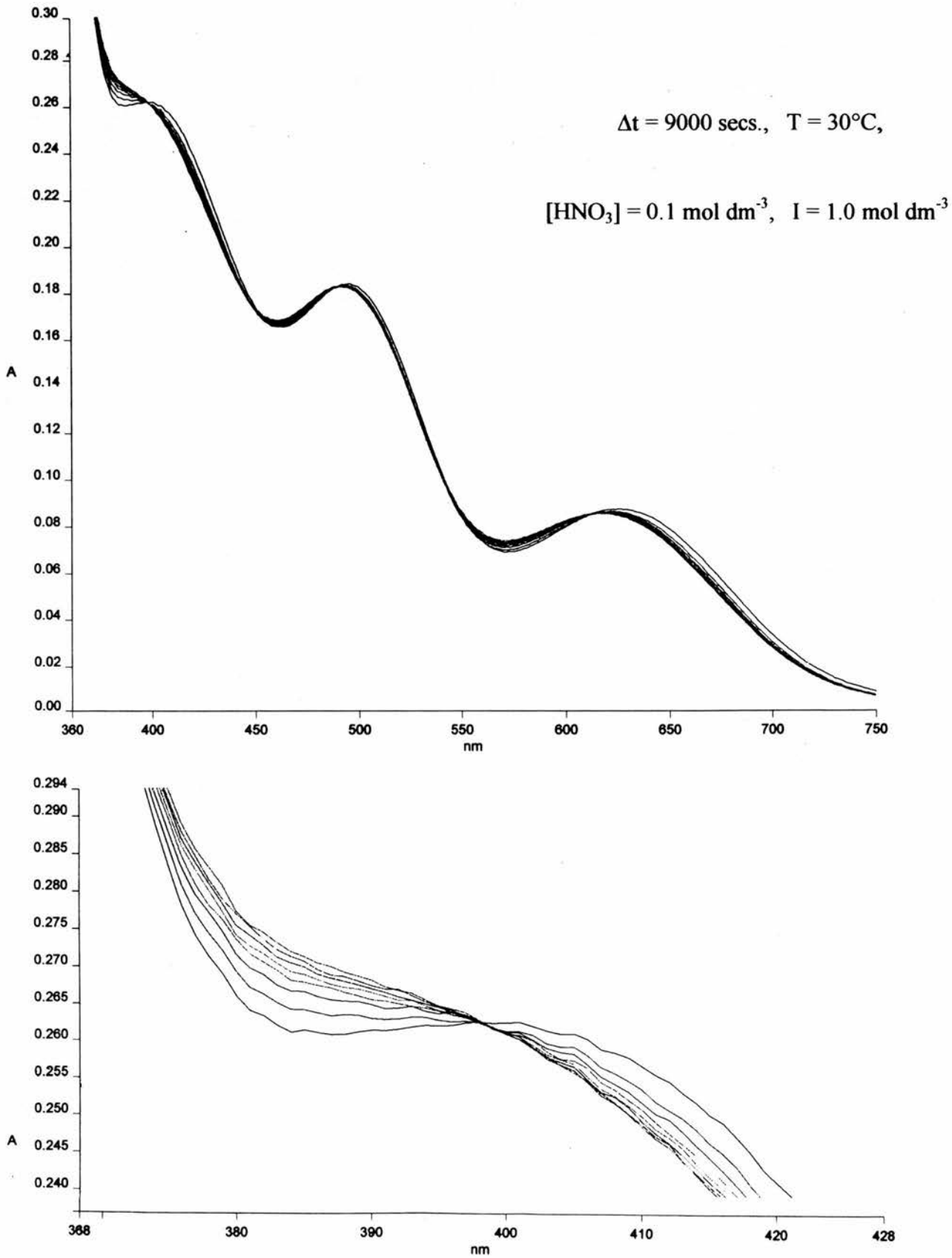

Figure 3.3.3.3. Conductivity *versus* time for the aquation of [Co([15]aneN$_4$)Cl$_2$]$^+$.

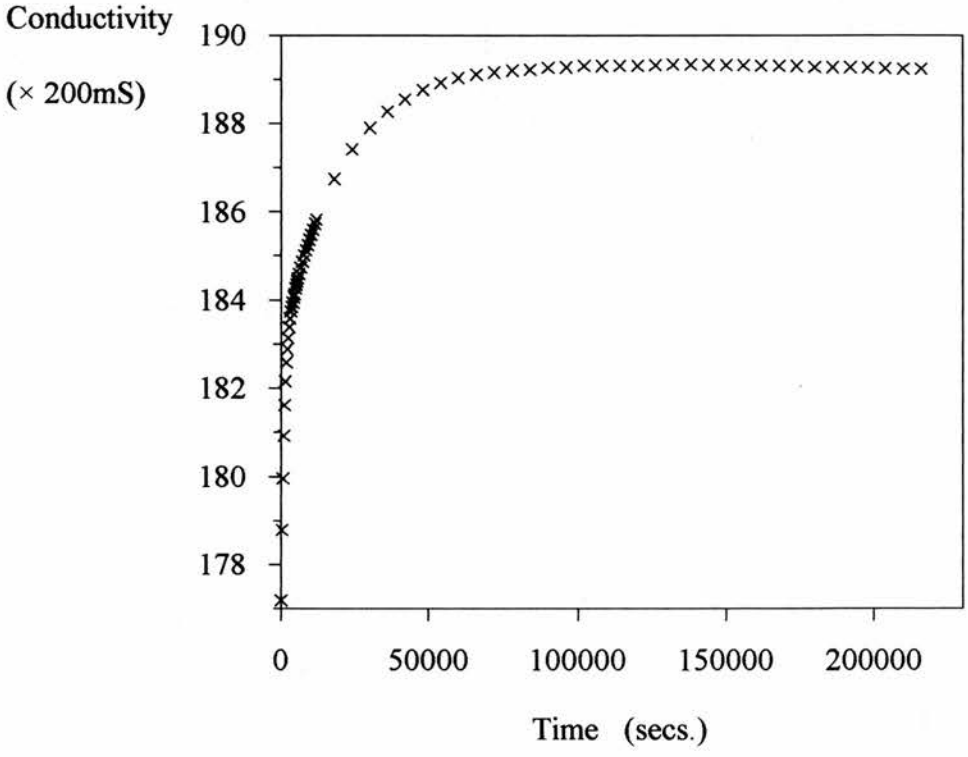

Our results indicate that the aquation reaction is a two step process. The initial step to form [Co([15]aneN$_4$)(H$_2$O)Cl]$^{2+}$ occurs with isosbestic points at 368, 432, 465, 522, 557 and 634 nm and $k = 1 \times 10^{-3}$ s^{-1}.

First Aquation Step:

$$[Co([15]aneN_4)Cl_2]^+ + H_2O \overset{k_1}{\rightleftharpoons} [Co([15]aneN_4)(H_2O)Cl]^{2+} + Cl^-$$

Second Aquation Step:

$$[Co([15]aneN_4)(H_2O)Cl]^{2+} + H_2O \xrightarrow{k_2} [Co([15]aneN_4)(H_2O)_2]^{3+} + Cl^-$$

The value of k_2 for the second aquation step is calculated to be 5.2×10^{-5} s^{-1} at 25°C. A separate experiment showed that the molar conductance upon completion of the reaction was 411 S cm^2 mol^{-1}. This result suggests that step 2 proceeds to completion giving a 3:1 electrolyte.

Except for the differences in isosbestic points these results confirm those of Busch *et al.*

3.4 References

1 E.B. Fleischer and J.H. Wang, *J. Am. Chem. Soc.*, 1960, **82,** 3498

2 R.W. Hay and M. T. Tarafder, *Trans. Met. Chem.*, 1993, **18,** 1

3 Y. Hung, L.Y. Martin, S.C. Jackels, A.M. Tate and D.H. Busch, *J. Am. Chem. Soc.*, 1977, **99,** 4029

4 C.K. Poon, *Inorg. Chim. Acta,* 1971, **6,** 322

5 L.Y. Martin, L.J. De Hayes, L.J. Zompa and D.H. Busch, *J. Am. Chem. Soc.*, 1974, **96,** 4046

6 R.W. Hay and M. T. Tarafder, *J. Chem. Soc., Dalton Trans.*, 1991, 823

7 F. Basolo and R.G. Pearson, *Mechanisms of Inorganic Reactions,* Wiley, New York, 1968

8 A. Palmer and H. Kelm, *Coord. Chem. Rev.*, 1981, **36,** 89

9 C-K. Poon, T-C. L. Lau and Y-P. Kan, *J. Chem. Soc. Dalton Trans.*, 1983, 1641 and references therin.

10 Y. Hung and D.H. Busch, *J. Am. Chem. Soc.*, 1977, **99,** 4977

11 R.W. Hay and B. Jeragh, *Transition Met. Chem. (Weinheim. Ger.),* 1979, **4,** 288

12 T.P. Dasgupta, *Inorg. Chim. Acta,* 1976, **20,** 33

13 J.A. Kernohan and J.F. Endicott, *J. Am. Chem. Soc.*, 1969, **91,** 6977

14 E.K. Barefield, F. Wagner and K.D. Hodges, *Inorg. Chem.*, 1976, **15,** 1370

15 M.S. Islam and M.M. Uddin, *Polyhedron,* 1993, **12,** 423

16 H.F. Bauer and W.C. Drinkard, *J. Am. Chem. Soc.*, 1960, **82,** 5031

17 D.H. Busch, *Inorganic Synthesis*, Wiley, New York, 1980, **20,** 105

18 T.P. Dasgupta and G.M. Harris, *J. Am. Chem. Soc.*, 1971, **93,** 91

19 D.A. Buckingham and C.R. Clark, *Inorg. Chem.*, 1994, **33,** 6171

20 D.A. Palmer and R. Van Eldik, *Chem. Rev.*, 1983, **83,** 651

21 T.P. Dasgupta and G.M. Harris, *J. Am. Chem. Soc.*, 1969, **91,** 3207

22 V.S. Sastri and G.M. Harris, *J. Am. Chem. Soc.*, 1970, **92,** 2943

23 K.E. Hyde, G.H. Fairchild and G.M. Harris, *Inorg. Chem.*, 1976, **15,** 2631

24 P.M. Coddington and K.E. Hyde, *Inorg. Chem.*, 1983, **22,** 2211

25 R.W. Hay and B. Jeragh, *J. Chem. Soc., Dalton Trans.*, 1979, , 1343

26 J.F. Glenister, K.E. Hyde and G. Davies, *Inorg. Chem.*, 1982, **21,** 2331

27 K.E. Hyde, E.W. Hyde, J. Moryl, B. Baltus and G.M. Harris, *Inorg. Chem.*, 1980, **19,** 1603

28 D.J. Francis and R.B. Jordan, *Inorg. Chem.*, 1972, **11,** 1170

29 L. Melander in; *Isotope Effects on Reaction Rates*, Ch. 6, Ronald Press Company, New York, 1960

30 G.M. Harris and K.E. Hyde, *Inorg. Chem.*, 1978, **17,** 1892

31 J.L. Kice and J.M. Anderson, *J. Am. Chem. Soc.*, 1966, **88,** 5242

32 R. van Eldik, T.P. Dasgupta and G.M. Harris, *Inorg. Chem.* , 1975, **14,** 2573

33 C.K. Poon and M.L. Tobe, *Inorg. Chem.*, 1968, **7,** 2398

Chapter 4

Studies of the Formation of *trans*[14]dieneN$_4$

4.1 Introduction.

Prior to 1960 the porphyrins and phthalocyanins were the only cyclic ligands known. However, since 1960 a very large number of synthetic macrocycles have been prepared. The first of a series of pioneering template reactions for the synthesis of macrocyclic complexes was reported by Curtis[1] in 1960. Curtis found that *tris*-(ethylenediamine)nickel(II) perchlorate reacts with dry acetone at room temperature to produce a yellow crystalline product. Initially it was thought that this compound was the tetra *N*-isopropylidene nickel(II) complex but the stability of the complex in boiling acid or base and a band in the infra-red spectrum at ~3200cm^{-1} which could be assigned as ν(N-H) did not support this view. Decomposition by cyanide solution gave the products mesityl oxide and ethylenediamine. This result suggested that the acetone moieties were part of a C_6 system in the compound. The product was later shown[2] to be a mixture of the *cis*- and *trans*-isomers of the macrocyclic complex (5,7,7,12,14,14-hexamethyl-1,4,8,11-tetraazacyclotetradecane-4,(11,14)-dieneN$_4$)nickel(II) shown in Figure 4.1.1. It was later found[3] that metal complexes of the *trans* isomer can exist as two diastereoisomers due to the presence of chiral *sec*-NH centres in the metal complex. The common abbreviated name which has been adopted for these compounds is [14]-dieneN$_4$. The nickel complex of the *trans* form is known as Ni(*trans*-[14]-dieneN$_4$) and the *cis* form as Ni(*cis*-[14]-dieneN$_4$).

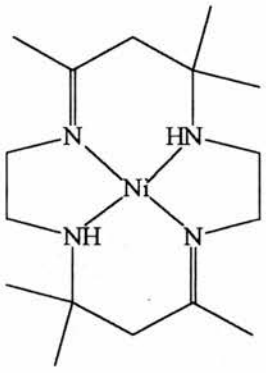

trans-[14]-dieneN$_4$

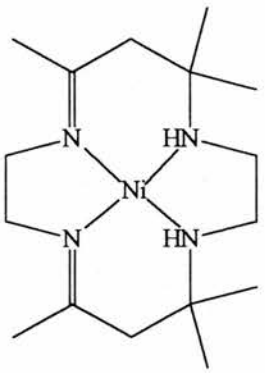

cis-[14]-dieneN$_4$

Figure 4.1.1. *trans*-[14]-dieneN$_4$ and *cis*-[14]-dieneN$_4$

The exact mechanism of the formation of the macrocycle is not known, but it is thought that it involves an initial condensation between an acetone molecule and a coordinated primary amine, followed by nucleophilic attack of the carbanion on the coordinated imine (Figure 4.1.2). In this reaction the nickel ion acts as a template for the reactants and thus the procedure is known as a template synthesis. Subsequent investigations have shown that the free ligand can also be synthesized without a metal template in greater than 80% yield[4]. However, in these reactions the proton can be considered to have a specific templating effect due to hydrogen bonding.

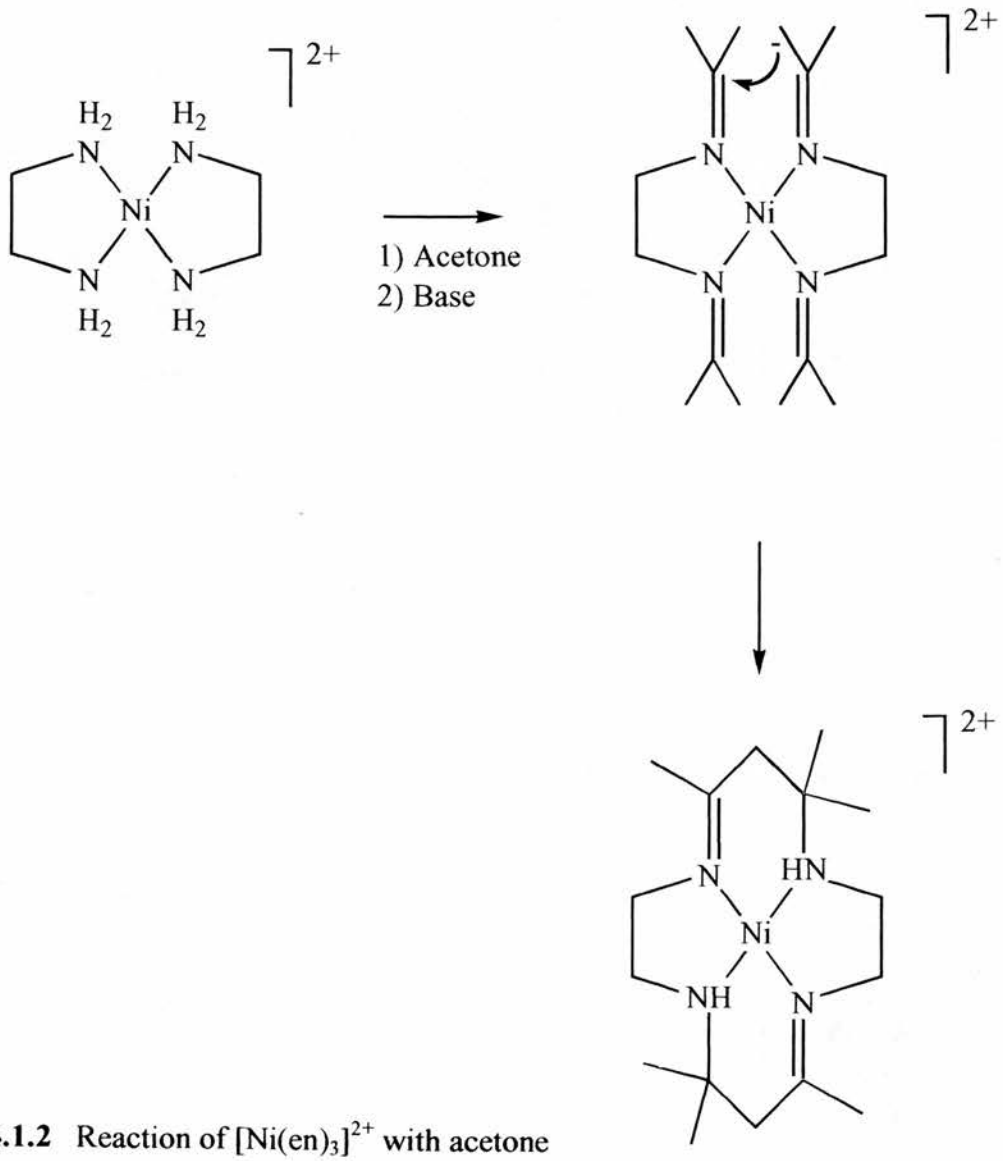

Figure 4.1.2 Reaction of $[Ni(en)_3]^{2+}$ with acetone

An analogous template reaction also occurs with copper(II) complexes[5]. *Bis*-(ethylenediamine)copper(II) perchlorate reacts slowly with acetone at room temperature to form a mixture of $[Cu(cis\text{-}[14]\text{-}dieneN_4)]^{2+}$ and $[Cu(trans\text{-}[14]\text{-}dieneN_4)]^{2+}$. As with the nickel complexes the *cis* complex is the least soluble and crystallizes first. There are two crystalline forms, one orange and one red, of $[Cu(trans\text{-}[14]\text{-}dieneN_4)](ClO_4)_2$ due to the chiral *sec*-NH centres. The orange

diastereoisomer is the *N-meso* form in which the two protons on the secondary amines are *trans* to one another whereas in the red form, the *N-racemic* diastereoisomer, the two protons are both up or both down[6], Figure 4.1.3. This type of isomerism was first observed in the nickel(II) complexes and was confirmed by the crystal structure of the two diastereoisomers[6] and also by using N.M.R. techniques[7]. The crystal structure of the two diastereoisomers of the copper(II) complexes have also been determined[8,9].

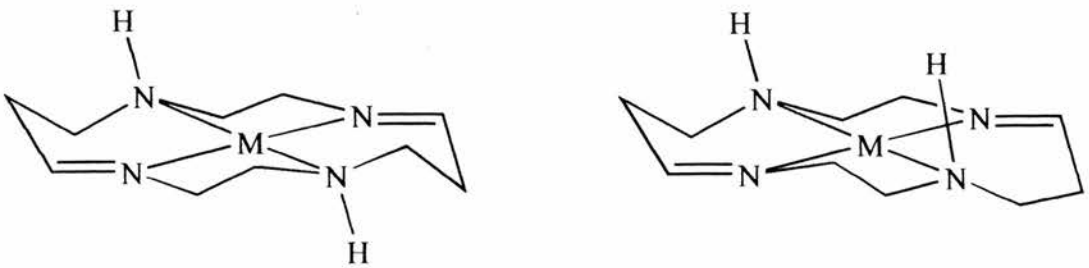

N-***meso*** N-***racemic***

Figure 4.1.3. N-*Racemic* and N-*meso* diastereoisomers of

$[M(trans\text{-}[14]\text{-}dieneN_4)]^{2+}$

Various intermediates can be isolated during the synthesis of [Cu(*trans*-[14]-dieneN$_4$)](ClO$_4$)$_2$. One such complex is [(4,4,9,11,11-pentamethyl-14-amino-5,8,12-triazatetradeca-8-ene-3-one)copper]$^{2+}$ (often abbreviated to [Cu(en-aib-βak)]$^{2+}$) is shown in Figure 4.1.4. . This compound is produced when *bis*-(ethylenediamine)copper(II) perchlorate is refluxed in acetone for 30 minutes[10]. The colour of the solution changes from magenta to blue as the complex [Cu(en-aib-βak)]$^{2+}$ is formed. This complex is rapidly converted to [Cu(*trans*-[14]-dieneN$_4$)](ClO$_4$)$_2$ under basic conditions. The kinetics of the base catalyzed conversion of [Cu(en-aib-βak)]$^{2+}$ to the [Cu(*trans*-[14]-dieneN$_4$)]$^{2+}$ complex have been studied in this work.

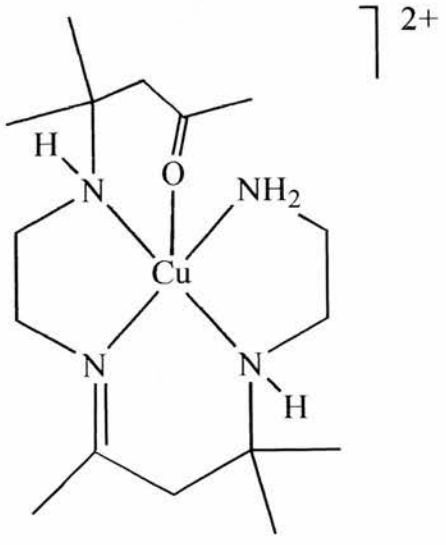

Figure 4.1.4. [(4,4,9,11,11-pentamethyl-14-amino-5,8,12-triazatetra-deca-8-ene-3-one)copper]$^{2+}$

Irradiation of [Cu(*trans*[14]dieneN$_4$)]$^{2+}$ in the region of the charge transfer bands (< 400 nm) has also been found[11] to generate [Cu(en-aib-βak)]$^{2+}$ when the medium was buffered at pH 6.

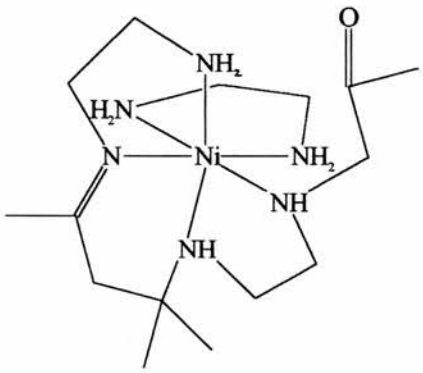

Figure 4.1.5. [Ni(en-aib-βak)(en)]$^{2+}$

There is no evidence that a nickel(II) complex analogous to the [Cu(en-aib-βak)]$^{2+}$ exists. However, [Ni(en-aib-βak)(en)]$^{2+}$ (Figure 4.1.5) has been reported along with the *bis*-β-amino-ketone nickel(II) complex shown in Figure 4.1.6. Curtis has recently[12] synthesised a pair of five coordinate complexes of nickel(II) and copper(II) with the triamine-diimine ligand 13-imino-4,4,6,11,11-pentamethyl-3,7,10-triazatetradec-6-en-1-amine (meim) shown in Figure 4.1.7.

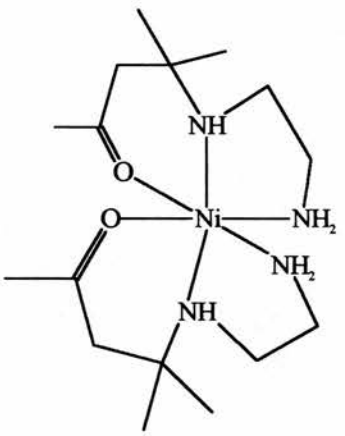

Figure 4.1.6. *bis*-β-aminoketone complex of nickel(II)

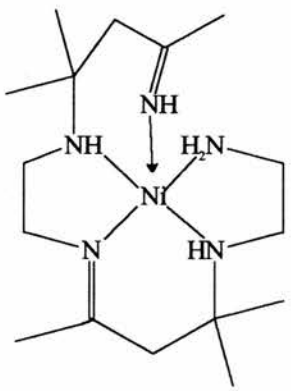

Figure 4.1.7. $[Ni(meim)]^{2+}$

Both complexes form the corresponding *trans*-[14]-dieneN$_4$ complex on heating in water. The nickel complex reacts more rapidly than the copper derivative.

4.2 Experimental

4.2.1 Synthesis

Synthesis of 5,7,7,12,14,14-hexamethyl-1,4,8,11-tetraazacyclotetradeca-4,11-diene hydrogen bromide

This synthesis followed that of Hay *et al*[4]. To 1,2-diaminoethane dihydrobromide (11.1 g, 0.05 mol) was added acetone (100 cm^3) and 1,2-diaminoethane (3.0 g, 0.05 mol). The mixture was heated to 45 °C for 45 minutes during which time the white product precipitated. This product was filtered off after cooling and washed with acetone then ether and dried in *vacuo*. (Yield 12.9 g, 67%) (Found: C, 39.76; H, 8.49; N, 11.50 %. Calculated for $C_{16}H_{32}N_4 \cdot 2HBr \cdot 2H_2O$: C, 40.08; N, 8.01; H, 11.71 %); m.p. 107 ± 1°C; I.R./cm^{-1};ν(N-H), 3180; ν(C:N), 1669, (KBr)

Synthesis of (5,7,7,12,14,14-hexamethyl-1,4,8,11-tetraazacyclotetradeca-4,11-diene)copper(II) perchlorate.

This complex was prepared essentially as described by Sadasivan and Endicott[13]. The perchlorate salt of *trans*[14]diene (2 g, 4.2 mmol) was dissolved in a 1:1 water-methanol mixture with copper(II) carbonate (2 g, 8.4 mmol) and heated on a steam bath for 15 minutes. Slow evaporation of the solvent yielded a mixture of the N-*meso* (20%) and N-*racemic* (80%) diastereoisomers. These

diastereoisomers were separated by recrystallsation from methanol. (Yield = 0.87 g N-*racemic* (38 %); 0.2 g N-*meso* (9 %)) (Found; C, 34.95; H, 6.05; N, 10.46 %. Calculated for $Cu[C_{16}H_{32}N_4](ClO_4)_2$: C, 35.40; N, 5.94; H, 10.32 %); λ_{max} (nm), ε ($dm^3\ mol^{-1}\ cm^{-1}$) N-*racemic* 507, (47), N-*meso* 502, (42); I.R./cm^{-1};*ν*(N-H), 3208; *ν*(C:N), 1669, (KBr)

Synthesis of (5,7,7,12,14,14-hexamethyl-1,4,8,11-tetraazacyclotetradeca-4,11-diene)nickel(II) perchlorate.

This complex was synthesised by two routes. The first using the template synthesis as described by Curtis[1] and the second using the hydrobromide salt of the ligand and nickel carbonate as for the preparation of the copper complex[13]. Both methods produced a yellow solid. No attempt was made to separate the two diastereoisomers. (Yield 35% (template), 45% (from ligand)); λ_{max} 436 nm, ε 54 $dm^3\ mol^{-1}\ cm^{-1}$; I.R./cm^{-1}; *ν*(N-H), 3177; *ν*(C:N), 1665

Synthesis of (4,4,9,11,11-pentamethyl-14-amino-5,8,12-triazatetradeca-8-ene-3-one)copper(II) perchlorate.

This complex was synthesised as described by Curtis[10]. A solution of *bis*-(ethylenediamine)copper(II) perchlorate (1.9 g, 0.005 mol) in acetone

(200 cm^{-3}) was refluxed for 30 minutes when the colour of the solution changed from magenta to blue. The product crystallised on removal of some of the solvent on a rotary evaporator and was recrystallised from methanol. (Yield = 2.07 g, 74%) (Found: C, 34.25; H, 6.05; N, 10.48 %. Calculated for $C_{16}H_{34}N_4Cu(ClO_4)_2$: C, 34.39; N, 6.1; H, 9.98 %); λ_{max} 628 nm, ε 80 dm^3 mol^{-1} cm^{-1}; I.R./cm^{-1}; $\nu(NH_2)$, 3350, 3268; ν(NH), 3237; $\delta(NH_2)$, 1595; ν(C=O) 1689 cm^{-1}

Synthesis of *bis*-(7-amino-4,4-dimethyl-5-azaheptan-2-one)nickel(II) perchlorate.

This compound was prepared as described for the copper(II) complex, substituting *bis*-(ethylendiamine)nickel(II) perchlorate (1.89 g, 0.005 mol) for *bis*-(ethylenediamine)copper(II) perchlorate. Fine needle like crystals were obtained and were recrystallized from ethanol and dried in *vacuo*. (Yield = 2.3 g, 80 %) (Found: C, 32.89; H, 5.77; N, 10.68 %. Calculated for $C_{16}H_{36}N_4O_2Ni(ClO_4)_2$: C, 33.47; N, 6.32; H, 9.76 %); λ_{max} 336 nm, ε 28.5 dm^3 mol^{-1} cm^{-1}; I.R./cm^{-1}; $\nu(NH_2)$, 3341, 3245; ν(NH), 3200; $\delta(NH_2)$, 1592; ν(C=O) 1680

Synthesis of (13-imino-4,4,6,11,11-pentamethyl-3,7,10-triazatetradec-6-en-1-amine)nickel(II) perchlorate.

This complex was prepared as described by Curtis[12]. To an aqueous solution (50 cm^3) of nickel chloride hexahydrate (6 g, 0.025 mol), ammonium chloride (6 g, 0.11 mol) and concentrated aqueous ammonia (20 cm^3) was added 5,7,7,12,14,14-hexamethyl-1,4,8,11-tetraazacyclotetradeca-4,11-diene hydrobromide (4.6 g, 0.012 mol). The mixture was stirred and heated on a water bath for 30 minutes. After cooling the product was isolated by the addition of sodium perchlorate. The lilac product was recrystallised from hot acetone and dried in *vacuo*. (Yield = 2.46 g, 37%) (Found; C, 34.51; H, 6.02; N, 12.87 %. Calculated for $C_{16}H_{36}N_5NiCl_2O_8$; C, 34.56; H, 6.52; N, 12.59 %); λ_{max} 528 nm, ε 24 $dm^3\ mol^{-1}\ cm^{-1}$; I.R./cm^{-1}; ν(NH); 3344, 3324; ν(C=N) 1665, 1638; $\nu(NH_2)$; 1596

Synthesis of (13-imino-4,4,6,11,11-pentamethyl-3,7,10-triazatetradec-6-en-1-amine)copper(II) perchlorate.

This complex could only be produced by metal ion substitution of the nickel complex. To an ethanolic solution of (13-imino-4,4,6,11,11-pentamethyl-3,7,10-triazatetradec-6-en-1-amine)nickel(II) perchlorate (1 g, 2.4 mmol) was added an excess of copper(II) chloride dihydrate (0.8 g, 4.8 mmol). The solution was

heated to reflux for 1 hour and then cooled. The blue product was isolated by evaporation of the solvent and recrystallising from methanol. (Yield = 1.08 g, 81%); λ_{max} 576 nm, ε 65 $dm^3\ mol^{-1}\ cm^{-1}$; I.R./cm^{-1}; ν(NH), 3285, 3182; ν(C=N), 1668; $\delta(NH_2)$, 1597

4.2.2 Kinetic Measurements.

The base catalysed cyclisation reactions of several of the non-macrocyclic ligands described above were studied. Conventional spectrophotometry was used to study the slower reactions using a Perkin Elmer Lambda 5 scanning spectrophotometer. The base catalysed cyclisation of $[Cu(en\text{-}aib\text{-}\beta ak)]^{2+}$ to $[Cu(\textit{trans}[14]dieneN_4)]^{2+}$ was studied over two pH ranges. At lower pH all measurements were made using borax buffers[14] adjusted to I = 0.1 mol dm^{-3} with sodium perchlorate. The pH of the buffers was checked using a Radiometer Titralab System. Hydroxide ion concentrations were obtained from the pH using the following pK_w values[15]; 14.0432 (25.1°C); 13.8731 (30.1°C); 13.7086 (35.1°C); 13.5524 (40.0°C). Activity coefficients were obtained from the Davies' equation[16]; 0.772 (25.1°C); 0.770 (30.1°C); 0.768 (35.1°C); 0.766 (40.0°C). The reactions were monitored at 500 nm (the formation of the copper(II) complex of ($\textit{trans}$[14]dieneN$_4$) and 650 nm (the decay of $[Cu(en\text{-}aib\text{-}\beta ak)]^{2+}$) and the values given are the mean values obtained from at least four runs at each wavelength. At higher pH ([NaOH] = 0.01 to 0.1 mol dm^{-3} (Volucon)) the cyclisation was monitored using stopped

flow methods using a Hi-Tech SF-51 Stopped Flow Spectrophotometer. The ionic strength of the solutions was adjusted to I = 0.1 mol dm^{-3} using KNO_3.

4.2.3 Crystal Structure Determination of [(14-amino-4,4,9,11,11-pentamethyl-5,8,12-triazatetradec-8-en-2-one)copper(II)]$(ClO_4)_2 \cdot CH_3CN$

A blue needle crystal grown from acetonitrile solution mounted on a glass fibre was used in the X-ray analysis.

Crystal Data.—— $C_{18}H_{37}N_5O_9Cl_2Cu$, M = 601.97, triclinic, a = 10.752(9), b = 15.980(10), c = 8.112(7) Å, α = 100.24(7)°, ß = 95.43(7)° γ = 93.54(6)°, U = 1361(1) $Å^3$ (by least squares refinement on diffractometer angles for 14 automatically centred reflections in the range $6.05 < 2\theta < 12.96°$, λ = 0.71069 Å), space group P1 (#2), Z = 2, D_{calc} = 1.469 g cm^{-3}, $F(000)$ = 630.00. Blue needle. Crystal dimensions: 0.25 × 0.05 × 0.05 mm, μ(Mo-K_α) = 10.51 cm^{-1}.

Data Collection and Processing.——Rigaku AFC7S diffractometer, ω–2θ mode with ω scan width = 0.73 + 0.35 tan θ, ω scan speed 16.0° min^{-1}, graphite monochromated Mo-K_α radiation; 3795 reflections measured (max. 2θ = 45.0°), 3553 unique [merging R = 0.074 after absorption correction (max.,min. transmission factors =)], giving 1825 with $I > 3\sigma(I)$. Lorentz, polarization and linear crystal decay was corrected during processing.

Structure Analysis and Refinement.——Direct methods[17] followed by expansion using Fourier techniques[18]. Non-hydrogen atoms refined anisotropically. Hydrogen ions were included but not refined. Full-matrix least-squares[19] refinement was based on 1825 observed reflections and 316 variable parameters and converged with unweighted and weighted agreement factors of:

$$R = \sum \| Fo| - |Fc| \| / \sum |Fo| = 0.058$$

$$R_w = \sqrt{\left(\sum \left(|Fo| - |Fc| \right)^2 / \sum wFo^2 \right)} = 0.052$$

The standard deviation[20] of unit weight was 1.88. The weighting scheme was based on counting statistics. Plots of $\Sigma w(|Fo|-|Fc|)^2$ versus $|Fo|$, reflection order in data collection, sin θ/λ and various classes of indices showed no unusual trends. The maximum and minimum peaks on the final difference Fourier map corresponded to 0.54 and −0.55 $e^-/Å^3$, respectively. Final R and R_w values are 0.058 and 0.052 respectively. All calculations were performed using the teXsan[21] crystallographic software package of Molecular Structure Corporation.

4.3 Results and Discussion

4.3.1 Synthesis

Refluxing a solution of *bis*-(diaminoethane)copper(II) perchlorate in acetone for 30 minutes gives a blue product which was recrystallised from acetonitrile to give clear blue needle like crystals. This product was characterised by elemental analysis, infrared spectroscopy and UV/Vis spectroscopy as the copper(II) complex [(14-amino-4,4,9,11,11-pentamethyl-5,8,12-triazatetradec-8-en-2-one)copper(II)] perchlorate ([Cu(en-aib-βak)](ClO$_4$)$_2$), Figure 4.3.1.1.

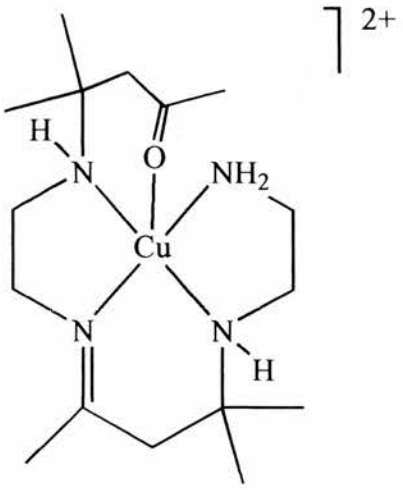

Figure 4.3.1.1. [(14-amino-4,4,9,11,11-pentamethyl-5,8,12-triazatetradec-8-en-2-one)copper(II)]$^{2+}$

The visible spectrum of $[Cu(en\text{-}aib\text{-}\beta ak)]^{2+}$ has λ_{max} = 628 nm, with a shoulder in the region of 800 to 900 nm. This additional band is indicative of five coordination in solution and such bands have previously been observed in five coordinate copper(II) complexes of pentaaza macrocycles[22]. An analogous compound with nickel(II) could not be formed, but the preparation of *bis*-(7-amino-4,4-dimethyl-5-azaheptan-2-one)nickel(II) perchlorate by literature methods[10] was successful. The complexes (13-imino-4,4,6,11,11-pentamethyl-3,7,10-triazatetradec-6-en-1-amine)nickel(II) perchlorate and (13-imino-4,4,6,11,11-pentamethyl-3,7,10-triazatetradec-6-en-1-amine)copper(II) perchlorate were synthesised successfully.

4.3.2 Crystal Structure of [(14-amino-4,4,9,11,11-pentamethyl-5,8,12-triazatetradec-8-en-2-one)copper(II)]$(ClO_4)_2 \cdot CH_3CN$.

The structure of $[CuL](ClO_4)_2 \cdot CH_3CN$ is built up of discrete molecules without any intramolecular interactions. The ORTEP molecular structure diagram of the cation is shown in Figure 4.3.2.1 along with the atomic numbering scheme. Final fractional atomic coordinates are given in Table 4.3.2.1 and selected bond lengths and bond angles in Table 4.3.2.2.

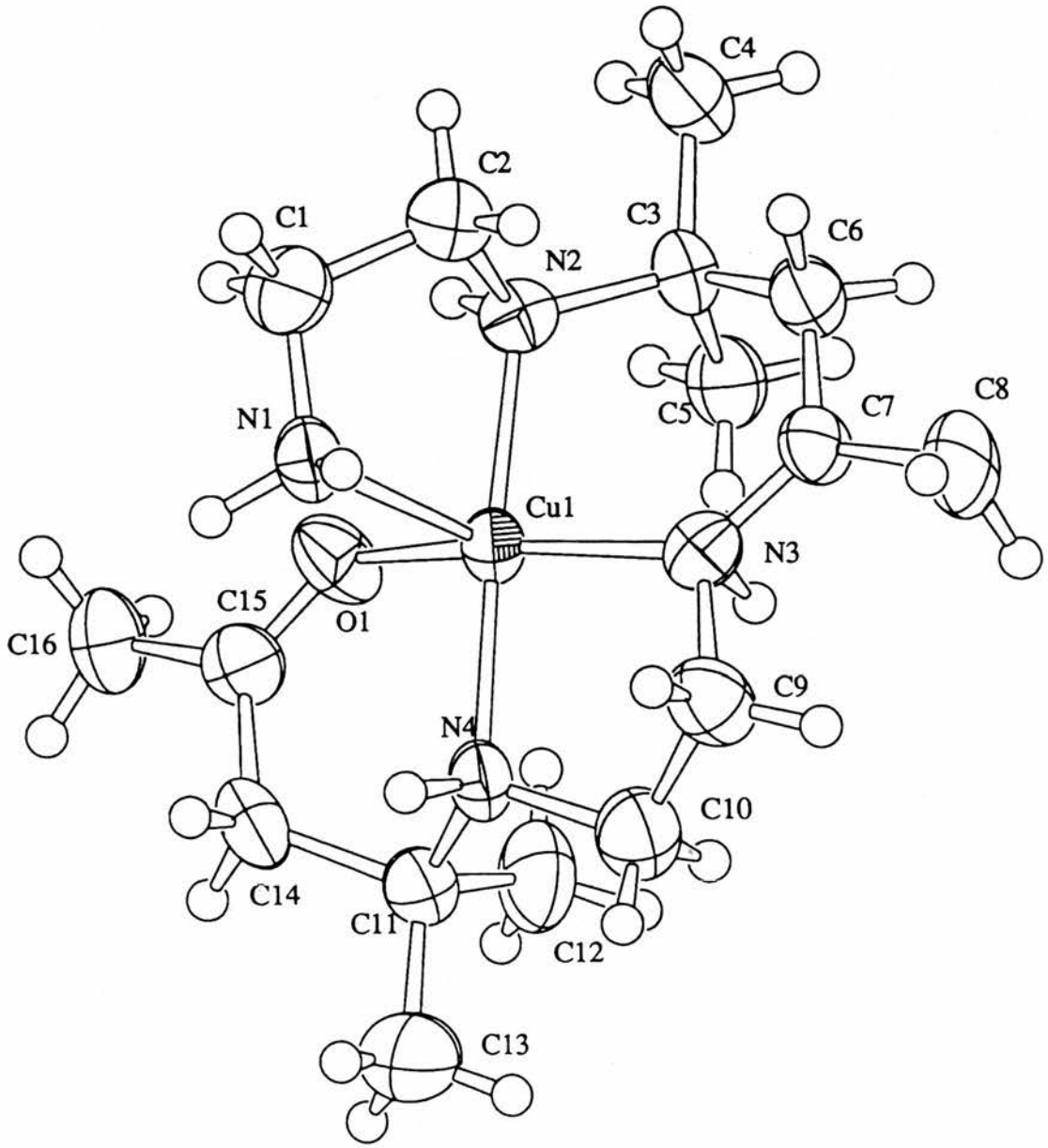

Figure 4.3.2.1. ORTEP diagram of [(14-amino-4,4,9,11,11-pentamethyl-5,8,12-triazatetradec-8-en-2-one)copper(II)]$(ClO_4)_2 \cdot CH_3CN$.

Table 4.3.2.1. Fractional atomic coordinates [(14-amino-4,4,9,11,11-pentamethyl-5,8,12-triazatetradec-8-en-2-one)copper(II)]$(ClO_4)_2 \cdot CH_3CN$

Atom	x	y	z
Cu(1)	0.8473(1)	0.23227(9)	0.8251(2)
N(1)	0.8922(8)	0.2206(5)	1.085(1)
N(2)	0.7013(7)	0.1509(5)	0.832(1)
N(3)	0.7395(9)	0.3276(5)	0.814(1)
N(4)	0.9904(7)	0.3131(5)	0.798(1)
O(1)	0.9389(7)	0.1252(5)	0.734(1)
C(1)	0.805(1)	0.1503(7)	1.107(1)
C(2)	0.679(1)	0.1553(7)	1.012(1)
C(3)	0.589(1)	0.1599(7)	0.714(1)
C(4)	0.485(1)	0.0899(7)	0.715(1)
C(5)	0.633(1)	0.1492(7)	0.537(1)
C(6)	0.538(1)	0.2477(7)	0.763(1)
C(7)	0.620(1)	0.3269(7)	0.794(1)
C(8)	0.554(1)	0.4083(7)	0.806(2)
C(9)	0.822(1)	0.4089(7)	0.846(1)
C(10)	0.938(1)	0.3926(7)	0.759(1)
C(11)	1.085(1)	0.2783(7)	0.680(1)
C(12)	1.019(1)	0.2520(8)	0.500(1)
C(13)	1.191(1)	0.3470(9)	0.685(2)
C(14)	1.136(1)	0.2003(8)	0.743(1)
C(15)	1.050(1)	0.1221(7)	0.726(1)
C(16)	1.108(1)	0.0378(8)	0.701(1)

Table 4.3.2.2. Molecular geometry dimensions (lengths in Å, angles in °)

Atoms		Distance (Å)	Atoms		Distance (Å)
Cu(1)	O(1)	2.084(7)	C(1)	C(2)	1.51(1)
Cu(1)	N(1)	2.157(8)	C(3)	C(4)	1.53(1)
Cu(1)	N(2)	1.987(8)	C(3)	C(5)	1.54(1)
Cu(1)	N(3)	1.979(8)	C(3)	C(6)	1.54(1)
Cu(1)	N(4)	2.001(8)	C(6)	C(7)	1.46(1)
O(1)	C(15)	1.21(1)	C(7)	C(8)	1.51(1)
N(1)	C(1)	1.47(1)	C(9)	C(10)	1.50(1)
N(2)	C(2)	1.49(1)	C(11)	C(12)	1.54(1)
N(2)	C(3)	1.50(1)	C(11)	C(13)	1.52(2)
N(3)	C(7)	1.28(1)	C(11)	C(14)	1.54(1)
N(3)	C(9)	1.50(1)	C(14)	C(15)	1.49(1)
N(4)	C(10)	1.49(1)	C(15)	C(16)	1.51(1)
N(4)	C(11)	1.53(1)			

Table 4.3.2.2. Molecular geometry dimensions (lengths in Å, angles in °) (cont.)

Atoms			Angle (°)	Atoms			Angle (°)
O(1)	Cu(1)	N(1)	93.2(3)	Cu(1)	N(4)	C(10)	108.0(6)
O(1)	Cu(1)	N(2)	86.1(3)	Cu(1)	N(4)	C(11)	117.0(7)
O(1)	Cu(1)	N(3)	156.9(3)	C(10)	N(4)	C(11)	113.5(8)
O(1)	Cu(1)	N(4)	93.0(3)	N(1)	C(1)	C(2)	109.7(9)
N(1)	Cu(1)	N(2)	84.3(3)	N(2)	C(2)	C(1)	106.6(9)
N(1)	Cu(1)	N(3)	109.5(3)	N(2)	C(3)	C(4)	110.7(8)
N(1)	Cu(1)	N(4)	100.2(3)	N(2)	C(3)	C(5)	106.3(8)
N(2)	Cu(1)	N(3)	92.2(4)	N(2)	C(3)	C(6)	110.5(8)
N(2)	Cu(1)	N(4)	175.4(4)	C(4)	C(3)	C(5)	109.0(8)
N(3)	Cu(1)	N(4)	86.8(4)	C(4)	C(3)	C(6)	109.3(9)
Cu(1)	O(1)	C(15)	126.7(8)	C(5)	C(3)	C(6)	110.9(9)
Cu(1)	N(1)	C(1)	104.1(6)	C(3)	C(6)	C(7)	122.0(9)
Cu(1)	N(2)	C(2)	107.8(6)	N(3)	C(7)	C(6)	122(1)
Cu(1)	N(2)	C(3)	114.0(6)	N(3)	C(7)	C(8)	122(1)
C(13)	C(11)	C(14)	110.3(9)	C(6)	C(7)	C(8)	116(1)
C(11)	C(14)	C(15)	118.0(9)	N(3)	C(9)	C(10)	108.2(9)
O(1)	C(15)	C(14)	122(1)	N(4)	C(10)	C(9)	110.0(9)
O(1)	C(15)	C(16)	121(1)	N(4)	C(11)	C(12)	109.4(9)
C(14)	C(15)	C(16)	117(1)	N(4)	C(11)	C(13)	109(1)
C(2)	N(2)	C(3)	115.9(8)	N(4)	C(11)	C(14)	107.4(9)
Cu(1)	N(3)	C(7)	129.9(8)	C(12)	C(11)	C(13)	110(1)
Cu(1)	N(3)	C(9)	108.0(6)	C(12)	C(11)	C(14)	110.4(9)
C(7)	N(3)	C(9)	121.9(9)				

The copper atom is five coordinate with approximate trigonal bipyramidal stereochemistry and an axial N(2)—Cu—N(4) bond angle of 175.4(4)°. The Cu—N bond lengths lie within the range 1.979 to 2.157 Å; the axial bond lengths Cu—N(2) = 1.987(8) and Cu—N(4) = 2.001(8) Å and the three equatorial bonds are Cu—N(1) = 2.157, Cu—N(3) = 1.979 and Cu—O(1) = 2.084. The equatorial bond angles N(1)—Cu—O(1), N(1)—Cu—N(3) and O(1)—Cu—N(3) are 93.2(3)°, 109.5(3)° and 156.9(3)° respectively, demonstrating considerable deviation from a regular structure. The axial equatorial bond angles range from 84.3(3)° for the N(1)—Cu—N(2) bond angle to 100.2(3)° for the N(1)—Cu—N(4) bond angle. The largest deviations from the expected 90° bond angles are to N(1). This terminal amine forms part of a five membered chelate ring but unlike the amines within the other five membered chelate ring is not constrained by being linked to other parts of the molecule. Therefore the strain within the ring decreases the bite angle. The other bond to a terminal atom is to the ketone oxygen atom, but this forms part of an unstrained six-membered chelate ring and therefore has bite angles close to the expected 90°. The two six membered chelate rings adopt a twist chair conformation. An interesting feature of the structure is that deprotonation of N(1) by base to give the amido species would allow ready attack on C(15) to generate a carbinolamine which would dehydrate to give *trans*[14]dieneN$_4$.

4.3.3 Kinetic studies

In basic solution $[Cu(en\text{-}aib\text{-}\beta ak)]^{2+}$ undergoes quite rapid ring closure to form the copper(II) complex of *trans*[14]dieneN$_4$. Attempts to perform the same base catalysed ring closure with the nickel(II) complex of *bis*-(7-amino-4,4-dimethyl-5-azaheptan-2-one) produced only nickel hydroxide. This is perhaps to be expected in view of the structure of the nickel(II) complex[23] in which the amines are not adjacent to the carbonyl groups. The complexes (13-imino-4,4,6,11,11-pentamethyl-3,7,10-triazatetradec-6-en-1-amine)nickel(II) perchlorate and (13-imino-4,4,6,11,11-pentamethyl-3,7,10-triazatetradec-6-en-1-amine)copper(II) perchlorate undergo very slow base catalysed ring closure to form complexes of *trans*[14]dieneN$_4$. These complexes also form *trans*[14]dieneN$_4$ complexes in acidic solution at a much faster rate than in basic solution.

In basic solution $[Cu(en\text{-}aib\text{-}\beta ak)]^{2+}$ undergoes quite rapid ring closure to form the copper(II) complex of *trans*[14]dieneN$_4$, with λ_{max} = 503 nm, Figure 4.3.3.1. Base catalysed ring closure in the pH range 9.1 to 9.7 was studied spectrophotometrically. Typical kinetic results are summarised in Table 4.3.3.1.

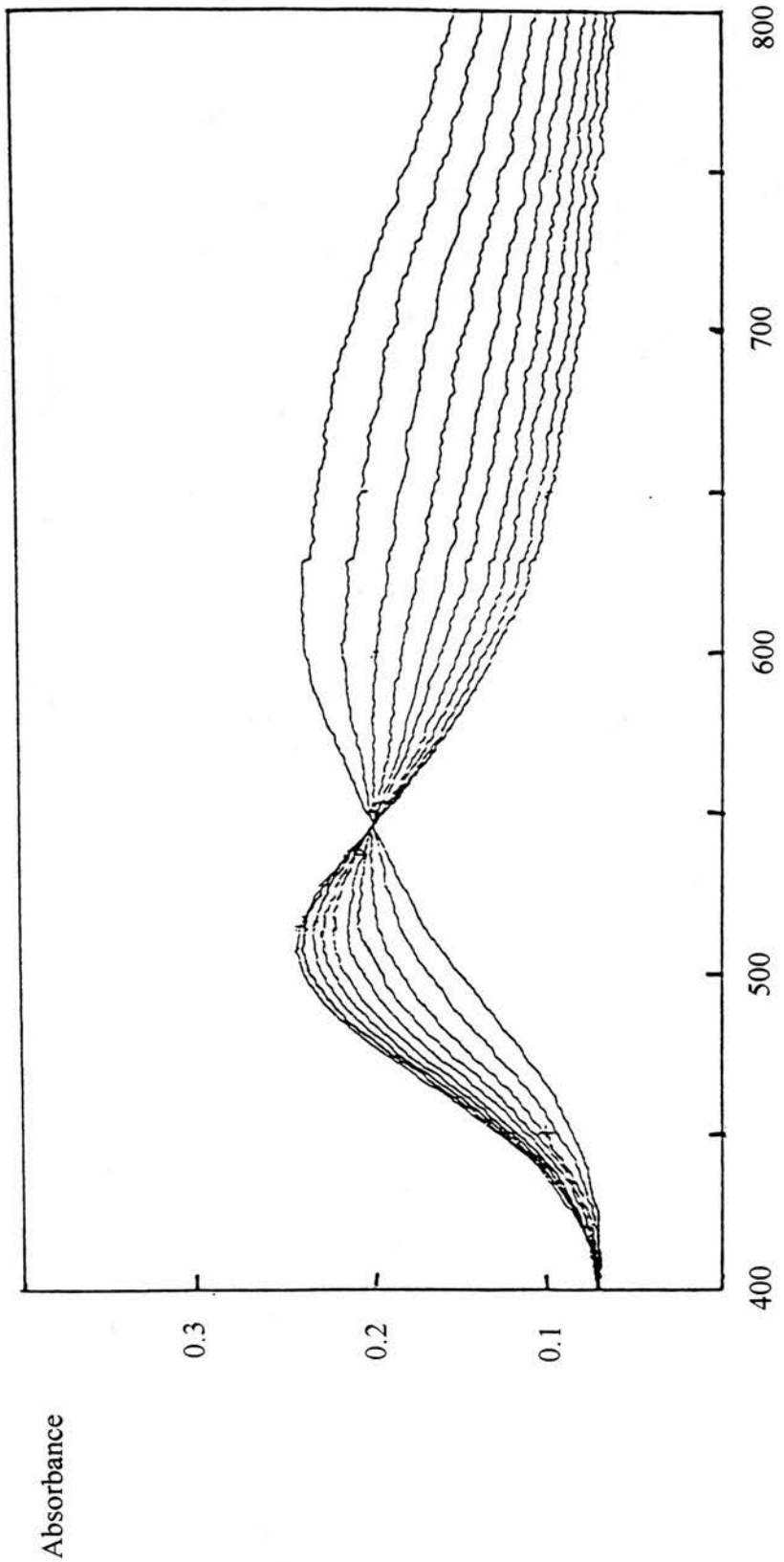

Figure 4.3.3.1. Interval scan spectra for the conversion of $[Cu(en\text{-}aib\text{-}\beta ak)]^{2+}$ to $[Cu(trans[14]dieneN_4)]^{2+}$.

Table 4.3.3.1 Ring closure of $[Cu(en\text{-}aib\text{-}\beta ak)]^{2+}$ in borax buffers at I = 0.1 mol dm^{-3}.

Temperature (°C)	pH	10^5 [OH$^-$] (mol dm^{-3})	10^4 k_{obs} (s^{-1})
30.1	9.70	8.72	4.98
	9.50	5.50	3.87
	9.30	3.47	2.84
	9.10	2.19	2.38
35.1	9.70	12.80	8.90
	9.50	8.06	6.72
	9.30	5.08	5.16
	9.10	3.21	4.08

A plot of k_{obs}, the observed first order rate constant at constant pH, *versus* the hydroxide ion concentration is linear with a positive intercept, Figure 4.3.3.2. The rate expression therefore takes the form

$$k_{obs} = k_0 + k[OH^-]$$

where k_0 relates to the water catalysed isomerisation and k to the base catalysed pathway. At 30.1°C, $k_0 = 1.50 \times 10^{-4}$ s^{-1} and k = 4.05 dm^3 mol^{-1} s^{-1}. Values of k_0 and k at the four temperatures studied are summarised in Table 4.3.3.2. The temperature dependence of k_0 gives $\Delta H^{\ddagger} = 77.6 \pm 2.0$ kJ mol^{-1} and $\Delta S^{\ddagger}_{298} = -62.5 \pm 4.0$ J K^{-1} mol^{-1}. For k, $\Delta H^{\ddagger} = 31.5 \pm 3.0$ kJ mol^{-1} and $\Delta S^{\ddagger}_{298} = -130 \pm 6.0$ J K^{-1} mol^{-1}.

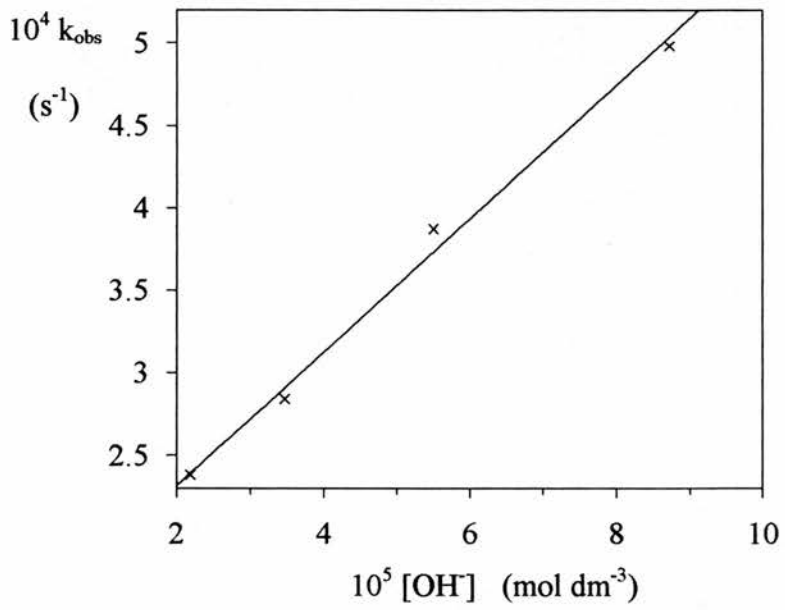

Figure 4.3.3.2. Plot of k_{obs} *versus* [OH$^-$] for the base catalysed conversion of [Cu(en-aib-βak)]$^{2+}$ to [Cu(*trans*[14]dieneN$_4$)]$^{2+}$ at 25°C and I = 0.1 mol dm^{-3}.

Table 4.3.3.2 Rate constants obtained using borax buffers solutions, I = 0.1 mol dm^{-3}.

Temp. (°C)	10^5 k_0 (s^{-1})	k (dm^3 mol^{-1} s^{-1})
25.1	9.1	3.25
30.1	15.0	4.05
35.1	25.7	5.00
40.0	41.9	6.26

At higher temperatures slight curvature of the plots of k_{obs} *versus* $[OH^-]$ was detectable. This result suggests that there may be an intramolecular reaction involving coordinated hydroxide. For example, it has previously been found[24] that the isomerisation of $[Cu(tet\ a)\ blue]^{2+}$ ((tet *a* blue) = C-meso-5,7,12,14,14-hexamethyl-1,4,8,11-tetraazacyclotetradecane) to the thermodynamically stable red isomer with the *trans* III chiral *sec*-NH configuration occurs by an intramolecular reaction involving coordinated hydroxide. The kinetic scheme is of the type;

$$[Cu(tet\ a]blue]^{2+} + OH^- \overset{K_{OH}}{\rightleftharpoons} [Cu(tet\ a)(OH)\ blue]^+ \qquad (1)$$

$$[Cu(tet\ a)(OH)blue]^+ \xrightarrow{k_{OH}} [Cu(tet\ a)red]^+ + OH^- \qquad (2)$$

For this scheme,

$$k_{obs} = \frac{k_{OH}K_{OH}[OH^-]}{\left(1 + K_{OH}[OH^-]\right)}$$

At low base concentrations where $K[OH^-] \ll 1$, $k_{obs} = k_{OH}K_{OH}[OH^-]$ and $k = k_{OH}K_{OH}$. For this reason stopped flow measurements were carried out using sodium hydroxide solutions in the concentration range 0.01 to 0.10 mol dm^{-3} adjusted to $I = 0.1$ mol dm^{-3}. The kinetic results obtained at 25°C are shown in Figure 4.3.3.3.

The solid line in Figure 4.3.3.3 is calculated using the constants $k_{OH} = 1.0 \times 10^{-2}$ s^{-1} and $K_{OH} = 78$ dm^3 mol^{-1}.

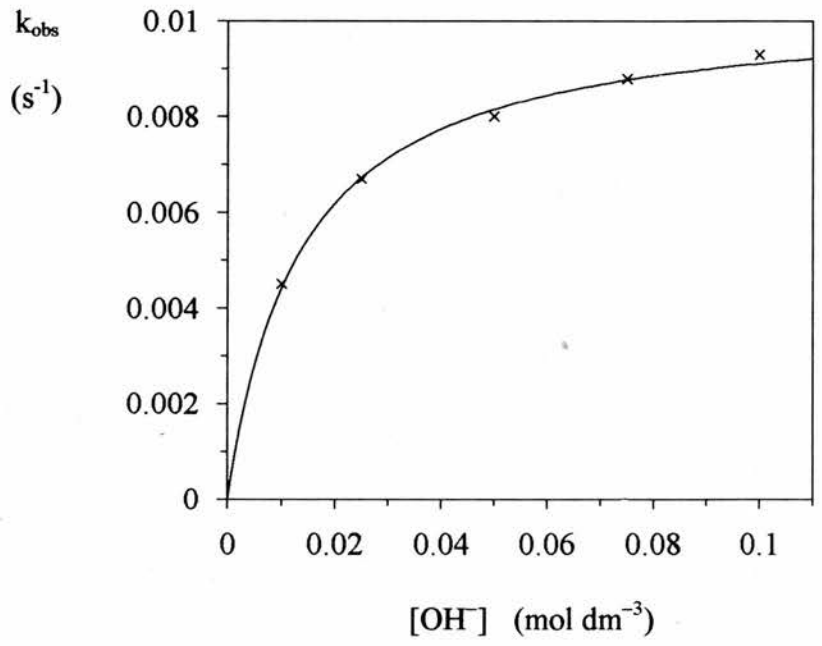

Figure 4.3.3.3. Plot of k_{obs} *versus* [OH$^-$] for the base catalysed conversion of [Cu(en-aib-βak)]$^{2+}$ to [Cu(*trans*[14]dieneN$_4$)]$^{2+}$ at 25°C and I = 0.1 mol dm^{-3}.

At higher hydroxide ion concentrations the reaction becomes independent of the hydroxide ion concentration consistent with a reaction scheme of the type illustrated in equations (1) and (2). Since,

$$k_{obs} = \frac{k_{OH}K_{OH}[OH^-]}{\left(1 + K_{OH}[OH^-]\right)}$$

it can be readily shown that,

$$\frac{1}{k_{obs}} = \frac{1}{k_{OH}K_{OH}[OH^-]} + \frac{1}{k_{OH}}$$

so that a plot of $1/k_{obs}$ *versus* $1/[OH^-]$ will be linear with a slope of $1/k_{OH}K_{OH}$ and an intercept of $1/k_{OH}$. Such a linear plot, Figure 4.3.3.4, gives K_{OH} = 78 dm^3 mol^{-1} and the limiting rate constant, k_{OH}, = 1.0 × 10^{-2} s^{-1} at 25°C and I = 1.0 mol dm^{-3}.

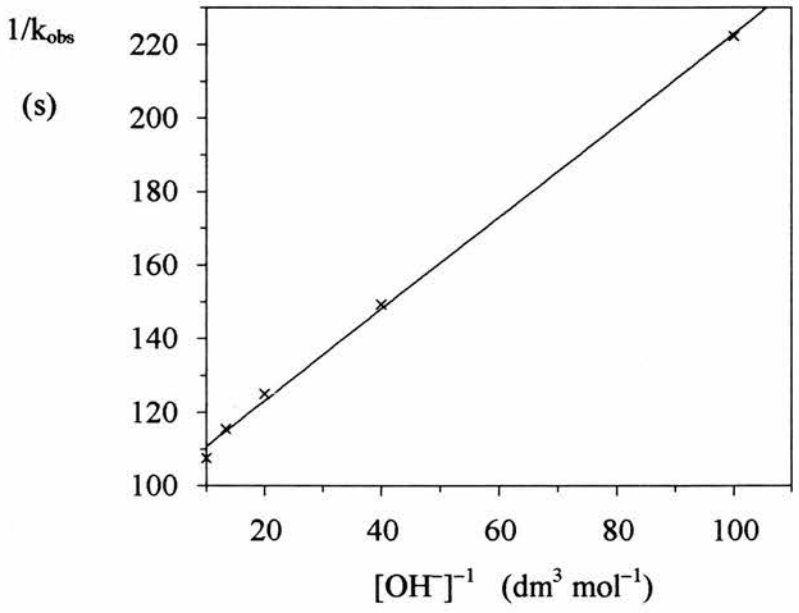

Figure 4.3.3.4. Double reciprocal plot of $1/k_{obs}$ *versus* $1/[OH^-]$ at high pH.

Temperature = 25°C, I = 0.1 mol dm^{-3}.

The equilibrium constant K_{OH} is the formation constant for the hydroxo complex. The ionization constant for the equilibrium;

$$CuL(OH_2)]^{2+} \overset{K_a}{\rightleftharpoons} CuL(OH)]^{+} + H^{+}$$

is given by $K_a = K_{OH}K_W = 7.8 \times 10^{-13}$ mol dm^{-3} leading to a $pK_a = 12.1$. The formation constant $K_{OH} = 78$ dm^3 mol^{-1} is similar to the value of 50.3 dm^3 mol^{-1} reported by Liang and Chung for the reaction of hydroxide ion with [Cu(tet *a*)blue]$^{2+}$. It is now clear that many base-catalysed reactions of copper(II) complexes occur by an intramolecular process involving coordinated hydroxide ion. Such reactions are well documented for kinetically inert cobalt(III) complexes[25], but have been more difficult to define with labile copper(II) complexes. In addition to the conversion of [Cu(tet *a*)blue]$^{2+}$ to [Cu(tet *a*)red]$^{2+}$ in which a Cu—OH species deprotonates an adjacent *sec*-NH centre in the macrocycle, the hydrolysis of the nitrile (A), Figure 4.3.3.5, to the amide (B) involves a similar mechanism[26].

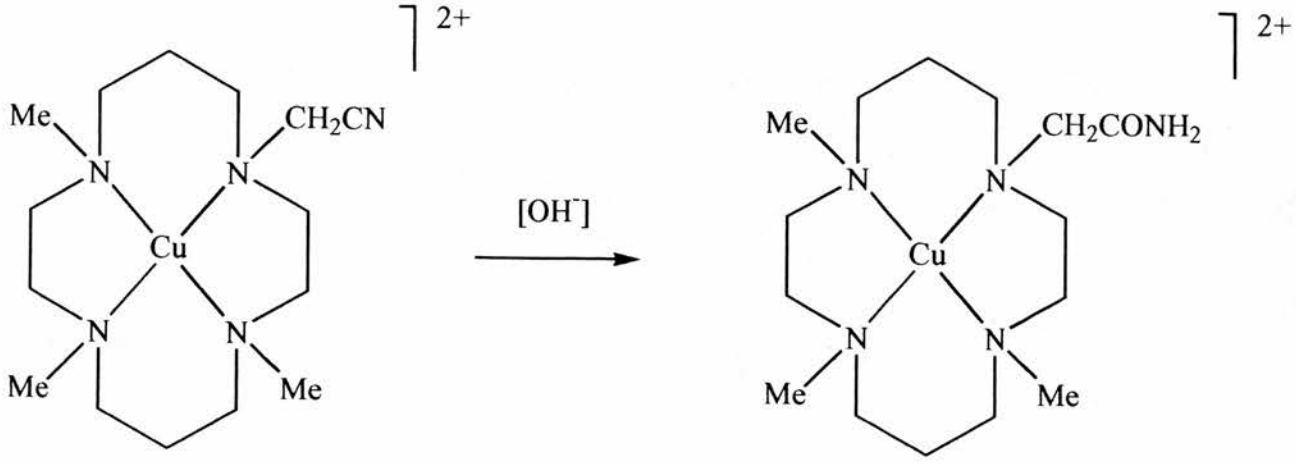

Figure 4.3.3.5. Conversion of nitrile to amide by intramolecular mechanism.

The reaction displays a first order dependence on the hydroxide ion concentration at low pH, but becomes independent of the hydroxide ion concentration at high pH when the Cu—OH species is fully formed.

Ring closure of the $[Cu(en\text{-}aib\text{-}\beta ak)]^{2+}$ to give [Cu(*trans*[14]dieneN$_4$) is expected to involve deprotonation of the NH_2 group at N(1) to generate the amido species which then attacks C(15) to generate the anion of the carbinolamine which accepts a proton from the solvent and dehydrates to the imine. It appears that the amino group on N(1) remains coordinated throughout the reaction so that nucleophilic attack can only occur in the presence of a base which allows the generation of the nucleophilic amido complex.

4.4 References

1 N.F. Curtis, *J. Chem. Soc.*, 1960, 4409

2 N.F. Curtis and D.A. House, *Chem. Ind.*, 1961, 1708

3 N.F. Curtis, Y.M. Curtis and H.K.J. Powell, *J. Chem. Soc. A*, 1966, 1015

4 R.W. Hay, G.A. Lawrance and N.F. Curtis, *J. Chem. Soc. Dalton Trans.*, 1971, 591

5 M.M. Blight and N.F. Curtis, *J. Chem. Soc.*, 1962, 3016

6 M.F. Bailey and I.E. Maxwell, *J. Chem. Soc. Chem. Comm.*, 1966, 908

7 L.G. Warner, N.J. Rose and D.H. Busch, *J. Am. Chem. Soc.*, 1967, **89,** 703

8 T-H. Lu, T-J. Lee, B-F. Liang and C-S. Chung, *J. Inorg. Nucl. Chem.*, 1981, **43,** 2333

9 T-H. Lu, C-S. Chung and T-J. Lee, *Acta Crystallogr., Sect. C,* 1984, **40,** 70

10 N.F. Curtis, *Coord. Chem. Rev.*, 1968, **3,** 3

11 G.J. Ferraudi and J.F. Endicott, *Inorg. Chem.*, 1977, **16,** 2762

12 N.F. Curtis, *Aust. J. Chem.*, 1988, **41,** 957

13 N. Sadasivan and J.F. Endicott, *J. Am. Chem. Soc.*, 1966, **88,** 5468

14 D.D. Perrin and B. Dempsey, in *Buffers for pH and Metal Ion Control,* Chapman Hall, London, 1974

15 R.A. Robinson and R.H. Stokes, *Electrolyte Solutions*, Second Edition, Butterworths, London, 1959

16 C.W. Davies, *J. Chem. Soc.*, 1936, 2093

17 A. Altomare, M.C. Burla, M. Camalli, M. Cascarano, C. Giacovazzo, A. Guagliardi and G. Polidori, *J. Appl. Crystallogr.* In preparation.

18 P.T. Beurskens, G. Admiraal, G. Beurskens, W.P. Bosman, R. de Gelder, R. Israel and J.M.M. Smits, *The DIRDIF-94 Program System,* Technical Report of the Crystallography Laboratory, University of Nijmegen, The Netherlands

19 Least squares:

Function minimised: $\sum \omega\left(|Fo| - |Fc|\right)^2$

where $w = \dfrac{1}{\sigma^2(Fo)} = \dfrac{4Fo^2}{\sigma^2(Fo^2)}$

$$\sigma^2(Fo^2) = \frac{S^2(C + R^2B) + (pFo^2)^2}{Lp^2}$$

S = Scan rate

C = Total integrated peak count

R = Ratio of scan time to background counting time

B = Total background count

Lp = Lorentz-polarization factor

p = p-factor

20 Standard deviation of an observation of unit weight:

$$\sqrt{\sum w\left(|Fo| - |Fc|\right)^2 / (No - Nv)}$$

where: No = number of observations

Nv = number of variables

21 teXsan: Crystal Structure Analysis Package, Molecular Structure Corporation, 1985 and 1992

22 R.W. Hay, R. Bembi and F. McLaren, *Inorganica Chimica Acta,* 1984, **85,** 23

23 N.F. Curtis, *Personal Communication*

24 B-F. Liang and C-S. Chung, *Inorg. Chem.*, 1980, **19,** 1867

25 R.W. Hay in *Comprehensive Coordination Chemistry, Vol 6,* eds; G. Wilkinson, J.A. McCleverty and R.D. Gillard, Pergammon Press, Oxford, 1987

26 T.A. Kaden, *Pure Appl. Chem.*, 1988, **60,** 1117

Chapter 5

Synthesis of Tetraamide Macrocycles

5.1 Introduction

As the subject of macrocyclic chemistry has matured chemists have sought to develop new ligands with increased functionality in the basic saturated polyamine structure. This has been accomplished in a number of ways; (i) replacement of N donors with S donors to produce thia ether ligands, (ii) affixing pendant arms with either donor atoms or sterically bulky groups, (iii) introduction of amide groups in place of the amine groups within the ligand to form oxo polyamine macrocycles.

Macrocyclic oxopolyamines are unique metal chelators possessing the dual characteristics of oligopeptides and macrocyclic polyamines. They display greater selectivity over metal ions than polyamines and have the added advantage of enhanced reversibility of metal uptake which can be controlled by pH. In addition, these ligands are also able to stabilize metal ions in high and unusual oxidation states since when deprotonated the ligands carry a negative charge and act as strong σ donors to hard metal centres.

5.1.1 Uses of Macrocyclic Oxopolyamines.

Selective Metal Ion Transport.

The selective liquid membrane transport of metal ions coupled to free energy gradients and against a concentration gradient is of both biological and industrial interest.

In biological systems mechanisms are required to control the transport of metal ions. Metal ions must be transported to cells that require them, they must be stored and any surplus must be excreted. Free metal ions may produce toxic effects due to non-specific

complexation with proteins or other molecules and therefore metal ions are usually transported and stored as metal complexes. Complexation also facilitates metal ion transport. For example, Cu(II) ions are usually transported complexed to peptides such as Gly-His-Lys[1] and Asp-Ala-His[2].

Industrially there are many applications for selective metal transport systems, for example, recovery and concentration of radioactive metal ions in the nuclear industry[3], metal recovery from effluents, selective extraction of metal ions prior to analysis[4], extraction of metal ions from ore[5] and waste water treatment. In the field of medicine systems are required that can selectively extract metal ions; excess Cu(II) ions must be removed in the treatment of Wilson's disease and after cancer treatment with *cis*-platin toxic Pt(II) ions must be excreted[6].

Several ligands have been found to be suitable for the transport of metal ions; crown ethers are efficient and selective in the transport of alkaline and alkaline earth metal cations[7] and macrocycles containing phenolic groups[8] have been used. The transport of transition metals has been achieved using macrocyclic polyaza ligands especially those containing amide donors in addition to amine donors. Macrocyclic amide ligands are particularly adept because of their unique chelating behaviour[9]. They will chelate metal ions with considerable selectivity in neutral or alkali conditions to form 1:1 complexes, which dissociate rapidly under to acidic conditions[10].

The transport of Cu(II) cations through a liquid membrane utilizing a functionalised analogue of dioxocyclam as a carrier has been demonstrated[11,12]. The ligand, with a

lipophilic group attached to its skeleton, is soluble in organic solvents but insoluble in aqueous media. Figure 5.1.1.1 illustrates a typical liquid membrane system and shows the transport of the Cu(II) cation. The ligand at the source phase/organic phase interface chelates a copper cation with simultaneous loss of two protons to the aqueous source phase. The complex then diffuses across the organic membrane to the organic phase/receiving phase interface where the two imido groups are protonated and the Cu (II) cation dissociates. The system relies on there being a pH gradient across the system.

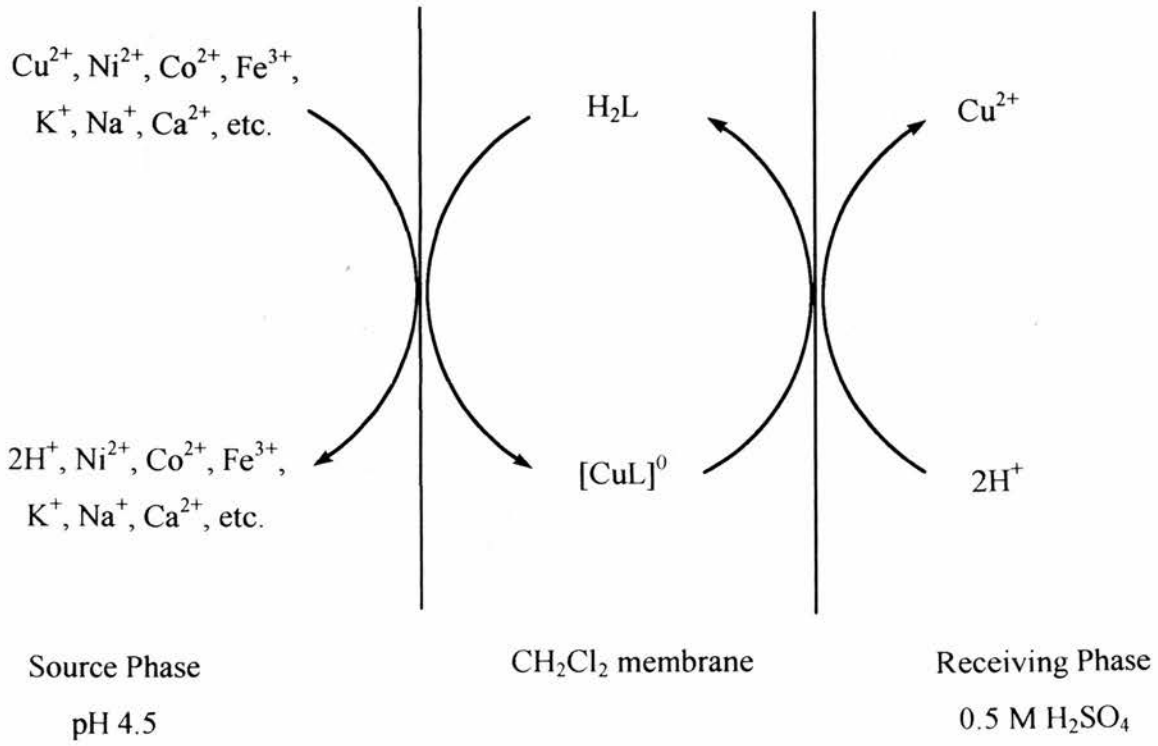

Figure 5.1.1.1. Selective transport of copper(II) ions using a liquid membrane transport system.

Biomimetics.

Two aspects of the chemistry of macrocyclic amides have ensured that they have been studied as biomimetic molecules; their similarity to oligopeptides and their ability to stabilize metal ions in high oxidation states.

Oligopeptides, such as Gly-Gly-His, have been used to model the active site of the Cu(II) specific transport site of serum albumin[13], Figure 5.1.1.2, which is responsible for the transport of copper in mammalian blood. Macrocyclic amides can be synthesised which have similar affinities for copper as the oligopeptides and such can be used to model the Cu(II) transport proteins.

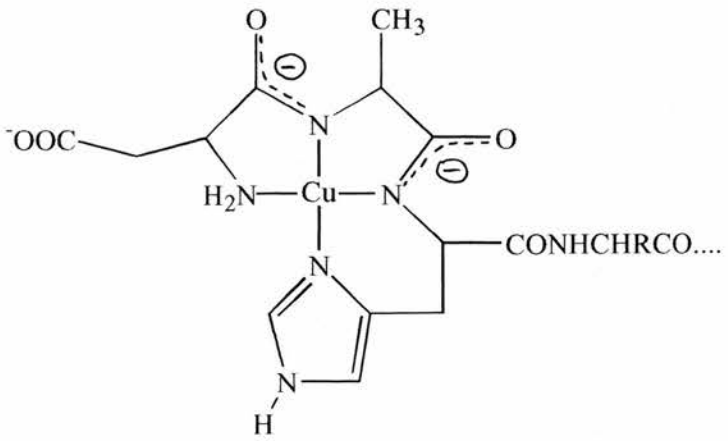

Figure 5.1.1.2. The active site of serum albumin

Biological oxygenases have been the subject of many studies into their chemistry which has proved to be extremely diverse. Model compounds have been used to investigate the

mechanism and applications of these enzymes. Macrocyclic amides, particularly dioxopentaamine[5], Figure 5.1.1.3, have proved particularly useful as mimics for mono-oxygenases[14]. The Ni(II) complex reacts with O_2 to give the Ni(III)—$O_2^{\cdot-}$ complex[15,16,17,18] and this complex has been shown to hydroxylate benzene to phenol and to cleave DNA[19].

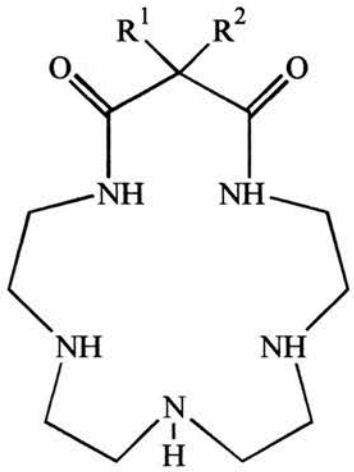

Figure 5.1.1.3 The macrocyclic amide, dioxopentaamine

A study of dioxygen uptake by a range of cobalt(II) complexes of saturated macrocyclic polyamines and oxopolyamines[20] has shown that the amide group plays a significant role in enhancing dioxygen uptake. This arises due to the increased donor strength of the deprotonated amide. Higher electron density at the metal increases the back donation to O_2 resulting in a stronger Co-O_2 bond. However, the structural framework of the ligand

also exerted some influence, the 14-membered dioxo ring system having the highest K_{O_2} value.

MRI Contrasting Agents.

Effective magnetic resonance imaging (MRI) contrast agents not only have to provide a significant enhancement of water relaxation rates but they must also be non-toxic at the effective administered dosage. Metal complexes are known to be less toxic than either of their constituent free ligands or metal ions[21]. However the toxicity of a metal complex is not only related to its thermodynamic stability. Metal ions available endogenously (eg. Cu(II) and Zn(II)) may compete for the ligand and dissociate Gd(III). A recent study[22] has shown that there is a good correlation between the relative stabilities of the Gd(III) and Zn(II) complexes and their toxicities demonstrating that a complex may have a small absolute thermodynamic stability and still be non-toxic as long as it is relatively higher than the stability of the potential displacing metal ion complex.

Macrocyclic amides have been shown to be effective ligands for MRI contrast agents[23]. Their structure has been considered to be "preorganised" for metal chelation[24] resulting in thermodynamically stable complexes. Allied to their metal ion selectivity and variable peripheral functionality, which can help them discriminate between different *in vivo* environments, they have the potential to be excellent contrast agents.

Oxidation Resistant Ligands.

There are relatively few examples of high valent middle and late transition metal complexes. Usually the metal centres in such complexes are highly oxidizing and, as the nearest source of electrons, the ligand is particularly vulnerable to oxidative attack. However ligands that are able to complex metal ions in high oxidation states can be designed if due consideration is given to optimizing two features of the ligand. The donor capacity of the ligand must be enhanced since strongly donating ligands reduce the oxidizing properties of high valent complexes and the ligand's resistance to oxidation must be optimized.

Amide ligands are particularly suitable for stabilizing high oxidation states because when deprotonated the amido-*N* anion is a strong donor group. Attention then turns to designing oxidation resistance in the ligand. An understanding of the processes by which a ligand may transfer electron density (be oxidized) to a complexed metal centre has aided this design process. Collins *et al*[25] have designed a pair of oxidation resistant macrocyclic tetra-amide ligands that stabilize Cr(V)[26], Ni(III)[27], Co(III)[28,29], Mn(V)[30,31,32] and Fe(IV)[33,34]. Certain structural features that enhance the ligands' resistance to oxidation have been incorporated into these ligands.

(i) all carbon atoms α to the amido-*N* are *gem*-methylated to prevent proton abstraction and subsequent $2e^-$ reduction of the metal centre, Figure 5.1.1.4. Margerum

et al[35] determined that such reductions were responsible for the instability of Cu(III) complexes of a macrocyclic tetra-amide.

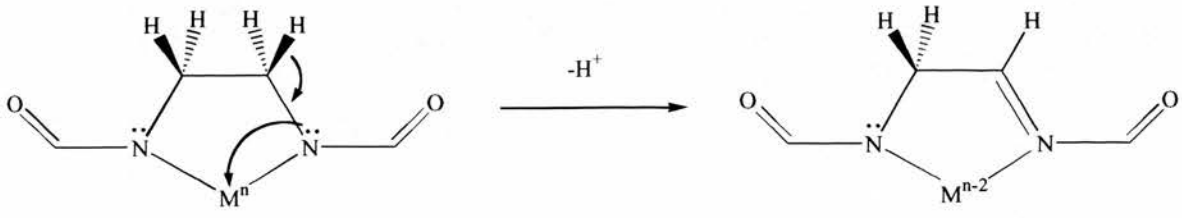

Figure 5.1.1.4

(ii) the 5-membered chelate rings do not contain any heteroatom substituents with lone pairs capable of overlapping with the σ* orbitals of the C-C bonds. In earlier studies such substituents were found to lead to destructive 2e– reductions of the metals, Figure 5.1.1.5.

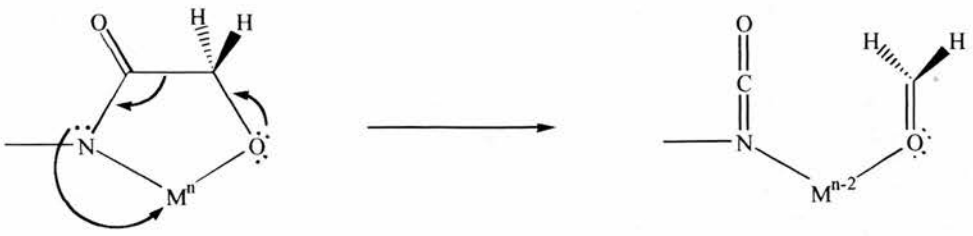

Figure 5.1.1.5.

(iii) the nitrogen lone pairs of the amide donor groups have minimal overlap with the σ* orbitals of the C-C bonds in the 5-membered chelate ring. Earlier studies found that other donors with more overlap with these orbitals were prone to heterolytic oxidative ligand decomposition, Figure 5.1.1.6.

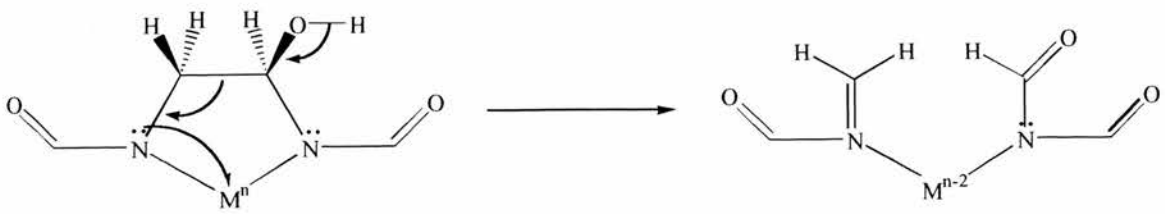

Figure 5.1.1.6.

(iv) the macrocyclic structure itself prevents homolytic oxidative ligand destruction.

Non-destructive oxidation can also occur which leads to ambiguities in the assignment of formal oxidation states to the metal. A particular feature that can lead to such problems is the presence of extended π-systems conjugated with the metal centre. Such ligands are classified as non-innocent whereas those without the conjugation are classified as innocent ligands[36].

5.1.2 Synthetic Strategies

The most common approach for the synthesis of macrocyclic amides utilizes the reaction between various carboxylic acid derivatives and amines.

Esters

The reaction between esters and amines (aminolysis) yields amides and is the most common synthetic procedure for macrocyclic amides. Diamides have commonly been synthesized from diesters and diamines, triamines[37], tetra-amines[38,39] and penta-amines[14] as shown in Figure 5.1.2.1.

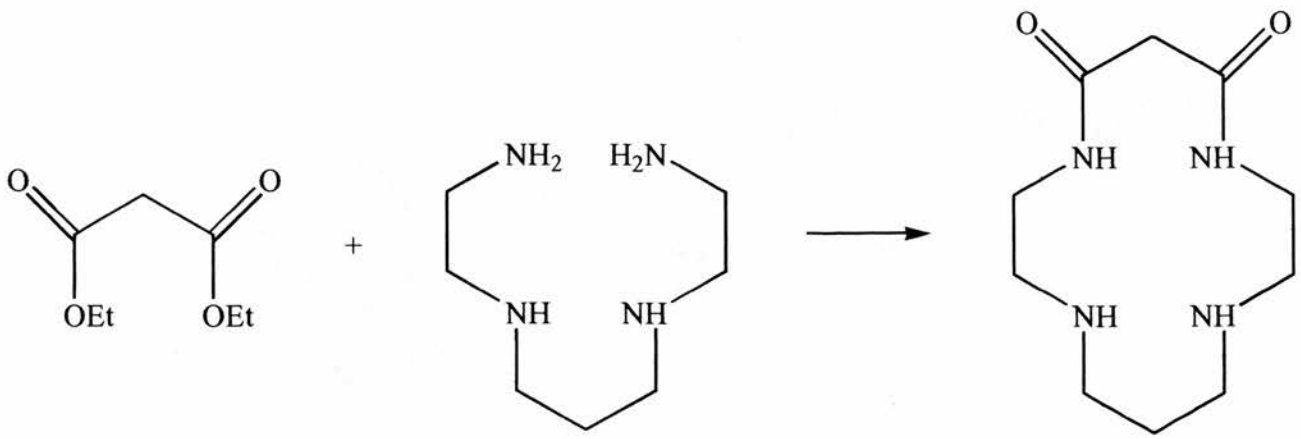

Figure 5.1.2.1.

Usually high dilution techniques (reactants at mmol concentrations) are required to prevent intermolecular reactions and the formation of polymeric products. However, some systems do not appear to require such techniques and give good yields of the macrocycle at high concentrations of reactants. An extension of this synthetic method is the introduction of one amide function into the macrocyclic ring using methyl acrylate[40].

Acid Chlorides

The reaction of acid chlorides with amines yields amides. Although less commonly used than esters, acid chlorides were used to synthesize the earliest examples of synthetic macrocyclic amides[41,42,43]. These reactions were all [1+1] additions to give diamides[44], however [2+2] additions have yielded tetra-amides[45], Figure 5.1.2.2.

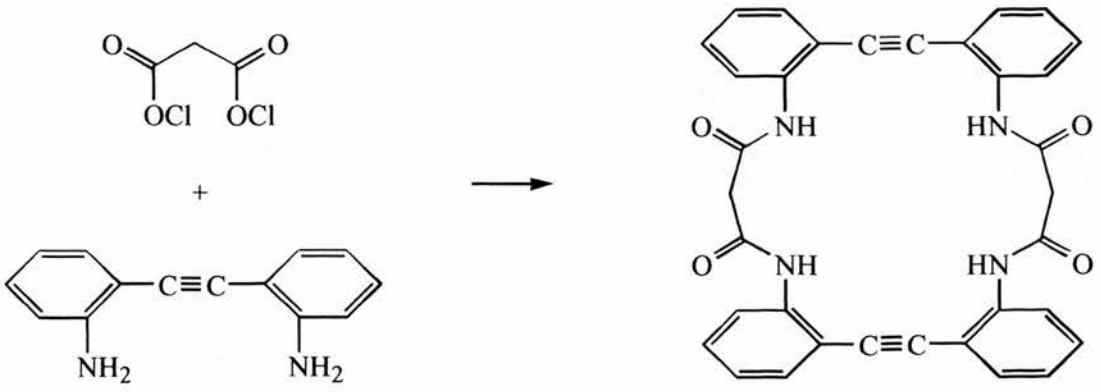

Figure 5.1.2.2.

Anhydrides

Several examples of the synthesis of macrocyclic amides from anhydrides and amines have been reported. Carvalho *et al*[23] utilized the reaction between cyclic anhydrides and diamines to produce macrocycles suitable for complexing to gadolinium(III) to provide MRI contrast agents.

Siddiqi and Mathew[46] claim to have synthesized a macrocyclic tetra-amide by the [2+2] addition of phthalic anhydride and ethylenediamine, Figure 5.1.2.3.

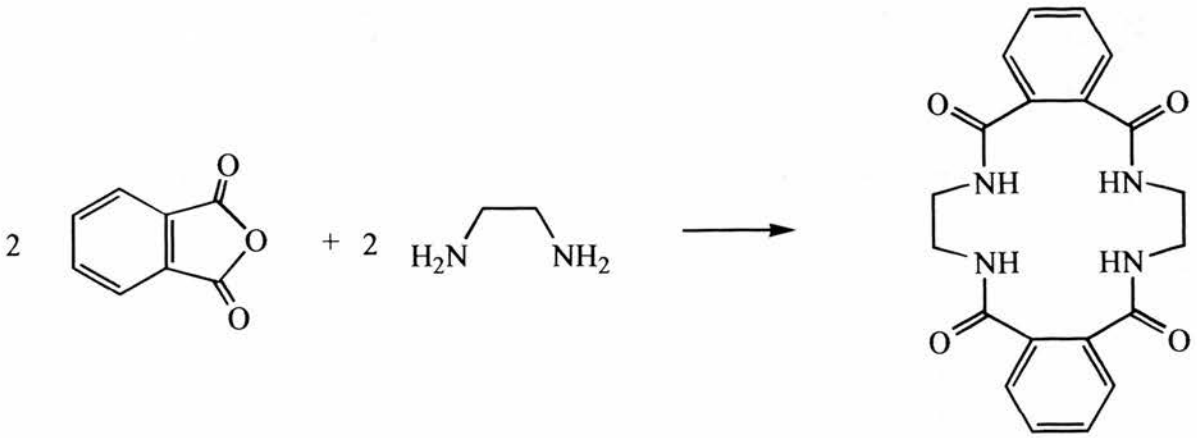

Figure 5.1.2.3.

Thiazolidine-2-thione derivatives

The aminolysis of thiazolidine-2-thione derivatives of dicarboxylic acids has been demonstrated to give high yields of macrocyclic diamides and tetra-amides[47], Figure 5.1.2.4. The reactions were performed under high dilution which was achieved by using mechanically driven syringes to introduce the reactants slowly into a large volume of solvent.

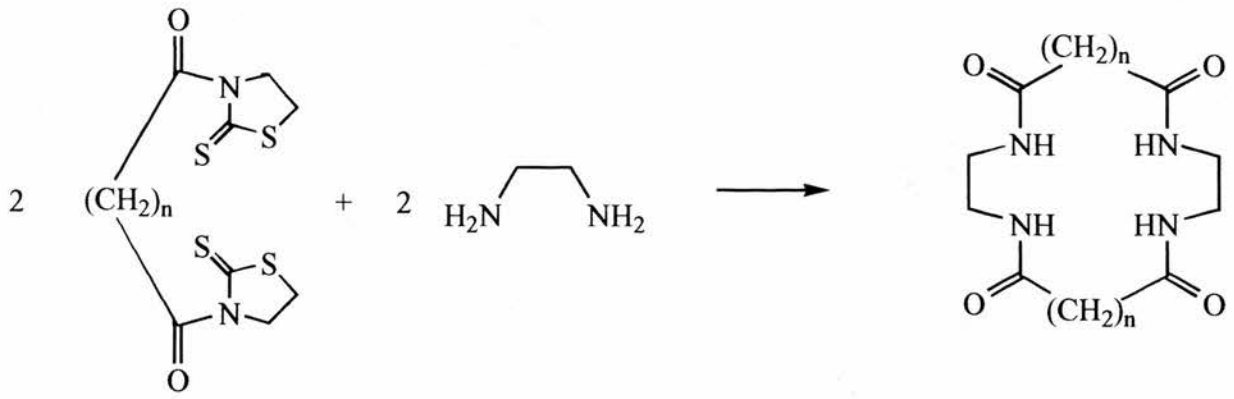

Figure 5.1.2.4.

In an attempt to overcome the polymerization problem without resorting to high dilution techniques several attempts at forming macrocyclic amides using a template synthesis have been reported. Silicon has been used as a covalent template by converting a diamine into the corresponding diazasilolidine[48] and subsequently condensing it with an activated carboxylic acid derivative (usually an acid chloride) to produce a macrocyclic tetra-amide[49].

Shakir has reported the synthesis of a large range of macrocyclic amides via metal ion template condensation of dicarboxylic acids with primary diamines[50]. It is claimed that the condensation works with a range of diacids and diamines and for several metal ion templates. Dinucleating macrocycles have been synthesized using the same procedure by substituting the diamine with a triamine[51].

Preliminary results and chemical intuition suggested that this method of synthesis would not yield the desired macrocyclic tetraamides. For this reason the reaction of diamines and diacids in the presence of a metal template was investigated.

5.2 Experimental

5.2.1 Synthesis

All materials were reagent grade and were obtained from either Aldrich Chemical Company or Avocado Research Chemicals Ltd.

Preparation of macrocyclic tetraamides

The reaction of malonic acid and the diamines, ethylenediamine and propylenediamine, in the presence of Cu(II), Ni(II) or Co(II) as templating ions was used to prepare the macrocyclic tetraamides as described by Shakir *et al*[50]. To an ice cold solution of the metal salt (0.005 mol) in methanol (50 cm^3) was added the diamine (0.01 mol) dissolved in methanol (50 cm^3), followed by the slow addition of malonic acid (0.01 mol) in methanol (50 cm^3). The resulting mixture was stirred for *ca.* 7 hours and the resulting precipitate was filtered off, washed with methanol and dried in *vacuo*. All synthetic work was performed under nitrogen.

Reaction of $CuCl_2.2H_2O$ with malonic acid and ethylenediamine.

Yield = 2.41 g, 61.7 %; (Found: C, 29.08; H, 3.54; N, 7.88 %. Calculated for $C_{10}H_{16}N_4O_4CuCl_2$: C, 30.74; H, 4.12; N, 14.34 %); UV/Vis λ_{max} 620-720 nm (variable)

Reaction of $CuCl_2.2H_2O$ with malonic acid and propylenediamine.

Yield = 2.17 g, 51.8 % (Found: C, 30.96; H, 4.67; N, 8.45 %. Calculated for $C_{12}H_{20}N_4O_4CuCl_2$: C, 34.41; H, 4.81; N, 13.38 %); λ_{max} 650 nm; I.R./cm^{-1}; ν(N-H) 3075, ν(C-H) 2960, 1615, 1584, 1418

Reaction of $NiCl_2.6H_2O$ with malonic acid and ethylenediamine.

Yield = 2.64 g, 63.8 %; UV/Vis; λ_{max} 391, 655, 727 nm; I.R./cm^{-1}; ν(N-H) 3039, 1584 cm^{-1}

Reaction of $NiCl_2.6H_2O$ with malonic acid and propylenediamine.

Yield = 2.34 g (Found: C, 33.76; H, 5.50; N, 10.47 %. Calculated for $C_{12}H_{20}N_4O_4NiCl_2$: C, 34.82; H, 4.87; N, 13.54 %); λ_{max} 389, 661 nm; I.R./cm^{-1}; ν(C-H) 2926, 1593, 1427

Reaction of $CoCl_2.2H_2O$ with malonic acid and ethylenediamine.

Yield = *ca.* 2 g, (Found: C, 26.35; H, 5.05; N, 8.93 %. Calculated for $C_{10}H_{16}N_4O_4CoCl_2$: C, 31.11; H, 4.18; N, 14.51 %); λ_{max} nm; I.R./cm^{-1}; ν(N-H) 3143, ν(C-H) 2954, 1621,1592, 1427

Reaction of $CoCl_2.6H_2O$ with malonic acid and propylenediamine.

Yield = 1.4 g; (Found: C, 24.58; H, 4.59; N, 7.61 %. Calculated for $C_{12}H_{20}N_4O_4CoCl_2$: C, 34.80; H, 4.87; N, 13.53 %); λ_{max} nm; I.R./cm^{-1}; ν(N-H) 3143, ν(C-H) 2954, 1621,1592, 1427

The copper(II) complex obtained with propylene diamine and malonic acid was purified by ion exchange methods using a Sephadex C-25 cation exchange column. The complex was absorbed on the column and a green complex slowly eluted with water. A blue band remained on the column and was eluted with 4 mol dm^{-3} sodium chloride.

The electronic spectrum of the green complex has λ_{max} = 854 nm which is very similar to that of $[Cu(mal)^2]^{2-}$. The cationic blue complex had λ_{max} = 578 nm which is identical to $[Cu(propylendiamine)^2]^{2+}$.

In a further experiment the prepared complex was sorbed on the Sephadex C-25 column and eluted with dilute HCl solution (pH = 3.5). A blue complex was eluted

from the from the column and on standing blue crystals formed. This complex gave a positive test for chloride with silver nitrate.

(Found: C, 27.73; H, 6.27; N, 14.36 %. Calculated for $C_{12}H_{20}N_4O_4CuCl_2$ (Shakir's complex): C, 34.80; H, 4.87; N, 13.53 %. Calculated for $C_9H_{24}N_4O_4CuCl_2$: C, 27.95; H, 6.26; N, 14.49 %); UV/Vis λ_{max} 624 nm; I.R./cm^{-1}; ν(N-H) 3143, ν(C-H) 2954, 1621,1592, 1427

5.2.2 Crystal Structure Determination of $[Cu(mal)(pn)Cl_2]^{2-}(pnH_2)^{2+}$

A blue needle crystal grown from aqueous solution mounted on a glass fibre was used in the X-ray analysis.

Crystal Data.—— $C_9H_{24}N_4O_4CuCl_2$, M = 386.77, orthorhombic, a = 9.080(4), b = 9.406(5), c = 18.403(4) Å, U = 1571(1) $Å^3$ (by least squares refinement on diffractometer angles for 19 automatically centred reflections in the range $9.10 < 2\theta < 16.75°$, λ = 0.71069 Å), space group Pnma (#62), Z = 4, D_{calc} = 1.634 g cm^{-3}, F(000) = 804.00. Blue, needle. Crystal dimensions: 0.10 × 0.15 × 0.35 mm, μ(Mo-K_α) = 17.46 cm^{-1}.

Data Collection and Processing.——Rigaku AFC7S diffractometer, ω-2θ mode with ω scan width = 1.57 + 0.35 tan θ, ω scan speed 16.0° min^{-1}, graphite monochromated

Mo-K_α radiation; 1265 reflections measured (max. $2\theta = 49.9°$), giving 847 with $I > 3\sigma(I)$. Lorentz, polarization corrected during processing.

Structure Analysis and Refinement.——Direct methods[52] followed by expansion using Fourier techniques[53]. Non–hydrogen atoms were refined anisotropically. Hydrogen atoms were included but not refined. Full-matrix least-squares[54] refinement was based on 847 observed reflections and 100 variable parameters and converged with unweighted and weighted agreement factors of:

$$R = \sum \| Fo| - |Fc| \| / \sum |Fo| = 0.035$$

$$R_w = \sqrt{\left(\sum \left(|Fo| - |Fc| \right)^2 / \sum wFo^2 \right)} = 0.032$$

The standard deviation[55] of unit weight was 2.34. The weighting scheme was based on counting statistics. Plots of $\sum w(|Fo|-|Fc|)^2$ versus $|Fo|$, reflection order in data collection, $\sin\theta/\lambda$ and various classes of indices showed no unusual trends. The maximum and minimum peaks on the final difference Fourier map corresponded to 0.41 and −0.58 $e^-/Å^3$, respectively. Final R and R_w values were 0.035 and 0.032 respectively. All calculations were performed using the teXsan[56] crystallographic software package of Molecular Structure Corporation.

5.3 Results and Discussion

Following the procedure described by Shakir *et al*[50] complexes were prepared for various combinations of di-acid, diamine and metal ion. However, characterisation of the products revealed that there was some discrepency between our results and the tetraamide structure suggested by Shakir. Elemental analysis, electronic spectra and infrared spectra varied significantly between different preparations of the same complex.

Mixing ethanolic solutions of $[Cu(pn)_2]^{2+}$ and $[Cu(mal)_2]^{2-}$ gives an immediate precipitate of a complex which is probably $[Cu(pn)_2][Cu(mal)_2]$ or a mixed ligand complex of the type [Cu(pn)(mal)]. This complex has an infrared spectrum identical to that of the complex prepared by Shakir *et al*. Shakir's complex does not have the properties expected for a cyclic amide. The complex most similar to that claimed by Shakir is the tetraamide ligand, *cyclo*-β-alanylglycyl-β-alanylglycyl (L), synthesised by Rybka and Margerum[57]. This ligand reacts as a slurry with $Cu(OH)_2$ in 0.1 mol dm^{-3} sodium hydroxide in 10 to 15 minutes to give the complex $[CuLH_{-4}]^{2-}$ in which the four amides are deprotonated, Figure 5.3.1.

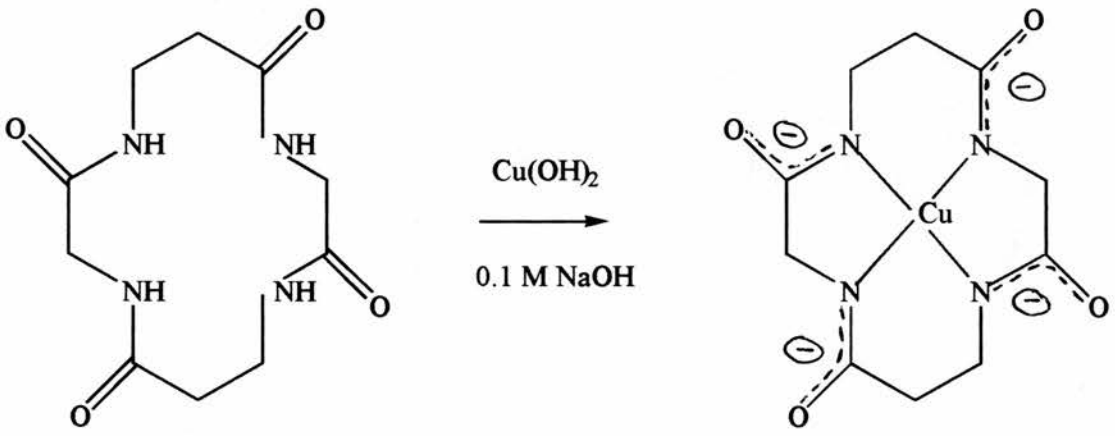

Figure 5.3.1 *cyclo*-β-alanylglycyl-β-alanylglycyl

The visible spectrum of $[CuLH_{-4}]^{2-}$ is characterised by a single band at 488 nm (ε = 54 dm^3 mol^{-1} cm^{-1}). The position and intensity of the band is independent of pH from pH 8.2 to 14.0 indicating that all four amide groups are deprotonated at pH 8.2. The position of the copper(II) *d—d* transition can be estimated using the rules developed by Billo[58]. The *d—d* band is predicted to occur at 520 ± 20 nm on the basis of four deprotonated amide nitrogens. The lower wavelength found with the macrocyclic complex is considered to be due to the constriction of the macrocyclic ring cavity which leads to a somewhat stronger ligand field. The available spectroscopic data indicates that the copper(II) complex of a macrocyclic tetraamide in basic solution should give rise to a *d—d* band at 500 ± 20 nm due to the strong ligand field exerted by the deprotonated amide groups. The copper(II) complex

prepared by Shakir's procedure gives a band in basic solution at *ca.* 620 nm which suggests that the macrocyclic tetraamide is not produced.

The product eluted from the Sephadex C-25 column with dilute hydrochloric acid was characterised. The elemental analysis suggested that it was a copper(II) complex with two propylenediamine molecules (one diprotonated), malonate and two chlorides. Titrating this complex with sodium hydroxide gave a molecular weight of 392.75 g mol^{-1}. Finally the crystal structure of the complex was determined. An ORTEP view of the structure is shown in Figure 5.3.2 along with the atomic numbering scheme and fractional atomic coordinates are given in Table 5.3.1. The molecular geometry dimensions are given in Table 5.3.2.

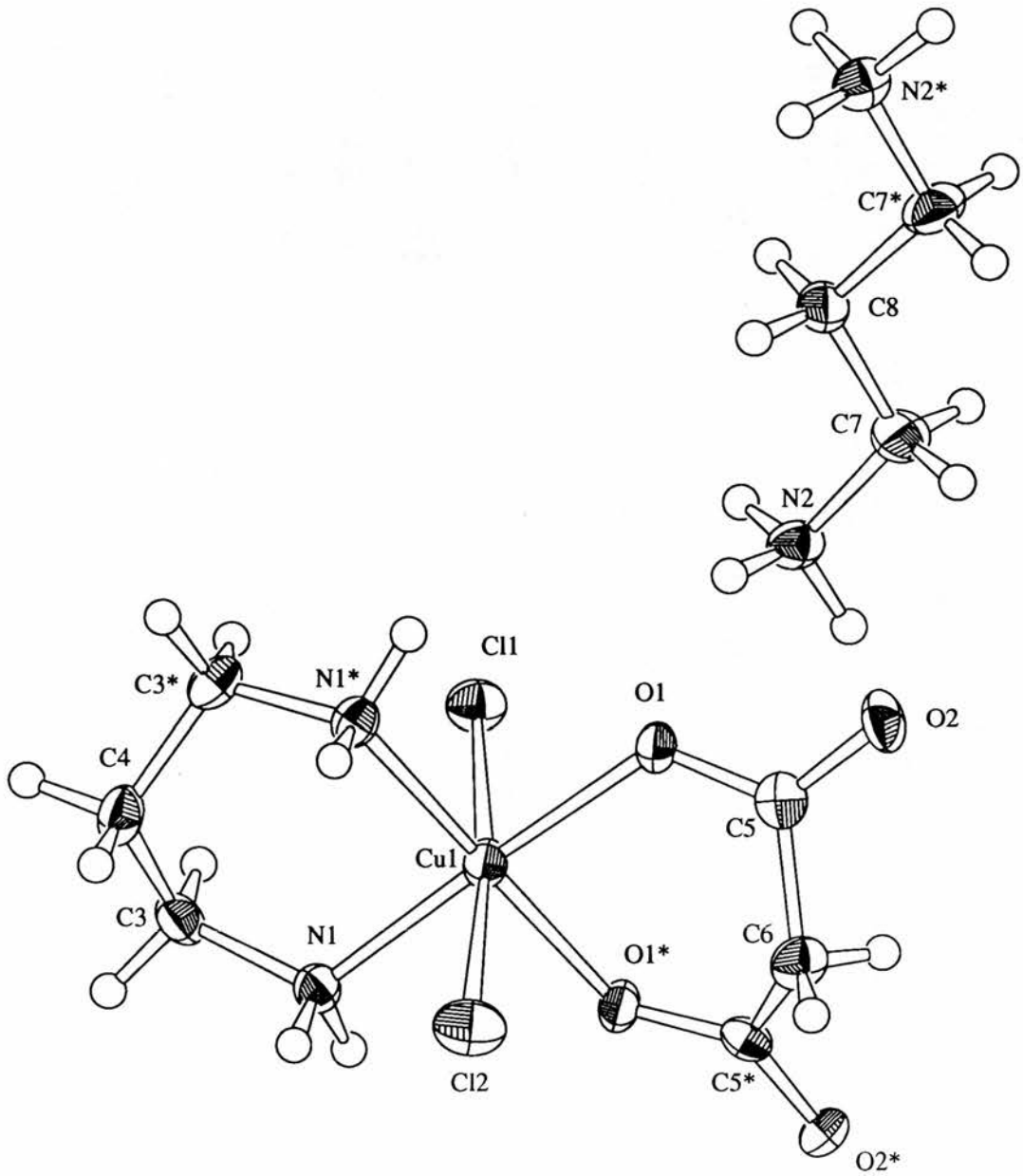

Figure 5.3.2. ORTEP view of $[Cu(pn)(mal)Cl_2]^{2-}(pnH_2)^{2+}$

Table 5.3.1. Fractional atomic coordinates $[Cu(pn)(mal)]^{2-}(pnH_2)^{2+}$

Atom	x	y	z
Cu(1)	0.0430(1)	0.25	0.07078(6)
Cl(1)	0.2222(2)	0.25	0.1987(1)
Cl(2)	-0.1250(2)	0.25	-0.0722(1)
O(1)	-0.0832(3)	0.3976(4)	0.1138(2)
O(2)	-0.2959(4)	0.4851(4)	0.1490(2)
N(1)	0.1615(4)	0.0976(4)	0.0234(2)
N(2)	-0.0407(5)	0.4869(5)	0.2634(2)
C(3)	0.3227(6)	0.1149(6)	0.0187(3)
C(4)	0.3628(8)	0.25	-0.0208(4)
C(5)	-0.2224(6)	0.3865(6)	0.1233(3)
C(6)	-0.2955(8)	0.25	0.0997(4)
C(7)	-0.1137(6)	0.6195(6)	0.2880(3)
C(8)	-0.0284(9)	0.75	0.2675(4)

Table 5.3.2. Molecular geometry dimensions (lengths in Å, angles in °)

Atoms		Distance (Å)	Atoms		Distance (Å)
Cu(1)	Cl(1)	2.862(2)	N(1)	C(3)	1.475(6)
Cu(1)	Cl(2)	3.042(2)	N(2)	C(7)	1.483(6)
Cu(1)	O(1)	1.966(3)	C(3)	C(4)	1.509(7)
Cu(1)	N(1)	1.993(4)	C(5)	C(6)	1.509(6)
O(1)	C(5)	1.281(6)	C(7)	C(8)	1.500(6)
O(2)	C(5)	1.237(6)			

Atoms			Angle (°)	Atoms			Angle (°)
Cl(1)	Cu(1)	Cl(2)	175.47(7)	Cu(1)	O(1)	C(5)	124.9(4)
Cl(1)	Cu(1)	O(1)	90.0(1)	Cu(1)	N(1)	C(3)	118.8(3)
Cl(1)	Cu(1)	N(1)	93.1(1)	N(1)	C(3)	C(4)	111.1(5)
Cl(2)	Cu(1)	O(1)	93.2(1)	C(3)	C(4)	C(3)	114.7(6)
Cl(2)	Cu(1)	N(1)	83.8(1)	O(1)	C(5)	O(2)	121.6(5)
O(1)	Cu(1)	O(1)	89.8(2)	O(1)	C(5)	C(6)	117.7(5)
O(1)	Cu(1)	N(1)	176.7(2)	O(2)	C(5)	C(6)	120.7(5)
O(1)	Cu(1)	N(1)	89.0(1)	C(5)	C(6)	C(5)	116.5(6)
O(1)	Cu(1)	N(1)	176.7(2)	N(2)	C(7)	C(8)	112.4(4)
N(1)	Cu(1)	N(1)	92.0(2)	C(7)	C(8)	C(7)	109.9(6)

The copper(II) ion is coordinated to the two nitrogen atoms of the propylenediamine molecule, the two oxygen atoms of the malonate ion at a distance of *ca.* 2 Å in a planar manner. The fifth and sixth coordination sites about the octahedral copper(II) ion are occupied by chloride ions with a Cu—Cl interatomic distance of 2.95 Å. There is a slight deviation from octahedral geometry about the copper(II) ion. The 1,3-diaminopropane molecule and malonate ion form six membered chelate rings with the copper(II) ion. The rings have different conformations; the copper-amine ring has a chair conformation while the copper-malonate ring has a boat conformation. This arrangement of conformations is the same as found for the similar complex[59], malonato-(1,3-diaminopropane)copper(II). The complex ion has a discrete diprotonated 1,3-diaminopropane counter ion.

It is commonly understood that the addition of an aliphatic amine to a carboxylic acid at room temperature results in a salt. Conversion of this salt to an amide requires high temperatures which are normally too high for the survival of the amide.

$$RCOOH + RNH_2 \longrightarrow RCOO^-NH_3^+R \xrightarrow{\Delta} RCONH_2 + H_2O$$

Formation of an amide is generally carried out after conversion of the carboxyl component to a more reactive acyl derivative which can react with the amino group under milder conditions. Suitable acyl derivatives with good leaving groups are esters, acid chlorides and acyl azides.

It appears that only simple complexes of the type $[Cu(pn)_2][Cu(mal)_2]$ or mixed ligand complexes [Cu(pn)(mal)] are formed by the described procedure. Experiments using

the other metal ions cobalt(II) and nickel(II) gave similar results and therefore it is concluded that macrocyclic amides are not produced by the procedure described by Shakir *et al.*

5.4 References

1 H. Sigel and B. Sarkar, *Chem. Rev.*, 1982, 82, 385

2 G. Rakhit and B. Sarkar, *J. Inorg. Biochem.*, 1981, 15, 233

3 R. Perrin, R. Lamartine and M. Perrin, *Pure and Applied Chemistry,* 1993, 65, 1549

4 T. Kumamara, Y. Nitta, H. Matsuo and E. Kimura, *Bulletin of the Chemical Society of Japan,* 1987, 60, 1930

5 *Chemistry and Engineering News,* 1985, 58

6 E. Kimura, Y. Lin, R. Machida and H. Zenda, *J.C.S. Chemical Communications,* 1986, 1021

7 J.D. Lamb, J.J. Christensen, S.R. Izatt, K. Bedke, M.S. Astin and R.M. Izatt, *Journal American Chemical Society,* 1980, 102, 3399

8 R.M. Izatt, J.D. Lamb, R.T. Hawkins, P.R. Brown, S.R. Izatt and J.J. Christensen, *Journal American Chemical Society,* 1983, 105, 1782

9 M. Kodama and E. Kimura, *J.C.S. Dalton Transactions,* 1979, 325

10 M. Kodama, T. Yatsunami and E. Kimura, *J.C.S. Dalton Transactions,* 1979, 1783

11 E. Kimura, C.A. Dalimunte, A. Yamashita and R. Machida, *J.C.S. Chemical Communications,* 1985, 1041

12 M. Di Casa, L. Fabrizzi, A. Perotti, A. Poggi and P. Tundo, *Inorganic Chemistry,* 1985, 24, 1610

13 E. Kimura, *Tetrahedron,* 1992, 48, 6175

14 E. Kimura, A. Sakonaka and R. Machida, *Journal American Chemical Society,* 1982, 104, 4255

15 E. Kimura and R. Machida, *J.C.S. Chemical Communications,* 1984, 499

16 D. Chen, R.J. Motekaitis and A.E. Martell, *Inorganic Chemistry,* 1991, 30, 1396

17 D. Chem and A.E. Martell, *Journal American Chemical Society,* 1990, 112, 9411

18 R. Machida, E. Kimura and Y. Kushi, *Inorganic Chemistry,* 1986, 25, 3461

19 Chien-Chung Cheng, S.E. Rokita and C.J. Burrows, *Angewante Chemie (Eng),* 1993, 32, 277

20 R. Machida, E. Kimura and M. Kodama, *Inorganic Chemistry,* 1983, 22, 2055

21 R.B. Laufer, *Chemical Reviews,* 1987, 87, 901

22 W.P. Cacheris, S.C. Quay and S.M. Rocklage, *Magnetic Resonance Imaging,* 1990, 8, 467

23 J.F. Carvalho, S-H. Kim and C.A. Chang, *Inorganic Chemistry,* 1992, 31, 4065

24 D.J. Cram, *Science,* 1988, 240, 760

25 T.J. Collins, K.L. Kostka, E.S. Uffelman and T.L. Weinberger, *Inorganic Chemistry,* 1991, 30, 4204

26 T.J. Collins, C. Slebodnick and E.S. Uffelman, *Inorganic Chemistry,* 1990, 29, 3433

27 T.J. Collins, T.R. Nichols and E.S. Uffelman, *Journal American Chemical Society,* 1991, 113, 4708

28 T.J. Collins and E.S. Uffelman, *Angewante Chemie,* 1989, 28, 1509

29 T.J. Collins, R.D. Powell, C. Slebodnick and E.S. Uffelman, *Journal American Chemical Society,* 1991, 113, 8419

30 T.J. Collins and S.W. Gordon-Wylie, *Journal American Chemical Society,* 1989, 111, 4511

31 T.J. Collins, R.D. Powell, C. Slebodnick and E.S. Uffelman, *Journal American Chemical Society,* 1990, 112, 899

32 T.J. Collins, D.F. Bocian, A.D. Procyk, R.D. Powell and J.M. Workman, *Inorganic Chemistry,* 1992, 31, 1550

33 T.J. Collins, K.L. Kostka, E. Munck and E.S. Uffelman, *Journal American Chemical Society,* 1990, 112, 5637

34 K.L. Kostka, B.G. Fox, M.P. Hendrich, T.J. Collins, C.E.F. Rickard, T.J. Wright and E. Munck, *Journal American Chemical Society,* 1993, 115, 6746

35 D.W. Margerum and J.S. Rybka, *Inorganic Chemistry,* 1981, 20, 1453

36 F.C. Anson, T.J. Collins, T.G. Richmond, B.D. Santarsiero, J.E. Toth and B.G.R.T. Treco, *Journal American Chemical Society,* 1987, 109, 2974

37 I. Tabushi, H. Okino and Y. Kuroda, *Tetrahedron Letters,* 1976, 4339

38 I. Tabushi, Y. Taniguchi and H. Kato, *Tetrahedron Letters,* 1977, 1049

39 Q-H. Lou, S-R. Zhu, M-C. Shen, S-Y. Yu, Z. Zhang, X-Y. Haung and Q-J. Wu, *J.C.S. Dalton Transactions,* 1994, 1873

40 E. Kimura, *Journal Coordination Chemistry,* 1986, 15, 1

41 P. Ruggli, *Leibigs Annalen der Chemie,* 1913, 399, 174

42 P. Ruggli, *Leibigs Annalen der Chemie,* 1912, 392, 92

43 P. Ruggli, *Leibigs Annalen der Chemie,* 1917, 412, 1

44 H. Stettler and J. Marx, *Angewante Chemie,* 1957, 69, 439

45 F. Vallacio Jr., R.V. Punzar and D.S. Kemp, *Tetrahedron Letters,* 1977, 547

46 Z.A. Ziddiqi and V.J. Mathew, *Polyhedron,* 1994, 13, 799

47 Y. Nagao, K. Seno, T. Miyasaka and E. Fujita, *Chemistry Letters,* 1980, 159

48 E.W. Abel and R.P. Bush, *Journal of Organometallic Chemistry,* 1965, 3, 245

49 E. Schwartz and A. Shanzer, *J.C.S. Chemical Communications,* 1981, 634

50 M. Shakir, S.P. Varkey and P.S. Hameed, *Polyhedron,* 1993, 12, 2775

51 M. Shakir and S.P. Varkey, *Transition Metal Chemistry,* 1994, 19, 606

57 D.W. Margerum and J.S. Rybka, *Inorganic Chemistry,* 1980, 19, 2784

58 E.J. Billo, *J. Inorg. Nucl. Chem. Lett.,* 1974, 10, 613

59 Aarne Pajunen and Elina Näsäkkäla, *Finish Chem Letters,* 1977, 100

52 A. Altomare, M.C. Burla, M. Camalli, M. Cascarano, C. Giacovazzo, A. Guagliardi and G. Polidori, *J. Appl. Crystallogr.,* in press

53 P.T. Beurskens, G. Admiraal, G. Beurskens, W.P. Bosman, R. de Gelder, R. Israel and J.M.M. Smits, *The DIRDIF-94 program system,* Technical Report of the Crystallography Laboratory, University of Nijmegen, The Netherlands., 1994, ,

54 Least squares:

Function minimised: $\sum \omega\left(|Fo| - |Fc|\right)^2$

$$\text{where } w = \frac{1}{\sigma^2(Fo)} = \frac{4Fo^2}{\sigma^2(Fo^2)}$$

$$\sigma^2(Fo^2) = \frac{S^2(C + R^2B) + (pFo^2)^2}{Lp^2}$$

S = Scan rate

C = Total integrated peak count

R = Ratio of scan time to background counting time

B = Total background count

Lp = Lorentz-polarization factor

p = p-factor

55 Standard deviation of an observation of unit weight:

$$\sqrt{\sum w\left(|Fo| - |Fc|\right)^2 / (No - Nv)}$$

where: No = number of observations

Nv = number of variables

56 teXsan: Crystal Structure Analysis Package, Molecular Structure Corporation, 1985 and 1992

57 D.W. Margerum and J.S. Rybka, *Inorganic Chemistry,* 1980, 19, 2784

59 A. Pajunen and E. Näsäkkäla, *Finish Chem Letters,* 1977, 100

Appendix 1

Treatment of Kinetic Data.

Simple reactions

For a reaction that proceeds to completion in which the concentration of only one reactant, A, changes significantly the expression

$$-\frac{d[\mathrm{A}]}{dt} = k[\mathrm{A}]^a \qquad (1)$$

can be written. Such a situation may arise if;

1) there is only one reactant involved,

2) all other reactants are in large excess (> 10 fold) compared to A,

3) the concentration of other reactants is held constant during the reaction.

Since it is usually easier to measure concentrations rather than rate equation (1) is usually integrated. For the most common case where a = 1, first order in A, the integrated equation is;

$$\ln\frac{[\mathrm{A}]_0}{[\mathrm{A}]_t} = k_1 t$$

If a = 0, zero order in A,

$$-\frac{d[\mathrm{A}]}{dt} = k$$

and, integration gives,

$$[A]_t = [A]_0 - kt$$

For a second order reaction where a = 2,

$$-\frac{d[A]}{dt} = k[A]^2$$

$$\frac{1}{[A]_t} = \frac{1}{[A]_0} + kt$$

Parallel First Order Reactions

For the reactions shown below;

$$A \xrightarrow{k_1} B$$

$$A \xrightarrow{k_2} C$$

$$A \xrightarrow{k_3} D$$

the rate of the reaction equates to

$$-\frac{d[\mathrm{A}]}{dt} = k_1[\mathrm{A}]_t + k_2[\mathrm{A}]_t + k_3[\mathrm{A}]_t = (k_1 + k_2 + k_3)[\mathrm{A}]_t$$

$$-\frac{d[\mathrm{A}]}{dt} = k_{\mathrm{T}}[\mathrm{A}]_t$$

Therefore a simple exponential decay will be observed experimentally with

$$\ln\frac{[\mathrm{A}]_0}{[\mathrm{A}]_t} = k_{\mathrm{T}}t$$

For the individual products, presuming their concentrations at t = 0 to be zero,

$$[\mathrm{B}] = \left(\frac{k_1[\mathrm{A}]_0}{k_{\mathrm{T}}}\right)\left(1 - e^{-k_{\mathrm{T}}t}\right)$$

$$[\mathrm{C}] = \left(\frac{k_2[\mathrm{A}]_0}{k_{\mathrm{T}}}\right)\left(1 - e^{-k_{\mathrm{T}}t}\right)$$

$$[\mathrm{D}] = \left(\frac{k_3[\mathrm{A}]_0}{k_{\mathrm{T}}}\right)\left(1 - e^{-k_{\mathrm{T}}t}\right)$$

Experimentally simultaneous reactions can be distinguished from simple first order reactions involving just one product by the absence of isosbestic points.

Consecutive Reactions

For two irreversible first order or pseudo first order consecutive reactions of the form;

$$A \xrightarrow{k_1} B \xrightarrow{k_2} C \qquad (1)$$

analysis will vary according to the relative magnitudes of k_1 and k_2. If $k_1 \gg k_2$ then the two steps can be investigated separately. If $k_2 \gg k_1$ then only the first step will be observed and the only method of investigating k_2 will be by the isolation and separate examination of B. If k_1 and k_2 are similar in value conventional methods for monitoring the composition of the reactants and products can be employed and the values of k_1 and k_2 calculated from data collected.

The rate equations for the components of (1) are given below;

$$-d[A]/dt = k_1[A] \qquad (2)$$

$$d[B]/dt = k_1[A] - k_2[B] \qquad (3)$$

$$d[C]/dt = k_2[B] \qquad (4)$$

The concentrations of A, B and C with respect to time can be derived by integration of equations (2) and (3), followed by substitution into (4).

Integration of (2)

$$\ln \frac{[A]_0}{[A]_t} = k_1 t$$

$$\ln \frac{[A]_t}{[A]_0} = -k_1 t$$

$$\frac{[A]_t}{[A]_0} = e^{-k_1 t}$$

$$[A]_t = [A]_0 e^{-k_1 t} \qquad (5)$$

Substituting this value into (3) and integrating the result,

$$\frac{d[B]}{dt} = k_1 [A]_t e^{-kt} - k_2 [B]_t$$

Rearranging

$$\frac{d[B]}{dt} + k_2 [B]_t = k_1 [A]_t e^{-kt} \qquad (6)$$

Using the integrating factor method and using the factor shown below;

$$\text{IF} = e^{\int k_2 dt} = e^{k_2 t}$$

Multiplying each term in (6) by this factor gives,

$$e^{k_2 t}\frac{d[\text{B}]}{dt} + [\text{B}]_t k_2 e^{k_2 t} = k_1[\text{A}]_0 e^{-k_1 t} e^{k_2 t} \qquad (7)$$

Combining the functions,

$$e^{-k_1 t} e^{k_2 t} = e^{(k_2 t - k_1 t)} = e^{(k_2 - k_1)t}$$

and substituting,

$$k_2 e^{k_2 t} = \frac{d(e^{k_2 t})}{dt}$$

gives

$$e^{k_2 t}\frac{d[\text{B}]}{dt} + [\text{B}]_t \frac{d(e^{k_2 t})}{dt} = k_1[\text{A}]_0 e^{(k_2 - k_1)t} \qquad (8)$$

The left hand side of equation (8) is the formula for the derivative of a product of functions and can be rewritten as;

$$e^{k_2 t}\frac{d[\mathrm{B}]}{dt}+[\mathrm{B}]_t\frac{d(e^{k_2 t})}{dt}=\frac{d([\mathrm{B}]e^{k_2 t})}{dt}$$

Therefore equation (8) becomes;

$$\frac{d([\mathrm{B}]e^{k_2 t})}{dt}=k_1[\mathrm{A}]_0 e^{(k_2-k_1)t} \qquad (9)$$

Integrating,

$$\int d[\mathrm{B}]e^{k_2 t}=k_1[\mathrm{A}]_0\int e^{(k_2-k_1)t}dt \qquad (10)$$

Since it is a differential the left hand side of equation (10) is readily integrated to;

$$[\mathrm{B}]_t e^{k_2 t}+c$$

The right hand side must be solved by substitution;

$u=(k_1-k_2)t$ and therefore;

$$\frac{du}{dt}=k_2-k_1 \qquad \text{and} \qquad dt=\frac{du}{k_2-k_1}$$

Substituting gives;

$$k_1[\mathrm{A}]_0 \int e^{(k_2-k_1)t} dt = k_1[\mathrm{A}]_0 \int e^u du$$

$$= \frac{k_1[\mathrm{A}]_0}{(k_2-k_1)} e^u + \mathrm{c}$$

$$= \frac{k_1[\mathrm{A}]_0}{(k_2-k_1)} e^{(k_2-k_1)t} + \mathrm{c}$$

Finally, combining both constants of integration into one;

$$[\mathrm{B}]_t e^{k_2 t} = \frac{k_1[\mathrm{A}]_0}{(k_2-k_1)} e^{(k_2-k_1)t} + \mathrm{c} \qquad (11)$$

Applying the limits of the experiment, namely [B]=0 when t=0;

$$0 = \frac{k_1[\mathrm{A}]_0}{k_2-k_1} + c \qquad \text{since } e^0 = 1$$

$$c = -\frac{k_1[\mathrm{A}]_0}{k_2-k_1}$$

Equation (11) then becomes;

$$[\mathrm{B}]_t e^{k_2 t} = \frac{k_1[\mathrm{A}]_0}{k_2 - k_1} e^{(k_2 - k_1)t} - \frac{k_1[\mathrm{A}]_0}{k_2 - k_1}$$

Dividing through by $e^{k_2 t}$ gives;

$$[\mathrm{B}]_t = \frac{k_1[\mathrm{A}]_0}{k_2 - k_1} e^{-k_1 t} - \frac{k_1[\mathrm{A}]_0}{k_2 - k_1} e^{-k_2 t}$$

so,

$$[\mathrm{B}]_t = \frac{k_1[\mathrm{A}]_0}{k_2 - k_1}(e^{-k_1 t} - e^{-k_2 t}) \qquad (12)$$

Since $[\mathrm{A}]_0 = [\mathrm{A}]_t + [\mathrm{B}]_t + [\mathrm{C}]_t$ equations (5) and (12) can be substituted into this equation to calculate $[\mathrm{C}]_t$.

$$[\mathrm{C}]_t = [\mathrm{A}]_0 - [\mathrm{A}]_t - [\mathrm{B}]_t$$

$$[\mathrm{C}]_t = [\mathrm{A}]_0 - [\mathrm{A}]_0 e^{-k_1 t} - \frac{k_1[\mathrm{A}]_0}{k_2 - k_1}(e^{-k_1 t} - e^{-k_2 t})$$

$$[\mathrm{C}]_t = [\mathrm{A}]_0\left(1 - e^{-k_1 t} - \frac{k_1}{k_2 - k_1}(e^{-k_1 t} - e^{-k_2 t})\right)$$

Multiplying $e^{-k_1 t}$ by $\frac{k_2 - k_1}{k_2 - k_1} = 1$ gives;

$$[C]_t = [A]_0 \left(1 - \frac{k_2 - k_1}{k_2 - k_1} e^{-k_1 t} - \frac{k_1 (e^{-k_1 t} - e^{-k_2 t})}{k_2 - k_1} \right)$$

$$[C]_t = [A]_0 \left(1 - \frac{k_2 e^{-k_1 t}}{k_2 - k_1} + \frac{k_1 e^{-k_1 t}}{k_2 - k_1} - \frac{k_1 e^{-k_1 t}}{k_2 - k_1} + \frac{k_1 e^{-k_2 t}}{k_2 - k_1} \right)$$

$$[C]_t = [A]_0 \left(1 - \frac{k_2 e^{-k_1 t}}{k_2 - k_1} + \frac{k_1 e^{-k_2 t}}{k_2 - k_1} \right)$$

$$[C]_t = [A]_0 \left(1 - \frac{k_2 e^{-k_1 t} + k_1 e^{-k_2 t}}{k_2 - k_1} \right)$$

Rearranging gives;

$$[C]_t = [A]_0 \left(1 - \frac{k_2 e^{-k_1 t} - k_1 e^{-k_2 t}}{k_1 - k_2} \right) \qquad (13)$$

The analysis of a property to which each component contributes linearly should give a biphasic plot. Since the usual method for monitoring this type of reaction is electronic absorption spectroscopy the relationship between the concentrations of the reactants and products with respect to time and the optical absorption of the reacting solution is

required before further analysis can proceed. The optical absorbance D_t of the reacting solution at time t is given by;

$$D_t = \varepsilon_A l[A]_t + \varepsilon_B l[B]_t + \varepsilon_C l[C]_t \qquad (14)$$

where ε_A is the molar absorption of A at time t and l is the spectrophotometric path length in centimetres. By substituting the terms for $[A]_t$, $[B]_t$ and $[C]_t$ from equations (5), (12) and (13) respectively into (14) gives;

$$D_t = \varepsilon_A l\left([A]_0 e^{-k_1 t}\right) + \varepsilon_B l\left(\frac{k_1[A]_0}{k_2 - k_1}(e^{-k_1 t} - e^{-k_2 t})\right) + \varepsilon_C l[A]_0\left(1 - \frac{k_2 e^{-k_1 t} - k_1 e^{-k_2 t}}{k_1 - k_2}\right) \qquad (14)$$

Rearranging and introducing $D_\infty = \varepsilon_C l[A]_0$ gives;

$$D_t - D_\infty = \alpha e^{-k_1 t} + \beta e^{-k_2 t}$$

where the constants α and β are;

$$\alpha = \frac{(\varepsilon_B - \varepsilon_A)k_1 + (\varepsilon_A - \varepsilon_C)k_2}{k_2 - k_1}[A]_0$$

$$\beta = \frac{(\varepsilon_C - \varepsilon_B)k_1[A]_0}{k_2 - k_1}$$

Therefore a plot of $\log(D_t-D_\infty)$ versus time consists of two added straight line segments. These can be resolved provided the two rate constants k_1 and k_2 are sufficiently different. In the case where $k_1 > k_2$ at long times the plot $\log(D_t-D_\infty)$ versus time will be linear and will have a slope of k_2 and an intercept at $t = 0$ of β since at these times the first reaction will be complete. The difference Δ can then be calculated from;

$$\Delta = D_t - D_\infty - \beta e^{-k_2 t} = \alpha e^{-k_1 t}$$

A plot of $\log \Delta$ versus t then yields k_1. β will give the unknown molar absorption ε_B.

This treatment of

$$A \xrightarrow{k_1} B \xrightarrow{k_2} C$$

allows two mathematical solutions which will fit the data with equal precision. The two rate constants for the fast and slow steps are interchanged,

$$k_1 = k'_2 \quad \text{and} \quad k_2 = k'_1$$

and an alternative molar absorption for species B is given by;

$$\varepsilon'_B = \varepsilon_A + \frac{k_1(\varepsilon_B - \varepsilon_A)}{k_2}$$